SCIENCE • TECHNOLOGY • RESEARCH HIGHLIGHTS • VISIONS

Dissertation
138

Strategy for wireless transmission disturbances detection and identification in industrial wireless sensor networks

Marina Eskola

VTT

VTT SCIENCE 138

Strategy for wireless transmission disturbances detection and identification in industrial wireless sensor networks

Marina Eskola

Thesis for the degree of Doctor of Science to be presented with due permission for public examination and criticism in IT115, at the University of Oulu, on the 22nd of November 2016 at 12 o'clock noon.

ISBN 978-951-38-8468-0 (Soft back ed.)
ISBN 978-951-38-8467-3 (URL: http://www.vttresearch.com/impact/publications)

VTT Science 138

ISSN-L 2242-119X
ISSN 2242-119X (Print)
ISSN 2242-1203 (Online)
http://urn.fi/URN:ISBN:978-951-38-8467-3

JULKAISIJA – UTGIVARE – PUBLISHER

Teknologian tutkimuskeskus VTT Oy
PL 1000 (Tekniikantie 4 A, Espoo)
02044 VTT
Puh. 020 722 111, faksi 020 722 7001

Teknologiska forskningscentralen VTT Ab
PB 1000 (Teknikvägen 4 A, Esbo)
FI-02044 VTT
Tfn +358 20 722 111, telefax +358 20 722 7001

VTT Technical Research Centre of Finland Ltd
P.O. Box 1000 (Tekniikantie 4 A, Espoo)
FI-02044 VTT, Finland
Tel. +358 20 722 111, fax +358 20 722 7001

Juvenes Print, Tampere 2016

Academic dissertation

Supervisors

Docent Tapio Heikkilä
VTT Technical Research Centre of Finland Ltd
PO Box 1100
FI-90571 Oulu
Finland

Prof. Olli Silven
University of Oulu
PO Box 4500
FI-90014 University of Oulu
Finland

Prof. Markku Juntti
University of Oulu
PO Box 4500
FI-90014 University of Oulu
Finland

Reviewers

Prof. Hamid Sharif
University of Nebraska–Lincoln
1110 South 67th Street, Omaha
USA

Prof. Floriano De Rango
University of Calabria
87036 Arcavacata of Rende, Cosenza
Italy

Opponent

Prof. Jerker Delsing
Luleå University of Technology
97187 Luleå
Sweden

Preface

The research for this thesis was conducted at the VTT Technical Research Centre of Finland Ltd in Oulu, Finland during the years 2011-2016. The supervisors of this thesis are Docent Tapio Heikkilä from VTT, Prof. Markku Juntti and Prof. Olli Silven from the University of Oulu. The research work has mostly been performed during two projects; Reliable and Real-time Wireless Automation - RIWA (2011-2013) funded by Tekes – the Finnish Funding Agency for Innovation, and Dependable Embedded Wireless Infrastructure - DEWI (2014-2015) funded by ARTEMIS Joint Undertaking and by Tekes.

First and foremost, I would like to express my appreciation and gratitude to my supervisor Tapio Heikkilä for his support and patience during the whole period of my work, as well as for his guidance and teachings that have enabled me to learn the important aspects of research working and academic writing. My deepest gratitude to Pirkka Tukeva for his trust in my professional skills and for giving me the opportunity and encouragement to begin my doctoral studies. I want to thank Prof. Olli Silven for his guidance during my studies, for his help in carrying out my career plans, and for help in focusing my research in the right direction. I also want to thank Prof. Markku Juntti for his valuable comments and suggestions on this research.

I want to thank the members of my follow-up group; Tapio Seppänen for providing his insight on the mathematical aspects of classification procedure, Mikko Sallinen for his friendly guidance and encouragement, and Jarmo Prokkola for his kind help and advises on the spectrum measurements related issues from my first day at VTT.

I am grateful to reviewers of this thesis, Prof. Hamid Sharif from the University of Nebraska-Lincoln and Prof. Floriano De Rango for the University of Calabria, for reviewing my manuscript. I am also grateful to Anni Repo for revising the thesis.

I also want to thank the partners from industry for helping and advising me during the measurements campaigns, and for their incredible cooperation spirit and friendly reception.

My appreciation to Timo Lehikoinen for his support and motivation to finish my thesis, and for being a good leader for our team. I am also very thankful to Esa Viljanmaa for his kind encouraging words, for his support on my phd studies, especially on UML exam, and for his great and positive attitude.

This work would not be possible without support of my colleagues at VTT. I want to thank Tero Peippola for the numerous fruitful discussions and guidance that have helped me in my developing work. I want also to express my deepest gratitude to Marko Korkalainen for his great help, time and kindness. I am very grateful to Jari Rehu for his advices, support, and patience on teaching the aspects of embedded coding. I would also like to acknowledge Kalle Määttä, Känsälä Klaus and Jari Hämeenaho for being supportive and helpful during this work. My special thanks to my colleagues in Tampere; Henrik Huovila, Seppo Rantala, Jari Jankkari and Harri Siirtola for their friendly attitude and for their help in adapting to the new working environment. My special acknowledge to Matti Annala for his great support and help on the last stages of this work, and for his sense of humour which cheers everyone up around and makes the working days more delightful. In addition, I want to thank Marko Höyhtyä for the thought-provoking conversations during the lunch time and coffee breaks.

My sincere gratitude to my dearest friends Ekaterina Osmekhina and Antonina Shvetsova, to my little sister Anitta Eskola, to my parents Valentina Eskola and Toivo Eskola, and to my grandmother Tatjana Haajanen for their incredible support and care, for believing in me and pushing me forward. Without support of my friends and relatives this work would not be possible, and the hard times would have been much worse. Finally, I want to thank my son Denis Timonen, who has given me the best motivation to keep going and doing my best.

Tampere, October 2016 Marina Eskola

Contents

List of symbols

ABB	ASEA Brown Boveri
ADC	Analogue-to-Digital Converter
BER	Bit Error Rate
BW	Bandwidt
C/N	Carrier-to-Noise Ratio
CCA	Clear Channel Assessment
CCK	Complimentary Code Keying
CPU	Central Processing Unit
CRC	Cyclic Redundancy Check
CWSN	Cognitive Wireless Sensor Networks
DSSS	Direct Sequence Spread Spectrum
EIRP	Equivalent Isotropically Radiated Power
FCC	Federal Communication Commission
FFT	Fast Fourier Transformation
HART	Highway Addressable Remote Transducer Protocol
IEC	International Electrotechnical Commission
ISA	International Society of Automation
ISI	Intersymbol Interference
ISM	Industrial, Scientific, and Medical radio band
IWSN	Industrial Wireless Sensor Networks
LBT	Listen Before Talk
LO	Local Oscillator

LOS	Line-of-sight
MAC	Medium Access Control
MBER	Mean Bit Error Rate
NCS	Networked Control Systems
NLOS	Non-line-of-sight
NNR	Nearest Neighbour Root
OFDM	Orthogonal Frequency-Division Multiplexing
OSI	Open Systems Interconnection reference model
PDF	Probability Density Function
PER	Packet Error Rate
PRR	Packet Reception Rate
QoS	Quality of Service
RF	Radio Frequency
RMS	Root Mean Square
RSSI	Received Signal Strength Indication
SDR	Software Defined Radio
SIR	Signal-to-Interference Ratio
SNR	Signal-to-Noise Ratio
USRP	Universal Software Radio Peripheral
UWB	Ultra-Wideband
WISA	Wireless Interface for Sensors and Actuators
WLAN	Wireless Local Area Network
WSN	Wireless Sensor Networks

1. Introduction

The benefits brought by wireless technologies to industrial automation systems play an important role in today's competitive marketing situation. Greater awareness and control enabled by industrial wireless sensor networks (IWSN) improve the productivity and efficiency of such systems, leading to significant savings and ease the integration of business processes; see Figure 1.

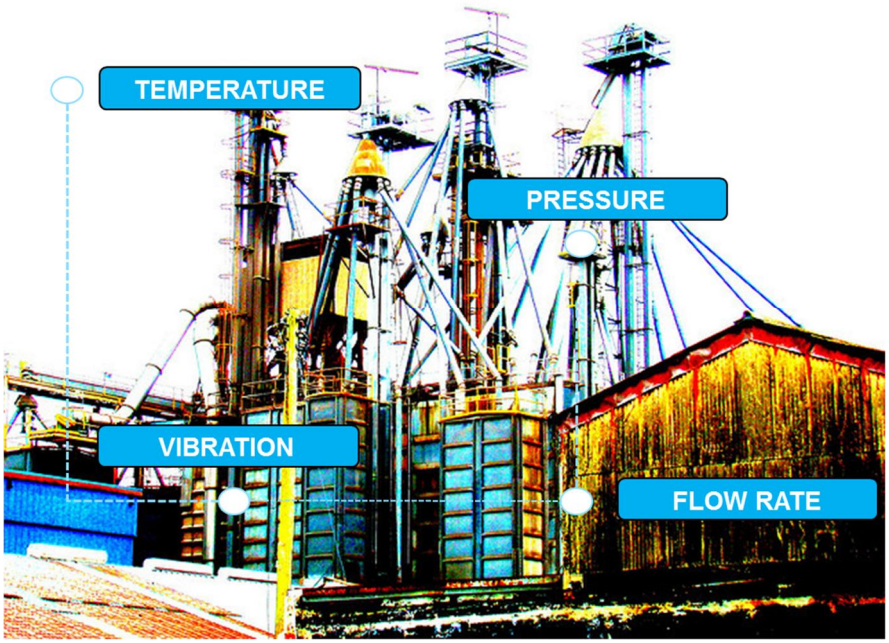

Figure 1. Wireless sensor technologies for better awareness and control of industrial automation systems

An industrial wireless sensor network consists of a number of sensor nodes, wirelessly connected and spatially distributed across a large field of interest. The task of sensor nodes is to measure different parameters from the industrial equipment

(e.g. vibration, temperature, pressure) or the surrounding environment (e.g. temperature, relative humidity, CO2), and send this data for analysis via the sink node. Real-time process control and maintenance systems equipped with wireless sensor networks can be integrated with back-end enterprise software as well as internet web services; see Figure 2. Data can be entered or acquired and the alerts/alarms can be notified through smartphones or tablets to the engineers at offices or remote locations; thus any drop in production efficiency can be prevented.

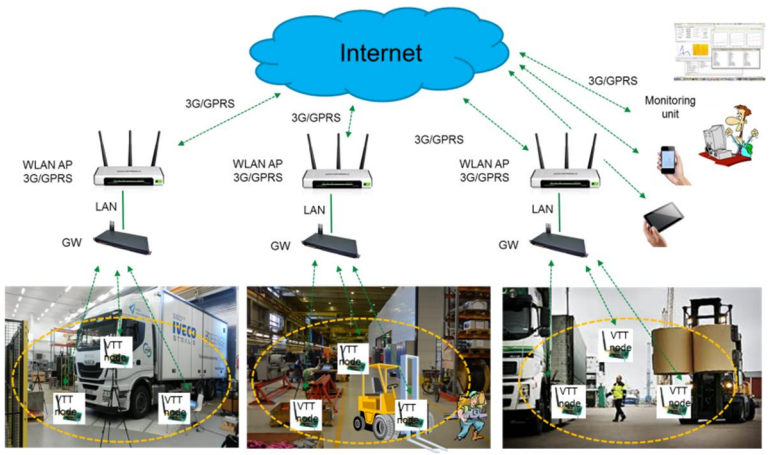

Figure 2. Different real-time industrial process control and maintenance systems equipped with wireless sensors networks integrated with the back-end enterprise

1.1 Background and motivation

IWSN technologies will contribute to solving the challenge whereby information and communication systems are invisibly embedded in the environment [6], [7], and [8]. The use of WSNs in industrial applications brings significant advantages and opens up new opportunities for real-time data acquisition and control. Wireless technologies have a large number of new opportunities and important application areas in industry, from wireless process automation to the monitoring and control of machines and devices. Simple deployment, significant cost savings in installations, lack of cabling, high mobility, and easy rearrangements related to device configuration and sensor locations make wireless sensor network technologies appealing for industrial applications [1], [2], [3], [4]. Some potentially interesting classes of industrial commercial applications are monitoring product quality, robot control and guidance in automatic manufacturing environments, factory process control and automation, monitoring disaster areas, machine diagnostics, transportation, factory instrumentation, vehicle tracking and detection, rotating machinery, and wind tunnels [5].

Within the industrial market, six different classes of sensor and control applications have been defined varying from critical safety (class 0) to condition monitoring and regulatory compliance (classes 4 and 5) [33]. The main differences between the classes are latency, timing and reliability requirements. In the closed-loop control applications involving mobile subsystems, coordination among mobile robots or autonomous vehicles, health monitoring of machines and tracking of parts, wireless data communications must satisfy tight real-time and reliability requirements at the same time, otherwise loss of time and money or even physical damage can occur as a result [2]. While in monitoring applications the requirements for real-time transmission are generally loose, reliability is important, especially for critical alarm messages.

As already mentioned, low latency and reliable communication are the key requirements for a wireless sensor network for industrial automation and process monitoring applications. However, the adaptation of resource-constrained wireless sensor nodes (limited energy and computational power) in industry poses extra challenges since the factory environments are typically harsh for wireless communications. Concerns arise due to variable link capacity, security, large-scale deployment, integration with other networks, and the harsh factory environment conditions; unpredictable variations in temperature, pressure, and humidity as well as strong vibrations, atmospheric precipitation, condensation, multipath propagation, interferences from ISM, and noise generated by equipment or heavy machinery; see Figure 3. In wireless access systems with terminals equipped with significant power resources, radio and baseband processing chains, different countermeasures against fading can be realised. In WSNs with often simpler and low-power sensor nodes, the situation is usually more complicated, and careful design of the overall system given the realisation constraints is needed. Due to restricted computing power, signal measurements and further analysis established in sensor nodes cannot be computationally demanding.

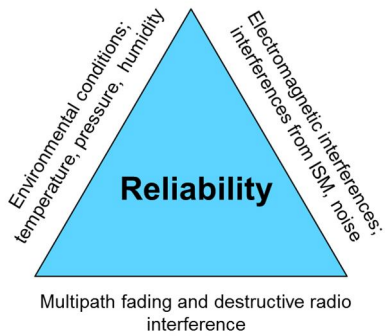

Figure 3. Common environmental concerns affecting the reliability of wireless transmission in industrial milieus

The reliability of data transmission in wireless sensor networks (WSN) is always an issue in harsh industrial environments and sets specific challenges for performance optimisation. Wireless transmission in an industrial environment filled with metal and concrete objects, water-filled human beings running around, trucks, etc. leading to signal strength variations by as much as 50 dB from that expected in free space [108], and so on, provides many challenges for maintaining the quality of transmission. Short-term signal disturbances in the form of multipath fading and destructive radio interference are of major concern due to signal path conditions (large concrete and metal surfaces), related line-of-sight (LOS) changes (incoming and outgoing trucks, forklifts and workers moving around), and radio frequency interferences. The resulting signal at the receiver is attenuated, delayed and dispersed in time in a complicated fashion. The effects can be dramatic and can significantly affect the ability of a radio link to function. There are three responses to this sort of complexity: 1) to attempt to understand each interaction in some detail, so that effects on the transmitted wave can be mitigated through careful network design; 2) to treat propagation on a statistical basis, and build radio systems so that reception is robust to variations in signal strength and delay, applying radio channel models; 3) to actively analyse radio channel state and overcome transmission problems in an efficient way. This third approach is used when the first two fail. Communication range and deployment cost must also be taken into account, since in a factory environment the communication path is obstructed, the reliable communication range of a network is reduced, and mesh networking solutions are applied to cover a larger area. This introduces more complexity and cost.

Interference from ISM disturbing channels is another important issue to be concerned about while installing WSNs in an industrial environment. The 2.4 GHz ISM band allows for primary and secondary uses. Secondary uses are unlicensed but must follow rules defined in the Federal Communications Commission Title 47 of the Code for Federal Regulations Part 15 [92] relating to total radiated power and the use of the spread spectrum modulation schemes. While the spread spectrum and power rules are fairly effective in dealing with multiple users in the band, provided the radios are physically separated, the same is not true for close proximity radios. Multiple users, including self-interference of multiple users of the same application, have the effect of raising the noise floor in the band, resulting in a degradation of performance. The impact of interference may be even more severe, when radios of different applications use the same band while located in close proximity. Thus, the interference problem is characterised by a time and frequency overlap [93].

Wireless local area networks (WLANs) based on the IEEE 802.11 specification, cordless telephones and Bluetooth devices have fully reached industrial environments, and when introducing WSNs to a plant, one must accept that the environment is under the influence of nearby interference sources. For example in case of WirelessHART, standard for industrial wireless communications, performance evaluation results for factory environments have shown that interference from a WLAN will cause increased packet loss rates; the probability for a collision be-

tween a WLAN beacon and a WirelessHART frame for 20 ms and 100 ms beacon intervals have been found to be 20% and 4%, respectively [34]. Exposing a WirelessHART network to attacks from a 2.4 GHz linear chirp jamming device has caused the WirelessHART network to break down completely, with no data reception on the gateway and a resulting reliability rate of 0% [13]. Zigbee does not have frequency diversity like WirelessHART, and thus is even more exposed to radio channel interferences [34]. The standards for industrial wireless communication will be described in more details in the next section.

1.2 Contribution of this thesis

The fundamental contribution of this dissertation is that it is a novel methodical approach to *improving the quality of wireless communication in IWSNs by identifying and classifying radio channel disturbances*. Availability has been depicted as one of most important research issues that need to be solved such that IWSNs can meet the expected market requirements; even short and transient communication errors can cause significant production outages [8,21]. Availability is a guarantee of reliable access and our methods aim to decrease the chance of network failure.

We have performed extensive measurements campaigns in real industrial environments to study the nature of the radio channel disturbances, to investigate the metrics that can be used to detect these radio channel disturbances, and to develop novel methods to identify these radio channel disturbances. The identification and classification of radio channel disturbances relies on the analysis of the signal propagation characteristics on the physical layer. Once the radio channel disturbances are identified and classified, this information is passed to the higher layers. Depending on the interference type (fading or radio interference), we must apply specific adaptation algorithms, like power control (PHY layer) or route diversity (Network layer) to overcome the transmission problems. The contribution of the thesis is visualised in Figure 4. Once the transmission problems have been detected, the received signal is analysed and the transmission problem is classified.

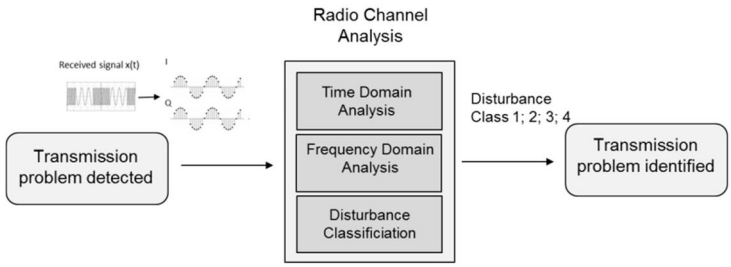

Figure 4. The main contribution of this thesis: radio channel analysis methods to identify radio channel disturbances

An increasing number of research papers have reported on radio interference cognition, spectrum sensing, monitoring and management. In our work, we aimed to expand the environmental awareness to also include *physical environment cognition* (obstacles, trucks). We used a software-defined radio (SDR) as the receiver to capture the transmitted signal and analyse the statistical properties of the captured signal with MATLAB/Simulink tools. Our studies led us to develop radio channel analysis methods which aim to detect and identify the temporal disturbances affecting the signal propagation: 1) *The probability density function (PDF) channel state analysis* method is based on the idea that changes in the statistical properties of the received signal are strongly correlated to the transitions of the channel states. It has been shown that temporal fading in the industrial environment exhibits Rician fading properties. Thus, by comparing these changes to the simulated theoretical Rician distributions and deriving the PDF's shape parameters, we can numerically characterise the effects of disturbances on the channel state. 2) *The spectrum analysis method* is based on calculating the spectrograms of the received signal and obtaining the statistical information of the radio interferences with image analysis tools. By combining the results of signal analysis methods in time and frequency domains, we constructed a 3) *classifier* to categorise the radio channel disturbances.

The channel analysis methods were designed and tested for the sensor nodes based on IEEE 802.15.4 networks. In our work, we aimed to avoid computing power consuming calculations, since the energy consumption of the low-powered sensor nodes must be considered: maximising the reliability may substantially increase network energy consumption. We tested the classifier functionality in a real industrial environment. The classifier proved to be a feasible solution for improving the reliability of wireless transmission and has the potential to be developed into a portable, small-sized SDR-based tool. The radio channel analysis SDR-based tool is a part of the *Auto-Fault-Diagnostic System*, a concept that will also be presented in this work.

1.3 Outline of the dissertation

The dissertation is organised as follows. In Chapter II the literature review and related background research work are described. In Chapter III an overview of the physical aspects and interferences of radio signal propagation is given. In Chapter IV the contribution of this work, the algorithmic solutions for radio channel disturbance identification and classification, is presented. In Chapter V the test results on methods evaluation in real environments are given. Finally, the work is concluded and results discussed in Chapters VI and VII.

2. Reliable industrial wireless sensor networks

In this chapter we provide a literature review of the ongoing research work related to industrial wireless sensor networks, and especially to the reliability issues. We introduce standardisation activities and compare several industrial organisations in term of applicability to the harsh industrial environments.

2.1 Standardisation activities

Several industrial organisations, such as ISA, HART, ZigBee and WISA have been actively pushing the applications of wireless technologies in industrial automation. In [18] Zheng describes the current situation of IWSN and standardisation activities. The international standardisation organisation IEC (International Electrotechnical Commission) TC65 technical committee started up the SC65C/WG16 working group for the standardisation of industrial wireless technology in 2008. The WirelessHART was approved as the first international standardisation for industrial wireless communications, IEC 62591 Ed. 1.0 in March 2010. In May 2009, the ISA100 standards committee voted to approve ISA100.11a, and in September 2009, the ISA officially released the ISA100.11a standard. It is interesting that members who drafted the WirelessHART and the ISA100.11a standardisation were almost the same, and both standards adopted the same technologies from DUST (a venture company in California), which is why the technical features are rather similar.

The brief overview of existing wireless sensor network solutions for industrial applications is given in [14]. Particularly for those wireless sensor networks which operate in the 2.4 GHz band of the ISM frequencies, it is necessary to have a strategy against radio channel interferences. ZigBee, WirelessHart and ISA100 standards are based on the same physical level of IEEE 802.15.4, but their medium access control (MAC) level is substantially different. WirelessHart and ISA100 are mesh solutions which adopt frequency agility and power adaptation methods to improve data transmission reliability. WirelessHART also applies channel hopping [29] and channel blacklisting in the MAC layer, while ZigBee uses only Direct Sequence Spread Spectrum (DSSS), as defined in IEEE 802.15.4. ZigBee shares the same channel without frequency diversity, and thus has no ability to fight against radio channel disturbances, disturbances caused by other radio transmis-

sions, or disturbances due to signal fading, particularly in harsh environments. In [12] it was shown that ZigBee cannot be reliably applied for industrial applications because of the stringent requirements of industrial control regarding deterministic delay and high dependability. In [12], WirelessHART is compared with ZigBee in terms of issues such as robustness, coexistence and security, proving that WirelessHART is more suitable than ZigBee in many aspects of industrial applications. The standards were compared in [12] on behalf of ABB, which has significant practical and theoretical knowledge of industrial applications and their standardisation. ISA100 Wireless is the only industrial wireless network protocol that satisfies the ETSI EN 300.328 v1.8.1 regulation coming into effect on 1 January 2015. ISA100 Wireless applies CSMA/CA (LBT – Listen Before Talk) CCA (Clear Channel Assessment) solutions to detect coexistence with other wireless transmissions on the same 2.4 GHz frequency channel, and spectrum monitoring to avoid congested channels by reconfiguring the data transmission to specific channels [14]. Wireless Interface for Sensors and Actuators (WISA) is based on the IEEE 802.15.1 physical layer and it was developed by ABB. The WISA standard was specially developed to satisfy the needs of factory automation. Because of the deterministic time behaviour of WISA, it is real-time capable and able to reduce the interference caused by other wireless networks by applying the frequency hopping method. Other industrial wireless sensor network solutions based on standards such as IEEE 802.11, Bluetooth, UWB and Internet Protocol version 6 (IPv6) over low-power wireless personal area networks (6LoWPAN) are not yet widely used for industrial applications. At the time of writing this report the most significant opponent standards for industrial automation are WirelessHART and ISA100.11a.

In [13] the theoretical comparison of WirelessHART and ISA100.11a, both from a technical and a systematically point of view, is provided. The main differences between the WirelessHART and ISA100.11a standards are in their operational flexibility (ISA100.11a is more flexible), protocol support (WirelessHART is restricted to use HART, while ISA100.11a can use any devices applying the tunnelling protocol, where the protocols of various devices are encapsulated and transported through the network), and methods to overcome the interference caused by the IEEE 802.11-Based Networks (ISA100.11a applies adaptive channel blacklisting which improves its robustness. In [9] the performance of WirelessHART in a factory environment has been investigated, and it showed that coexisting with IEEE 802.11-based WLAN networks, interference from the WLAN will cause increased packet loss rates in the WirelessHART network. The actual increase in WirelessHART packet loss depends on many factors, including the WLAN channel configuration, the distance between the WirelessHART devices and the APs, and, most importantly, the amount of WLAN traffic [9, 10]. Similar experiments are not yet available for ISA100.11a [11]. As the first generations of ISA100.11a products are just being shipped, the current market situation is naturally in favour of WirelessHART. Emerson is the current leading supplier of WirelessHART instruments. Other companies supplying WirelessHART are Siemens, ABB, Endress-Hauser, and Pepperl-Fuchs, while the main supporters of ISA100.11a are Honeywell and

Yokogawa [13]. Both WirelessHART and ISA100.11a mainly target application with quite relaxed requirements on latency and reliability, while for more time- and reliability-critical applications, some improvements in current standards need to be made.

The need to interconnect IEEE802.15.4-based low power networks to the Internet has triggered the birth of various working groups (WGs) within the Internet Engineering Task Force (IETF), including 6LoWPAN [109], ROLL (the group behind the RPL routing protocol [110]), and CORE (behind the CoAP web transfer protocol [111]) that have defined how to fit an IPv6 protocol stack on top of IEEE802.15.4. Given the appealing features of the IEEE802.15.4e for enabling ultra-low power and reliable low power and lossy networks (LLNs), the 6TiSCH WG aims at building IPv6-enabled LLNs, rooted in the IEEE802.15.4e TSCH MAC layer. The basic concept of TSCH (i.e. the combination of time synchronization and channel hopping) is not new. It was introduced by Dust Networks in 2006 in its proprietary Time Synchronized Mesh Protocol (TSMP) [112]. The core ideas of TSMP then made it into standards such as WirelessHART (2007) and ISA100.11a (2009). IEEE802.15.4e TSCH inherits directly from these industrial standards, which are already deployed as commercial products. TSCH is thus a proven technology. One important difference with existing industrial standards is that IEEE802.15.4e TSCH focuses exclusively on the MAC layer [113].

2.2 Wireless communication reliability

2.2.1 Design challenges

A significant body of research work related to emerging topics in general for wireless industrial communications exists. In [17] the most relevant research areas in wireless industrial networks are discussed. Here, Willing provides an introduction to important concepts of sensor networking and discusses a number of protocol design issues that are relevant to industrial applications, such as providing the required QoS in terms of reliability and real-time applications, tools and methodologies for network planning and configuration, run-time fault and performance monitoring, MAC protocol design issues, error-control schemes, routing, and transport protocols, etc. He also introduces techniques to mitigate channel fading and external interference that according to him are currently hot research topics in industrial wireless communication.

The design requirements for condition monitoring using commercial IWSNs systems are presented in [19]. These specific requirements of IWSNs are ability to process heterogeneous sensor signals, higher sampling rate, fast transmission rate, energy efficiency, higher data transmission reliability, and accurate time synchronisation. Gungor and Hancke discuss in [3] technical challenges and design principles in terms of hardware development, system architectures and protocols, and software development. Specifically, radio technologies, energy-harvesting techniques and cross-layer design for IWSNs are described. The au-

thors highlight that the efficient deployment of IWSNs in the real world is highly dependent on the ability to devise analytical models to evaluate and predict IWSNs performance characteristics, such as communication latency, reliability and energy efficiency. Other challenges are optimal sensor node deployment, localisation, security and interoperability between different IWSN manufacturers. To cope with RF interference and dynamic/varying wireless channel conditions in industrial environments, Gungor and Hancke propose porting a cognitive radio paradigm to a low-power industrial sensor node and developing controlling mechanisms for channel handoff.

Also, the following IWSN development issues can be found in the literature: coping with transient interferences: guaranteeing deterministic and timely data delivery in case of temporary link failures [22], real-time and reliable communication in heterogeneous networks [23], optimum design of resource-constrained sensor nodes [24, 25], energy efficiency exchanges [26] , deterministic node lifetime [26], scalability [26], capability for localisation, synchronisation and energy management (27), and safety and security [28]. In [20] the authors present the requirements for typical applications in process automations and outline the research direction for IWSNs; the major issues are safety, security and availability. In [21] the authors observed that one of most important research issues that needs to be resolved so that industrial wireless sensor networks (IWSNs) can meet the expected market requirements is availability; even short and transient communication errors can cause significant production outages.

Improving the reliability of wireless communication is crucial for WSN success in the industrial environment. A growing set of research results have been reported on such topics as reliable routing techniques [16], [53], [54] reliable transport protocols [55] for WSNs, scheduling, etc. [56], which aim to overcome the data transmission problems on MAC, network and higher layers. Less attention was paid to studying how to provide feedback on channel disturbances from the physical level and apply it to upper levels. Wireless industrial automation has strict requirements for quality of service (QoS), safety and security. The key aspect of QoS for industrial wireless sensor networks (IWSN) communication is to ensure the transmission of periodic or sporadic messages within predefined deadlines and in a reliable fashion [2]. The WINA technical committee has undertaken the development of a QoS design and assessment framework for IWSN [31]. The measures of performances that define QoS are throughput, latency, reliability, security, adaptability and affordability. Within the industrial environment, adaptability is one true advantage of wireless over wired networks, meaning the ability to adapt to changes in the environment while maintaining the required levels of QoS attributes [32].

2.2.2 Existing solutions for reliability improvement

The quality of signal transmission in WSNs varies in space and time and this can have severe consequences on system reliability. Amplitude histograms have previously been proposed for monitoring the performance of optical channels [105]

and for automation of modulation classification [106]. In our work we use a similar approach for the identification of radio channel interferences. The detailed characteristics of signal transmissions can only be determined practically by signal measurements, the results of which can later be utilised to overcome transmission problems in channelisation, protocol design, network management, and even in developing applications like Networked Control Systems (NCS).

In channelisation, to overcome the problem of spectrum scarcity in a WSN, a new concept of cognitive wireless sensor network (CWSN) has been proposed. The main difference between traditional WSN and CWSN is that in CWSN, nodes change their transmission and reception parameters according to the radio environment [35]. Spectrum sensing is a commonly used technique in cellular cognitive radio, helping to avoid the most crowded frequency channels, and it considerably improves radio channel reliability. In protocol design, the measurement data can be utilised in the form of error patterns as input for MAC protocol design, and also finding parameters for stochastic error models for performance analysis. In [36] the effects of wave propagation characteristics and the presence of noise or interference on transmission error behaviour have been studied. Quantitative results of mean bit error rates (MBERs) with related time-varying behaviour, presence, burstiness behaviour, and order of magnitude of packet losses and high variability of error burst lengths are useful for characterising similar environments, and are important for designing MAC protocols [36]. In network management, transmission-related measurements give updated indications on the network health and performance, like the state of network links and nodes [37]. A wider picture of the network state can be composed further: in [38] it has been shown how network tomography can be efficiently adapted to infer link loss performance, based on which a contour map technology can be used for the identification of lossy areas in large-scale WSNs.

There are applications that depend heavily on transmission quality and require spatial distribution and precise time performance. Networked control systems (NCS), or wireless NCS (W-NCS) employ event-triggered controllers and actuators to operate in response to time-triggered sensor nodes. Such NCSs require dedicated real-time networks, as total end-to-end latency of the system must be bounded to ensure proper operation [39]. The characteristics of the network can be considered during the design of such a control system. As transmission failures caused by bursty and recurrent wireless channel errors directly increase the latency of a W-NCS's packets, improving the quality of the wireless channel is the first challenge of design. Neighbours of a node can be utilised as a set of distributed antennas so that multiple nodes each with a single antenna function as a single multi-antenna system. Broadcasting is used to disseminate the data to the possible neighbours, called "co-operators", and via the cooperative transmissions the receiver is provided with multiple copies of the original signal coming from geographically separated transmitters. Using a cooperative MAC (COMAC) protocol, the cooperation of neighbouring nodes results in higher packet success rates under adverse wireless channel conditions when compared to regular IEEE 802.11 WLANs [39]. In [40] a practical wireless NCS is introduced. This shows

how to consider the characteristics of the network in the design of a control system based on a disturbance observer, which is used to compensate for the effect of transmission delays in measurement data.

3. Radio signal transmission in wireless sensor networks

In this chapter we describe the signal transmission issues common to all radio channels, such as absorption, reflection, refraction, diffraction, and scattering effects, and issues that are topical, especially for the radio channels in industrial environments. We will also present the research challenges related to signal transmission quality.

Signal propagation is defined as the travel of waves through or along a medium. There are many factors that affect the propagation of radio waves, such as reflection, diffraction and scattering. These phenomena give additional radio propagation paths between the radio transmitter and receiver, see Fig. 5.

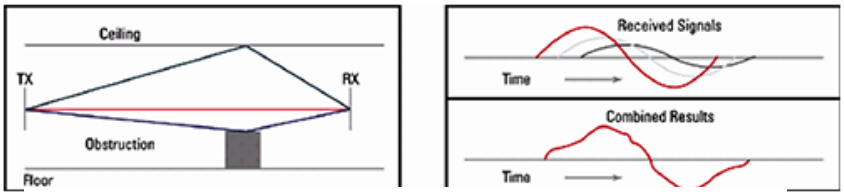

Figure 5. Signal multipath reception

The resulting potential at the antenna is the sum of all paths with their unique phase, amplitude and polarisation. An electric current element ***J*** at some location induces a potential ***A*** at other remote locations. The magnitude of the induced potential falls inversely at the distance and shifts in phase relative to the phase of current.

$$\boldsymbol{A} = \mu_0 \cdot \boldsymbol{J} \cdot \frac{e^{-jkr}}{4\pi r} \cdot e^{jwt} \tag{1}$$

Where

r = distance
k = $w\sqrt{\mu\varepsilon} = \frac{w}{c}$

$w = 2\pi f$
$\mu_0 = 4\pi \times 10^{-7}$ Henry/metre
$\varepsilon_0 = 8.86 \times 10^{-12}$Farad/metre.

The vector potential is a vector field, an entity that associates a unique direction and amplitude with every point in a three-dimensional space. However, the primary interest of the potential values lies at comparably long distances from the transmission antenna and other obstacles, and thus there is no need to characterise ***A*** at every point: the whole potential can be represented with a ray with a given direction, phase and wave number. Rays are a valid approximation of the vector field, as long as the phase and direction of neighbouring rays does not change much over a distance. In that case, the propagation problem can be divided into distinct rays following identifiable paths and add the resulting phase and intensity at the end to estimate the received signal (=geometric optics approximation). Accurate estimation of the relative phase of different paths requires knowledge of path length with high accuracy, as well as detailed understanding of obstacles to similar precision. Such accuracy is unlikely to be achieved in a real life environment, but practical analysis of a propagation environment can set bounds on possible amplitude values and increase the understanding of a complex propagation environment.

3.1 Radio signal transmission: How does it work?

3.1.1 Path loss

Signal path loss is a power attenuation of an electromagnetic wave as it propagates through the environment between antennas. Path loss includes all of the propagation losses associated with distance and the interaction of the propagating signal with the objects between the transmitter and receiver, for example free-space losses, absorption losses and diffraction losses. Free-space path losses occur as the signal travels over a line-of-sight path in free space. Absorption losses occur if the signal passes into a medium which is not totally transparent to the electromagnetic waves. Diffraction losses occur when radio waves encounter a large object on their path and diffract around the object. The other reasons for signal path loss are terrain, vegetation and atmosphere.

Free-space path loss depends only on distance and wavelength; it is proportional to the square of the distance between the transmitter and receiver and to the square of the frequency of the radio signal. The equation for free-space path loss or FSPL is:

$$FSPL = \left(\frac{4 \cdot \pi \cdot d}{\lambda}\right)^2 = \left(\frac{4 \cdot \pi \cdot d \cdot f}{c}\right)^2 \quad (2)$$

Where
d = distance of the receiver from the transmitter (metres)
λ = the signal wavelength (metres)
f = the signal frequency (Hertz)
c = the speed of light in a vacuum (metres per second).

The same formula expressed in logarithmic format:

$$FSPL(dB) = 20\log_{10}\frac{4\cdot\pi\cdot d\cdot f}{c} = 32.4 + 20\log_{10} d + 20\log_{10} f \qquad (3)$$

Where
d = distance of the receiver from the transmitter (km)
f = signal frequency (MHz)
c = speed of light in a vacuum (metres per second).

The free-space path loss equation can be used to predict the signal strengths that may be expected, but only in ideal scenarios without any interactions such as reflections or refractions. For this reason it is not applicable in real life scenarios.

3.1.2 Multipath propagation

Radio waves travel to the receiver antenna along several different paths. Reflection, diffraction and scattering are the phenomena that cause the additional propagation paths beyond the direct optical line-of-sight path between the transmitter and the receiver; see Fig. 6. Due to the different path delays, signal components are received at the receiver antenna at slightly different moments in time. The received signal is the sum of these incoming signal components and depending on their phase, the sum can be destructive or constructive. Because the relative phase of the various contributions can vary considerably with small changes in the positions of the transmitter, receiver and reflector, the total received amplitude becomes a sensitive function of position. This effect is known as fading.

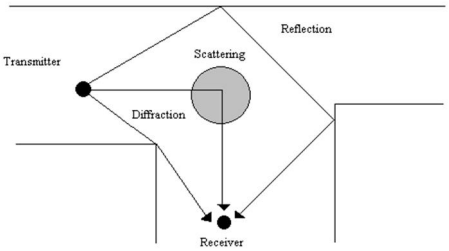

Figure 6. Multipath propagation

Reflection

Radio wave reflection occurs when it encounters a surface that is large in comparison to its wavelength. The reflection coefficient depends on the reflecting material, wave polarisation, the angle of incidence and the frequency of the propagating wave. The angle of incidence is equal to the angle of the reflection. Reflecting materials are divided into two groups: dielectric materials and conducting materials. For short range communications, metallic surfaces in particular are excellent reflectors of radio signal energy. In metals, the conductivity is so high that the change in amplitude of the transmitted signal takes place over a much shorter distance than a wavelength. This distance, known as skin depth δ, is typically a few microns for common metals at microwave frequencies. If the thickness of the metal is much greater that the skin depth, essentially no signal will be transmitted into the metal object. Because the amplitude change on the metal surface is so abrupt, on the scale of wavelength we can essentially assume that the potential instantly goes to zero at the metal surface.

$$A_i e^{i(wt-kx)} + A_r e^{i(wt+kx)} = 0, if\ A_r = -A_i \quad (4)$$

Where
A_i = incident potential
A_r = reflected potential
k = w√(με)=w/c
w=2πf.

Thus, a metal object reflects almost all the impinging energy, with a sign change in reflective wave. For those metal objects the size of which is in the order of some tens of wavelengths, the reflected beam is broadened and will interfere

with the incident beam to create a complex potential distribution in the reflected direction, and may lead to deep fading.

If the material is a dielectric, some of the signal energy is reflected and some of the energy travels through the material. The amount of incident radiation that is reflected and refracted is a function of the refractive indices of media, the angle of incidence, and the polarisation of the radiation. The realistic values of the reflected radiation on the incident wave values are in the order of 2:1; about a third of the impinging radiation is reflected at an interface for normal incidence leading to a loss of about 10% to 30% of the power due to reflection at a single interface. Reflection is on average more significant for **A** perpendicular to the plane of incidence, for example in case of a vertical antenna bouncing off the wall.

Diffraction and scattering

Signal diffraction occurs when the radio wave encounters sharp corners of a large obstacle or wavelength range gaps on its way from the transmitter to the receiver. As a result, radio waves diffract around the object.

Diffraction occurs when propagating waves graze the top of an object. A sharp surface will cause small losses of up to 6 dB, but a smooth, rounded object can cause losses of up to 30 dB. The concept of diffraction loss can be explained by Fresnel zones. Fresnel zones represent successive regions around the line-of-sight signal propagation path between the transmitter and the receiver. The Nth region is the region where the path length of the secondary waves is nλ/2 greater than the total path length of a line-of-sight path. In the first Fresnel zone, the propagating waves interfere with each other constructively, and in the successive Fresnel zones the interference is alternately constructive or destructive. If an obstruction does not block the first Fresnel zone, then the diffraction losses will be negligible. In order to minimise diffraction losses in line-of-sight microwave links, it is sufficient to keep 55% of the first Fresnel zone clear. The dimensions of the Fresnel zone can be defined by simple geometry; the radius of the Nth Fresnel zone circle can be calculated by Eq. 5, where d_1 and d_2 are the distances from obstacle to the link end points in metres. Note that the Fresnel zone radius depends on the wavelength.

$$r_n = \sqrt{\frac{n \cdot \lambda \cdot d_1 \cdot d_2}{d_1 + d_2}} \tag{5}$$

Where
r = the nth Fresnel Zone radius (metres)
λ = the signal wavelength (metres)
d_1 = distance from obstacle to one end point
d_2 = distance from obstacle to the other end point.

Obstacles of finite size relative to a wavelength do not create abrupt shadows, but rather scatter weakly outside the geometric shadow. The scattered potential is

similar in magnitude to the incident potential within much of the shadow and almost opposite in direction. The exact magnitude of scattered potential varies from point to point because of the changes in the relative phase of various parts of the obstacle, and these variations are magnified when the incident potential is added because the difference is small, so that narrow regions of deep shadowing occur within a background shadow with attenuations of typically 10-20 dB relative to the unobstructed power.

We must take into account that the Fresnel approximation reaches its limits at an observer distance of 1m from the plate; any closer than this and the shadow will be deep, so proximity to the obstacle and only reflections from other objects in a space will save our link budget.

Fading

Fading is the reduction of the signal level at the receiver input due to changes in external environmental factors and radio conditions. Deep fading (below the sensitivity of the receiver) leads to distortions or loss of signal. Fading can be divided into two categories, depending on its variation speed: large-scale fading and small-scale fading. There are two types of small-scale fading: fading caused by multipath time delay spread; and fading caused by Doppler spread.

Large-scale fading is the change in the average signal level over large distances due to changes in terrain, visual obstacles, or weather changes between the transmitter and receiver. The receiver is often represented as being shadowed by such obstacles. Large-scale fading is also known as log-normal fading.

Small-scale fading means the rapid changes to the signal level due to multipath propagation or movement of the receiver. *Delay spread* caused by multipath leads to temporal dispersion and frequency-selective fading, while *Doppler spread* caused by communications device movement leads to frequency dispersion and time-selective fading.

Delay spread is the difference between the time of arrival of the first and last signal component in a multipath channel. It can be calculated from the channel impulse response. The root mean square (RMS) delay spread is the metric that qualifies the multipath nature of the channel. Its range is μs in outdoor situations and ns in indoor situations. Coherence BW (bandwidth) characterises the channel response – frequency flat or frequency-selective fading. Let the baseband signal bandwidth be B_s, coherence bandwidth B_C, delay spread T_D and symbol period T_S, then

- flat fading: $B_S < B_C$ or $T_D < T_S$
- frequency-selective fading: $B_S > B_C$ or $T_D > T_S$

Delay spread causes intersymbol interference (ISI). When various components of the signal arriving at the receiver have a maximum time delay that is greater than one symbol duration, this delayed signal component will accumulate in the next signal components. The influence of this phenomenon is dependent on the

symbol duration. For high speeds (when the pulse duration is short), there is a lot of intersymbol interference, while at low speeds (when the pulse duration is sufficiently long), the ISI impact is very small. A channel can be considered stable when the RMS delay / T_s is less than 0.1, where T_s is the time of the symbol period.

Doppler spread is a measure of spectral broadening caused by the time-varying nature of a channel. Coherence time is the time domain dual of Doppler spread; it is the time duration over which the channel impulse response remains essentially invariant. If the Doppler spread is far smaller than the baseband signal bandwidth, or alternatively, if the coherence time of the channel is greater than the symbol period, then the effects of Doppler spread are negligible and the channel is considered as a slow fading channel. Let the baseband signal bandwidth be B_s, Doppler spread B_D, symbol period T_S and coherence time T_C, then

- Slow fading channel: $T_s << T_C$ or $B_S >> B_D$
- Fast fading channel: $T_S > T_C$or $B_S < B_D$

3.1.3 Noise

Electrical noise is any unwanted energy that tends to distort the reception and reproduction of the transmitted signal. Sources of noise can be external, for example industrial or atmospheric noise, or internal. Internal noise is generated by any devices found in the receiver.

Signal-to-noise ratio (SNR) is a ratio of the signal power P_S to the noise power P_N, see Eq.6. It compares the level of a transmitted signal to the level of the undesired noise. The SNR parameter is the key parameter of any receiver. The greater the difference between the signal and the unwanted noise, the better receiver sensitivity performance is.

$$SNR = \frac{P_S}{P_N} \tag{6}$$

Where
P_s = power of the signal
P_N = power of the background noise.

3.1.4 Interference

The two main types of system-generated interference are *co-channel interference* and *adjacent channel interference*. Co-channel interference is a crosstalk caused by two or more simultaneous transmissions that use the same frequency channel. The co-channel interference cannot be reduced simply by increasing the transmitting power, because it would increase the interference with neighbouring co-channel cells. To decrease the co-channel interference, the co-channel cells must be physically separated to a proper distance. Adjacent channel interference is

caused by transmitters that use the adjacent frequency channel. The reason for this kind of interference is the imperfect receiver filter, which allows nearby frequencies to leak into the pass band. There are two ways to reduce the adjacent channel interference: careful filtering and channel assignment. The larger the frequency separation between channels, the less adjacent channel interference occurs.

3.1.5 Transmission losses

Link budget defines the maximum allowable path loss in the communication system. It is a balance of all the gains and losses on a transmission path. For a line-of-sight system, a link budget equation can be written as:

$$P_{RX} = P_{TX} + G_{TX} - L_{TX} - L_{FS} - L_M + G_{RX} - L_{RX} \quad (7)$$

Where
P_{RX} = received power (dBm)
P_{TX} = transmitter output power (dBm)
G_{TX} = transmitter antenna gain (dBi)
L_{TX} = transmitter losses (coax, connectors...) (dB)
L_{FS} = free space loss or path loss (dB);
L_M = miscellaneous losses (fading margin, body loss, polarisation mismatch…) (dB);
G_{RX} = receiver antenna gain (dBi); and
L_{RX} = receiver losses (coax, connectors,...) (dB).

The overall transmission loss is presented in Fig. 7. The target for MAC layer transmission is to forward data packets (or frames) from the transmitting node to the receiving node. This takes place via several conversion and transmission operations as follows.

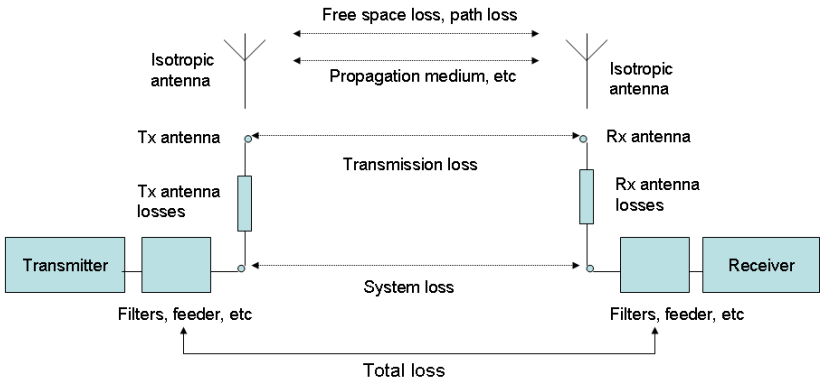

Figure 7. Transmission losses

1. Encode the MAC frame to a binary (bit)stream and access the RF channel
2. Convert and filter the bit-stream to a modulated analogue waveform and transmit the analogue waveform to the antenna
3. Propagate the analogue waveform in the air to the receiver's antenna
4. Receive, filter and demodulate the analogue waveform to a digital bit-stream
5. Decode the bit-stream to a MAC frame

Each phase from 1 to 5 may degrade the transmitted signal due to errors in SW or HW implementation or disturbances from the environment [94].

3.2 Radio signal transmission in industrial environments

The investigation of radio channel disturbances in the industrial environment showed that the most disruptive disturbances are caused by other wireless devices (co-channel and adjacent interference), environmental characteristics such as metal constructions, and the presence of heavy equipment (signal fading) and electrical and mechanical equipment (noise).

In [43] and [44], the sources of disturbances in wireless communication in three different factory environments are studied. The studies show that electrical and mechanical equipment such as electrical engines, power converters, charging devices for battery-driven equipment and frequency converters produce low frequency, high-impulsive and wideband disturbances. For example, mopeds and 4-wheeled motorcycles generate disturbances of up to 1 GHz [44].

In addition, the environmental issues related to variations in pressure, temperature and humidity create challenges to the use of WSNs in industry. In [45] the authors have presented WSN design requirements and solutions to improve wireless transmission in harsh environments with extreme temperature, pressure and humidity. Based on the real environment experiments performed, the authors offer a list of practical suggestions to consider related to the choice of electronic and passive components, printed circuit boards, and insulation of the enclosure of the electronic board.

The disturbances caused by metal constructions and heavy equipment (trucks etc.) as well as interference from other radio transmissions are difficult to predict, and challenging to eliminate by careful design since the industrial environment is dynamic and interferences are occasional with coming and going trucks, workers etc. For this reason, we decided to focus our work on investigating these disturbances in more details.

3.2.1 Signal fading

Large metal constructions and heavy machinery in the industrial environment cause multiple reflections of the transmitted signal, and lead to signal fading. The resultant received waveform is a sum of time- and frequency-shifted versions of the original transmitted signal, and depending on transmission conditions, the received signal may be greatly distorted [60]. Multipath has historically been identified as the most important factor limiting wireless radio communication systems [46], [47], [48]. For narrowband transmissions, multipath causes large fluctuations (fading) in the received signal levels due to the sum of signal components arriving at the receiver antenna at the different phases via different paths. Temporal variations in the radio channel states and changing environmental geometry lead to signal fading. Additional signal loss will occur when the wireless sensor node is shadowed by inventory or machinery. In wideband systems, signal scattering creates intersymbol interference and causes frequency-selective fading. In an extensive study, [46], it was shown that in the case of stationary transmitters and receivers, the continuous motion of people and machinery in factory environments causes Rician fading for narrowband communication systems. Similarly, measurements were repeated and analysed in [49] leading to the same conclusion; in factory environments for the light clutter situation, the probability functions and the distribution of path gain can be modelled using Rician distribution.

Statistical modelling of fading

The approach typically used in this area is to attempt to fit measured data to an analytic probability distribution, thereby extracting a handful of parameters that characterise the likelihood of a given signal amplitude. A large number of analytical formulae are used by different researchers in the field, with no simple consensus on which to apply in what circumstances.

We considered three different models before settling on one. The first model was the Rayleigh fading model, which describes small-scale rapid amplitude fluctuation in the absence of a strong received component. The Rayleigh distribution is widely used to describe multipath fading because of its elegant theoretical explanation and the occasional empirical justification. However, in deriving this distribution, a critical assumption made is that all signals reaching the receivers have equal strength. The studies show that a dominant line-of-sight (LOS) component exists that is not accounted for by this distribution [57], [58], [59]. Hence, we did not use this distribution. The second model we considered was the Rician distribution model. The Rician distribution occurs when a strong path exists in addition to the low level scattered path. This strong component may be the LOS path or a path that encounters much less attenuation than others. The Rayleigh distribution is a special case of the Rician distribution; when the strong path is eliminated, the amplitude distribution becomes Rayleigh. In literature, these two probability models are commonly used to characterise the propagation channels with fast and/or temporal fading [17]. The probability density of the received signal amplitude in a case of Rayleigh distributed fading is defined by Eq. 8.

$$f_\rho(\rho \mid a,\sigma) = \frac{\rho}{\sigma^2}\exp\left(-\frac{\rho^2}{2\sigma^2}\right) \tag{8}$$

Where

ρ = magnitude value measured at the receiver

a = signal amplitude due to the LOS path in the absence of all other multipath components

σ = standard deviation of the real part of the time-harmonic multipath component.

The Rician probability model corresponds to situations where one strongly dominant path exists. In this case the probability density of the magnitude is given by Eq. 9.

$$f_\rho(\rho \mid a,\sigma) = \frac{\rho}{\sigma^2}\exp\left(-\frac{\rho^2+a^2}{2\sigma^2}\right) I_u\left(\frac{a\rho}{\sigma^2}\right) \tag{9}$$

Where

I_u = modified zeroth-order Bessel function of the first kind

ρ = magnitude value measured at the receiver

a = signal amplitude due to the LOS path in the absence of all other multipath components

σ = standard deviation of the real part of the time-harmonic multipath component.

Furthermore, ρ is given by Eq. 10.

$$\rho(t) = \sqrt{I^2(t) + Q^2(t)} \tag{10}$$

Where

I = in-phase component of the received signal

Q = quadrature component of the received signal.

The Rician distribution is often described in terms of the Rician factor K, defined as the ratio between the deterministic signal power (from the direct path) and the diffuse signal power (from the indirect paths). K is usually expressed in decibels as

$$K(dB) = 10 \log_{10}\left(\frac{a^2}{2\sigma^2}\right) \tag{11}$$

In Eq. 11, if *a* goes to zero, the direct path is eliminated and the amplitude distribution becomes Rayleigh, with K (dB) = -∞. If the Rician K-factor becomes large (K >>1), it is possible to approximate the Rician distribution with Gaussian PDF. In our work we did not use K-factor to characterise the Rician distribution since it only reflects a ratio between the a and sigma values. In our analysis we use the valuable information brought by both a and sigma values.

The Rician distribution is fully described by two shape parameters: '*a'* and 'sigma'. The '*a'* value reflects the amount of the specular power of the received signal, while the sigma value is related to the amount of the received signal's scattered power. Figure 8 presents several different kinds of Rician PDFs simulated in MATLAB with various '*a'* and 'sigma' values. In Fig. 8, in the upper plot the sigma value is constant and a value is changed; the greater an *'a'* value is, the more specular power it reflects and the more PDF resembles Gaussian PDF. In the second plot the *'a'* value is constant and the sigma value is changed: here it shows how different sigma values reflect the scattering power of the received signal. The y-axis indicates the probability density value, and the x-axis the sample value.

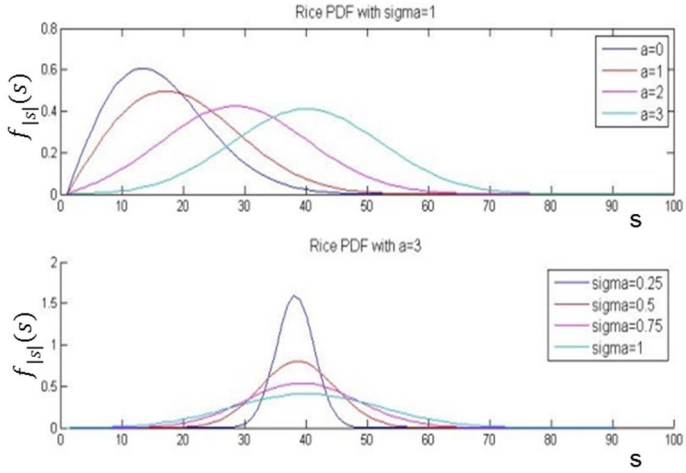

Figure 8. Simulated Rician PDFs

The Rician channel does not require a line-of-sight in the sense that the receiver needs to be visible from the transmitter. The Rician model is also applicable in scenarios where one strong dominant path exists: sometimes this dominant path may be subject to a specular reflection, for example.

The third model we considered is a Nakagami model. The Rician and Nakagami models behave approximately equivalently near their mean value. This observation has been used in many recent papers to advocate the Nakagami model as an approximation for situations where a Rician model would be more appropriate. In the analysis of outage probabilities or bit error rates, it is the behaviour of the model for signals in deep fades that has the determining effect. As the behaviour of the probability density functions for amplitudes near zero differ significantly, approximations based on behaviour near the mean are inappropriate. Modelling a Rician fading signal using a Nakagami distribution of the amplitude leads to overly optimistic results, and discrepancies can be many orders of magnitude [90]. The Nakagami model does not provide a clear intuitive picture of the fading mechanism (in contrast to the Rician model with its superposition of specular and scattered received signal components). The goodness of fit tests used by ionospheric physicists to match measured scintillation data to a Nakagami-m distribution do not usually give special weighting to the deep-fading tail of the distribution. As a result, we sometimes have a better fit near the median of the distribution than in the tail region, although it is the tail behaviour that is of greater significance to communications systems performance [90]. Thus, Rician distribution appears to be the best suited model for our case.

Other useful distributions include the Suzuki distribution, used for modelling a mixture of fast and slow fading in mobile links and forest environments, the Nakagami-q or Hoyt distribution, used for modelling fading in satellite links, and the

Weibull distribution, also used for modelling mobile radio channels. Many of these distributions are based on curve fits to empirical data, and that is why the interpretation of such empirical results should be made with caution to avoid overgeneralisations. It should be also noted that differences in many of these distributions in the domain of high occurrence are often very small; major discrepancies are present primarily in the “tails” of the PDFs [68].

3.2.2 Co-Channel and adjacent channel interference

“Coexistence among wireless devices is dependent on three main factors: 1) frequency, 2) space and 3) time. In terms of frequency, the probability of coexistence increases as the frequency separation of channels increases between wireless networks. In terms of space, the probability of coexistence increases as the signal-to-interference-ratio (SIR) of the intended received signal increases. In terms of time, the probability of coexistence increases as the overall channel occupancy of the wireless channel decreases. The key to achieving coexistence lies in the ability to at least control one of the three aforementioned factors. Coexistence is possible given one of the three following conditions: 1) adequate frequency separation between wireless networks; 2) sufficient distance between wireless networks, effectively decreasing the SIR in each; or 3) relatively low overall occupancy of the wireless channel [71].

The number of available channels provided by the IEEE 802.15.4 standard is limited, which creates the problem of cross-channel interference from co-located IEEE 802.15.4 networks. Coexistence issues between different co-located IEEE 802.15.4 networks working at the same time on separate channels can be solved by careful design of the network architecture and the whole system, in terms of wisely choosing transmitting power levels and distances between nodes [50].

The impact of IEEE 802.11 on IEEE 802.15.4 is more dramatic. In [51] the authors introduce a model in order to estimate the packet error rate obtainable in interference conditions. In [52] the same authors extend the model, deriving the packet error rate of IEEE 802.15.4 networks under combined interference from WLANs and Bluetooth networks. Here the authors conclude that interference from IEEE 802.11 networks can have an extremely critical impact on IEEE 802.15.4 if overlapping radio frequencies are used, while interference from Bluetooth networks and microwave ovens usually has a limited impact.

In the presence of multiple WLANs, available channels for IEEE 802.15.4 significantly decrease since a WLAN channel occupies 22 MHz bandwidth, which corresponds to the four consecutive IEEE 802.15.4 channels. To improve the performance of IEEE 802.15.4 networks in the presence of co-channel interference in the ISM band, different approaches have been suggested. In [69] the proposed scheme can rapidly detect the presence of co-channel interference in a distributed manner. In the presence of interference, it transmits the signal using multiple channels in a frequency hopping manner and finds out the best channel for the handoff, efficiently avoiding the interference effect. In [70] the interference mitiga-

tion technique is demonstrated, which detects and mitigates the channel interference based on packet error detection and repeated channel handoff command transmission. Interesting coexistence studies concerning 802.15.4 and 802.11 devices in medical environment have been performed and reported in [71]. Here, a reproducible NLOS coexistence test protocol was designed, which aims to gain helpful information towards efficiently overcoming coexistence problems between heterogeneous networks, while optimising their set-up in real-life conditions. The proposed protocol is used to determine the distance at which a medical device telemetry system can coexist with other wireless technologies that operate in a similar band.

Spectrum sensing

To avoid co-channel interference and mitigate induced performance degradation, cognitive radio solutions have recently been envisioned in the context of wireless sensor networks [81], [15]. The main idea is to allow sensor nodes to monitor the available frequency bands and opportunistically select their transmissions' unused frequency bands of spectrum. Two different approaches have been proposed; the first aims to exploit spectrum holes in the frequency domain through frequency agility: once interference is detected on a certain channel, nodes are reconfigured to use another available channel [78], [79]. Another approach is to take advantage of white spaces in the time domain accessing the medium during idle intra-packet periods, when interfering devices are not transmitting [80]. Both approaches require sensor nodes to identify suitable spectrum holes through spectrum sensing.

Spectrum sensing can be accomplished through a real-time wideband sensing capability to detect weak primary signals in a wide spectrum range. Generally, spectrum sensing techniques can be classified into three groups: primary transmitter detection, primary receiver detection, and interference temperature management [84]. Transmitter detection is based on the detection of a weak signal from a primary transmitter through the local observations of cognitive radio (CR) users. Three schemes are generally used for transmitter detection: matched filter detection, energy detection and feature detection [83]. The most efficient way to detect spectrum holes is to detect the primary users that are receiving data within the communication range of a CR user, but because the local oscillator (LO) leakage signal is typically weak, implementation of a reliable detector is not trivial. Recently a new model for measuring interference, referred to as interference temperature, has been introduced by the Federal Communications Commission (FCC). Here, the interference at the receiver is limited by an interference temperature limit, which is the amount of new interference the receiver could tolerate. As long as CR users do not exceed this limit, they can use the spectrum band. The challenge of this approach is to accurately define the interference temperature limit [84].

A typical concern in WSNs is energy consumption due to the resource-constrained nature of sensor nodes. Moreover, additional energy is consumed in the WSNs to support cognitive radio functionality such as spectrum sensing and switching, which could shorten the sensor node lifetime. In [81] the algorithm for

spectrum sensing adopting a cross-layer approach has been introduced. The algorithm aims to minimise the average energy required for the successful delivery of a packet. Their results show that using the short length packets in sensor networks can significantly improve energy efficiency, leading to gains of up to 50% when compared to other spectrum sensing algorithms presented in the literature. However, this solution is not appropriate for channels with heavy interference. In [82] a novel clustering-based spectrum sensing algorithm for cognitive radio wireless sensor networks is presented. The solution proposed by the authors reduces energy consumption by involving fewer nodes in spectrum sensing. They apply an improved clustering algorithm, where sensor nodes are grouped into different sets based on their similarity in sensing result. The simulation results show that the proposed scheme can effectively reduce the energy consumption of a sensor node and improve overall detection probability.

3.3 Radio signal transmission quality analysis

The studies on radio transmission quality have revealed the existence of three distinct reception regions in a wireless link: connected, transitional and disconnected [73], [75]. The transitional region is often quite significant in size and is generally characterised by high variance in packet reception rates (PRRs).

Empirical studies and measurements show that the coverage area of sensor radios is neither circular nor convex, and packet losses due to fading and obstacles are common at a wide range of distances and keep varying over time, thus the network simulation tools using idealised unit disk graph models do not give a realistic picture of radio channel quality [76], [75]. Studies have also revealed that a significant percentage of radio links suffer from link asymmetry and radio irregularity, especially when the communication distance is large or the transmit power is low [77], [73]–[75]. Link asymmetry occurs when a node can successfully send packets to another node but not vice versa, even if both nodes are set to the same transmit parameters.

The undesirable influence of the propagation environment on signal parameters makes the radio channel links unreliable. The degradation in the quality of the received signal is measured using one or more quality measures like signal-to-noise ratio, bit error rate (BER) and signal outage. An important measure of the received signal is the carrier-to-noise ratio (C/N). In the case of analogue representation, signal quality may be gauged by the receiver output signal-to-noise ratio (SNR). For digital signals, the equivalent measure is the average bit error rate (BER).

The transmission measurements play an important role, regardless of the point of view for dealing with transmission problems in WSNs. A common approach for the physical layer measurements is to rely on the received signal strength indication (RSSI) values provided by the chipset. The main attraction to RSSI as a metric is that the measurements and calculations involved in RSSI are less complicat-

ed, and RSSI values are easily available from the chipsets [41]. The drawbacks of using RSSI values are the differences between the RSSI values reported by the individual chips, which may originate from differences in antenna design, hardware design or driver, and the accuracy of time resolution. RSSI is a dimensionless quantity, which represents the signal strength observed at the receiver's antenna during packet reception, and for example, for the Chipcon cc2420 chipset it is calculated over eight symbol periods and stored in the RSSI registers [41]. However, this also introduces problems when using RSSI measurements: no RSSI value is attained unless the quality of the received signal is good enough for successful decoding. There is neither a standardised relationship between RSSI value and power level in mW or dBm and it is up to the chipset manufacturer to provide mapping between them, nor is the RSSI measured over the whole received packet [42]. In some cases, the RSSI reported from a packet reception represents the signal strength only during reception of the PCLP (physical layer convergence preamble) and PLCP header (IEEE 802.11) [43]. Thus, if the interference affects only the average received signal strength, the effect of interference will not be captured in the RSSI measurements [42].

RSSI data can be used to analyse signal attenuation, but it is important to note that RSSI does not relate to the quality of a signal. Signal strength is the power level received at the input to the decoder, while signal quality is a representation of the bit error rate (BER) after decoding, which in turn is proportional to the signal-to-noise ratio. In a digital transmission, BER is the percentage of bits with errors divided by the total number of bits that have been transmitted. The BER is not reported by default by wireless transceivers, so to derive the BER value, the CRC functionality has to be disabled in order to have access to erroneously received packets. The packet error rate (PER) and bit error rate (BER) values can be used to detect the degradation of connection quality on the MAC level. Note though that the BER can be computed only from the received packets (correct or corrupted). In high interference conditions, in which some packets may not be received at all, the BER cannot be calculated.

In [72] the author describes the principles of bit error rate (BER), the factors that affect it, and the methods for its measurement. The main factors affecting the BER are noise introduced by the circuitry, which can be described with Gaussian probability density function, and the disturbances affecting the signal path. The quantisation errors also reduce BER performance through incorrect or ambiguous reconstruction of the digital waveform. Quantisation errors are primarily a function of the accuracy of the digital-to-analogue and analogue-to-digital conversion processes.

There are some design issues that can increase or decrease the BER: one is to reduce the bandwidth, but we are limited by the bandwidth required to transmit the desired bit rate (Nyquist criteria). The energy per bit can also be increased by using higher power transmission, but interference with other systems can limit that option. A lower bit rate increases the energy per bit, but we lose capacity. Ultimately, optimising Eb/No is a balancing act among these factors [72].

4. Identification of radio channel disturbances

In Chapter 4 the contribution of this thesis is described: the time domain signal analysis, frequency domain analysis and classification procedure.

Studies on the physical phenomena behind the transmission problems led us to develop signal analysis methods that help to identify the radio channel disturbances: the probability density function (PDF) analysis method and the spectrogram analysis method. The PDF channel state analysis method is based on the idea that changes in statistical properties of the received signal are strongly correlated with the transitions of the channel states. Especially for the cases when the errors are too severe for successful demodulation of the signal, and RSSI or BER values cannot be accessed due to the lost packets, the PDF parameters can provide the necessary information on the current channel state and possible disturbance objects. The spectral analysis is based on calculating the spectrograms of the received signal and obtaining the statistical information of the radio interferences with image analysis tools. By combining the results of signal analysis in time and frequency domains, we constructed a classifier to classify the radio channel disturbances.

4.1 Time domain signal analysis

As already mentioned, it has been shown that temporal fading in the industrial environment exhibits Rician fading properties [57], [58], [59]. Measurements performed in different factory environments indicate that temporal fading caused by frequently moving trucks or other heavy machinery may cause deep fades and require 20 or 30 dB more transmitter power to achieve low bit error rates [46]. Here, we present a method which helps to track and predict these deep fades by analysing the statistical properties of the received signal.

Environmental changes in radio channels (e.g. trucks, other radio transmissions) cause fluctuations in the strength of the received signal and consequently in the histogram of the received signal. The histogram is calculated from the received signal magnitude samples and matched with theoretical Rician PDFs. There are two common ways to fit the data to a distribution: using the moments, or maximum likelihood estimation. In our work we used the ‘fitdist’ matlab function to match the signal magnitude samples of the received signal to Rician distribution, and the

'fitdist' function uses maximum likelihood estimation method. The shape and scale parameters, '*a'* and 'σ', are derived from the theoretical Rician PDF which best matches the histogram calculated from the received signal, see Fig. 9. The x-axis shows the signal sample strength values and the y-axis their probability distribution. Due to a large number of factors contributing to what we see as digital amplitude, the Software Defined Radio (SDR) receiver must be calibrated in order to convert the digital signal sample strength values obtained from the USPR, for example, to dBm values. We did not do this conversion, since in this work the metric of the signal magnitude value is not important. Our analysis is based on the variations of the signal sample magnitudes under different conditions, not on the absolute signal strength value.

In the Rician distribution the '*a'* value reflects the amount of the specular power of the received signal, while the *sigma* value is related to the amount of the scattered power of the received signal.

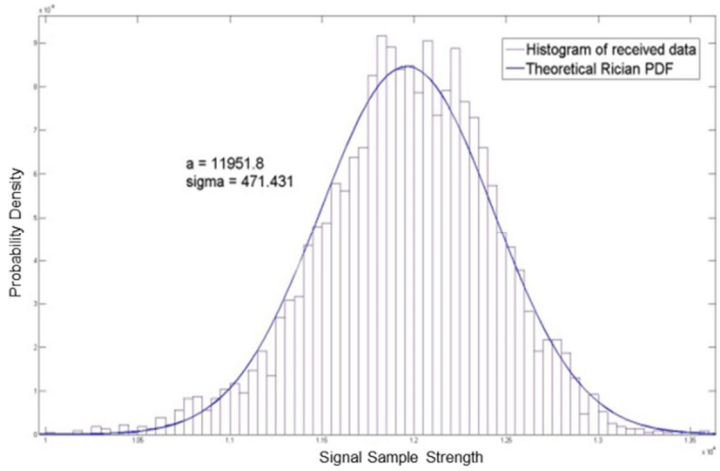

Figure 9. Received signal magnitude histogram and matching theoretical Rician PDF

In our work we studied the correlation between the temporal fading caused by the large objects and a and *sigma* parameter variations [96], [98]. During our measurements a vehicle (a car, a van and a truck) approached the line-of-sight between two radios and stopped for a moment to block the direct signal, and then drove away. In a situation where no vehicle is blocking the signal, we call this LOS channel state, meaning that the signal with shortest propagation path is not blocked or disturbed. And again, the situation where a vehicle drives between the radios and blocks the signal, we call NLOS channels state, meaning that the signal with shortest propagation path is blocked or disturbed. The behaviour of the received signal magnitude is illustrated in Fig. 10, where both LOS and NLOS

cases are given. The samples of the signal magnitudes are shown as histograms, with corresponding PDFs. In the NLOS case, the *a* value obtained from the theoretical PDF is decreased, but the PDF still follows the Rician PDF. As mentioned earlier, if the *a* value goes to zero, the amplitude distribution becomes Rayleigh.

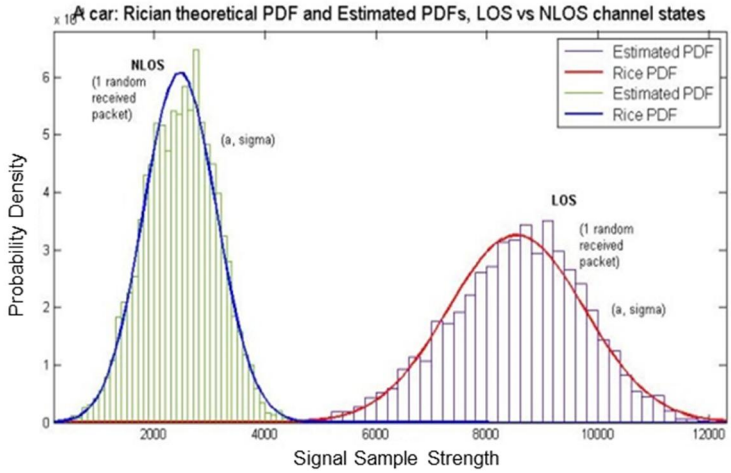

Figure 10. Received signal magnitude PDF in LOS (right) and NLOS (left) cases as measured for the passenger car

We also investigated the behaviour of received signal magnitudes in situations of strong radio interference. Here, the shape of the histograms changes due to the effect of two signals summing up; see Fig. 11. The WLAN 802.11b base station was used to create an interference signal. The sum of added signals does not follow the Rician PDF, and matching error occurs.

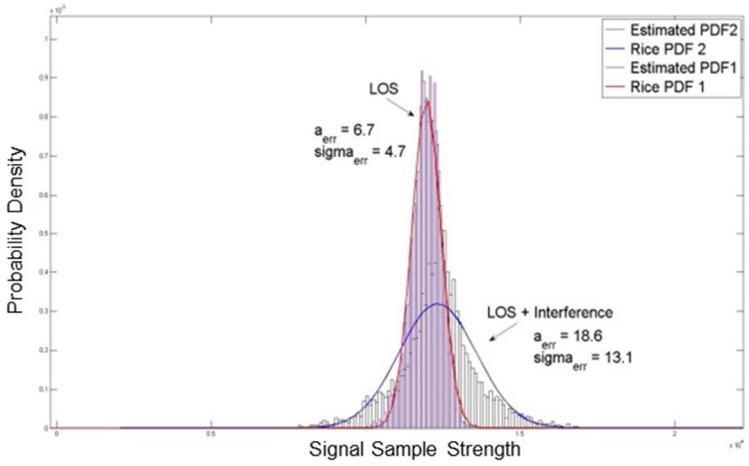

Figure 11. Received signal magnitude histogram and theoretical Rician PDF with a clear matching error for the interference signal

4.2 Frequency domain signal analysis

The spectrum analysis is based on calculating the spectrograms of the received signal magnitude and obtaining the statistical information of the radio interferences with image analysis methods. A spectrogram is a visual representation of the spectrum of frequencies, and it is calculated from the time space signal using the Fast Fourier Transformation (FFT). The horizontal axis of the spectrogram represents time and the vertical axis frequency; a third dimension indicating the magnitude of a particular frequency at a particular time is represented by the intensity or colour of each point in the image. The spectrograms can be used to extract distinctive features of the received signals and to identify the modulation of the signals. The instantaneous amplitude, phase and frequency transitions of the different types of modulated signals will have different spectral characteristics in the time-frequency domain [11]. In our work we will focus on extracting the frequency- and time-related features of the received signals to detect and characterise the radio interference.

Figs. 12-13 present the example spectrograms recorded with the software defined radio (SDR) in the industrial environment. In Figure 12 our signal is not disturbed by other radio transmissions (mostly WLAN), and the spectral trace is easily observed (indicated by an arrow).

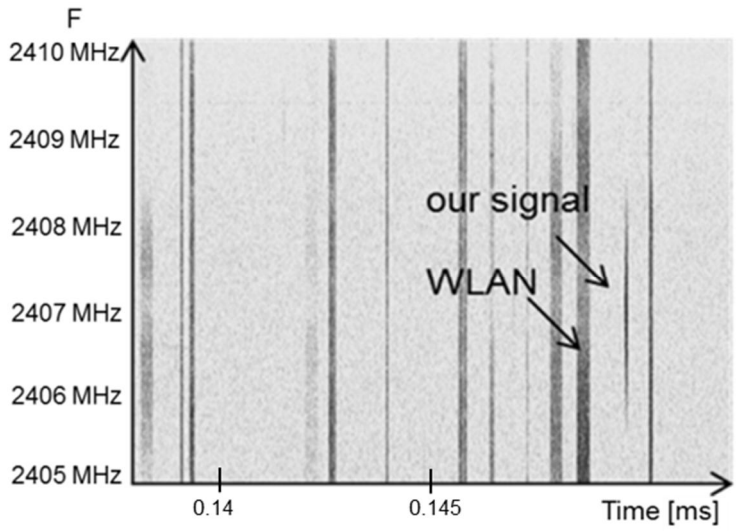

Figure 12. Exemplary spectrogram for industrial environment; our signal is not disturbed

In Figure 13 the situation is more complicated; here, our signal was strongly disturbed by other radio transmitting (WLAN) on the same frequency channel.

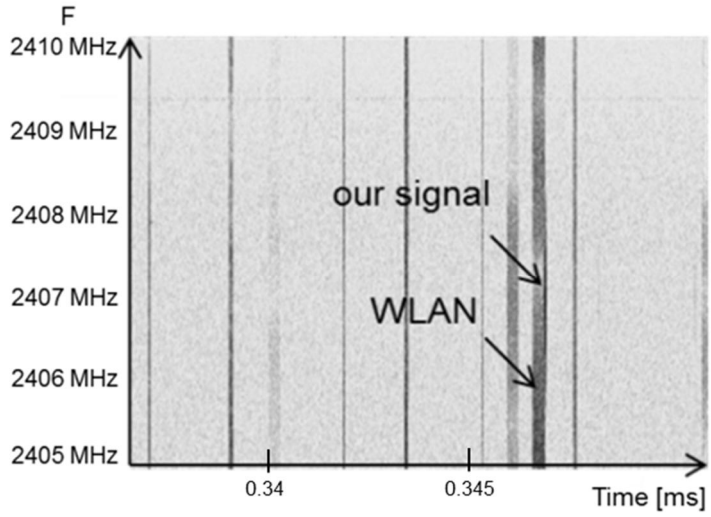

Figure 13. Exemplary spectrogram from industrial environment: our signal is disturbed

RF spectrograms are processed with image analysis tools to find transmission or disturbance entities, which we call RF objects, see Fig. 14. RF objects are transmissions or disturbances having a frequency band and duration time. After the objects are detected, they are transformed to the numerical representation by obtaining the frequency (y-axis), time and duration information (x-axis) of each object.

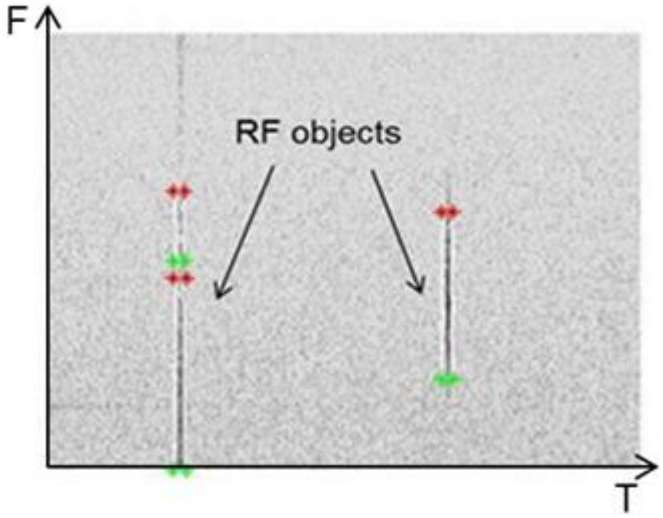

Figure 14. Radio interferences detection process performed using image analysis techniques

4.3 Classification

The recognition and identification of the radio disturbance is based on fusion of the signal magnitude analysis and spectrogram analysis with a classifier [99]. We follow the typical pattern for classification algorithms, presented in Fig.15.

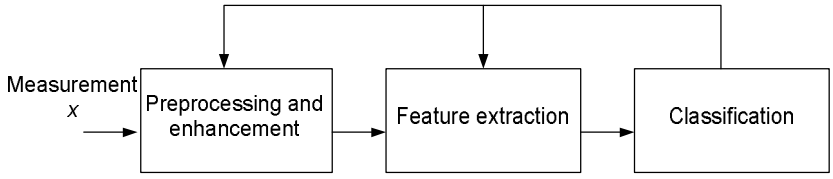

Figure 15. General pattern for classification procedure

The algorithm includes the following phases: pre-processing of measured data, feature extraction from the measured data, and classification. In addition, the data

already classified can be used to train the system to improve the performance of the classifier. The features are arranged in an n-dimensional feature vector, which yields a multidimensional measurement feature space. The classification is accomplished by portioning the feature space into class-labelled decision regions, and assigning the measured feature vector to the nearest region.

In our work, the received digitised I(n) and Q(n) samples are pre-processed and analysed both in time and frequency domains. For each received packet, the PDF of the signal magnitude is estimated as a signal magnitude histogram, and matched to the theoretical Rician PDFs, see Fig. 16. In parallel, the spectrogram is created from the received signal magnitude values, and the RF objects are extracted from the spectrogram with image analysis tools. The RF objects are compared to the transmitted packets (own or interference), and are shown as ridges, plains or otherwise distinguishable forms of the spectrogram. The parameters of the detected RF objects and related Rician parameters comprise features which are used in channel state classification. The feature extraction mechanism and classification algorithm are described in detail below.

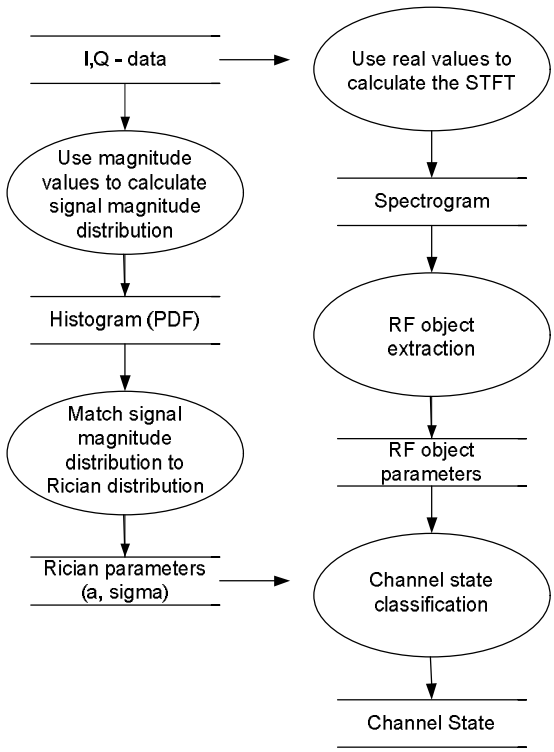

Figure 16. Fusing results of PDF analysis and spectrogram analysis to classify radio disturbances

4.3.1 Feature extraction

The feature vector comprises six parameters:

$$F = \begin{bmatrix} a \\ sigma \\ fit_{err} \\ f \\ \Delta f \\ \Delta t \end{bmatrix} \quad (12)$$

Where
a = amount of the specular power
sigma = amount of the scattered power
fit_{err} = goodness of fit
f = start frequency of the signal
Δf = width of the frequency band
Δt = duration of the signal.

To reduce computation, the parameters are calculated only for the estimated time slots of our own signal. The parameter values *a* and *sigma* are derived by matching the histogram calculated from the magnitude values of the received signal (=one packet) to the simulated Rician PDF.

The goodness of this fit is defined by the fit_{err} parameter. The less the histogram of the received packet resembles the simulated Rician PDF, for example in case of stronger radio disturbance, the larger the distributions match error.

The last three parameters *f, Δf* and *Δt* are obtained as characteristics of the RF object from the spectrogram of the received signal; *f* defines the mean of the frequency band*, Δf* the width of the frequency band, and *Δt* the duration of the signal, see Fig. 17.

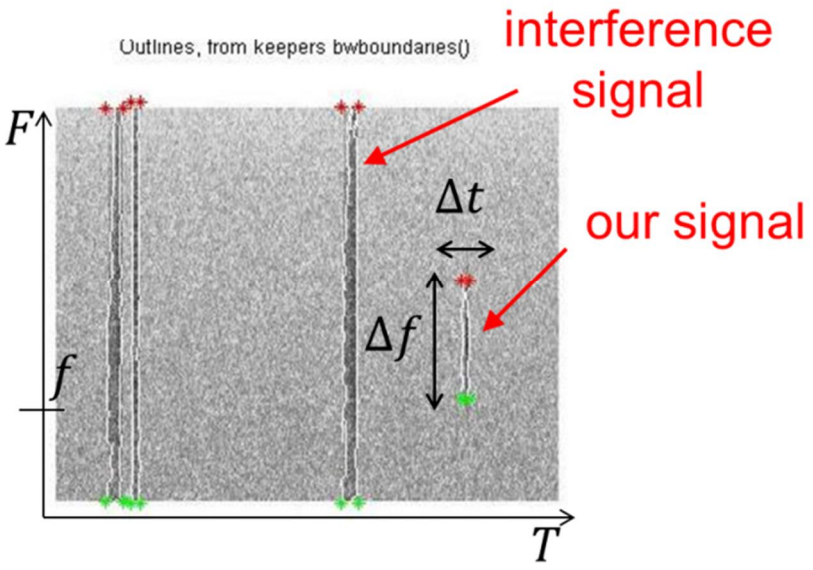

Figure 17. Spectrogram of the received signal

4.3.2 Reference classes and the classification procedure

We use a practical and simple approach for the classification – the Nearest Neighbour Rule (NNR). The underlying idea is quite simple: samples that are 'close' in the feature space are likely to belong to the same class. The NNR uses a training set directly to implement a classifier. Classification capability is achieved by considering samples in a training set to be typical representations of each class and by employing a similarity measure. The determination of a good and suitable similarity measure is a one of the difficult problems in the classification procedure. In this work, we chose the minimum Euclidean distance in order to minimise the computational expense. A training set will be specific to each environment due to different environmental geometrics, dimensions, wall/ceil materials, transmitting parameters (transmit power, distances between the nodes), and thus need to be obtained for each case individually. We call this phase of classification calibration, and it is need to be performed only once during the WSN installation in the new environment. In Fig. 18 the classification procedure is presented.

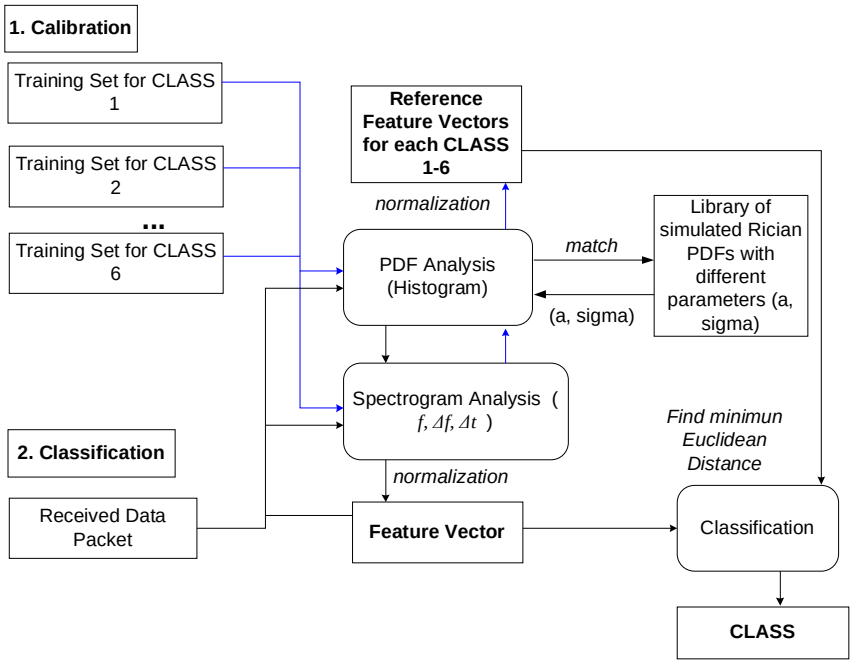

Figure 18. Classification and calibration phases

The reference feature vectors represent class-labelled decision regions where we want the measured feature vector calculated from each received data packet to be assigned. The reference feature values are the mean values per training set. Thus, a feature vector representing a class is a set of measured mean feature values. Both the feature vector calculated from a received data packet and reference feature vectors are normalised to a nominal feature vector. The normalisation is needed because otherwise some feature values will have larger variance than others, and thus dominate the classification results.

$$F_{norm} = \begin{bmatrix} a/a_n \\ sigma/sigma_n \\ fit_{err}/fit_{err\,n} \\ f/f_n \\ \Delta f/\Delta f_n \\ \Delta t/\Delta t_n \end{bmatrix} \quad (13)$$

Where
a_n = normalised *a* value
$sigma_n$ = normalised *sigma* value
$fit_{err\,n}$= normalised goodness of fit value
f_n = normalised value of centre frequency of the signal

Δf_n = normalised value of frequency bandwidth of the signal
Δt_n = normalised duration of the signal.

The nominal feature vector $[a_n\ sigma a_n\ fit_{errn}\ f_n\ \Delta f_n\ \Delta t_n]$ is acquired from a training set in the absence of any kind of disturbances (Class 1: LOS). The nominal feature vector is dependent on the transmission settings (transmit power) and the environment (industrial or office), and needs to be trained for the specific case (industrial or office). In this work, the analysis is performed assuming that the distance between the transmitter and the receiver is known and is static. The distance dependency will be avoided by scaling the signal magnitude values to a predefined magnitude interval. The absolute distance between the sensor nodes is not important for the classification procedure; only the relative changes of the magnitude values comparing to the nominal case matter.

In our work, we wanted to focus on classifying the dominant radio channel disturbances; active disturbances such as electromagnetic interference (co-channel interference) and passive disturbances such as trucks or other large objects blocking the signal partly or completely. Investigation of the real-life measurement results led us to the formation of four reference classes.

- Class 1: Nominal case, line-of sight = LOS
- Class 2: LOS + Co-channel channel interference
- Class 3: Non-line-of-sight = NLOS
- Class 4: NLOS + Co-channel channel interference

Class 1 is the nominal case; the data transmission link is not affected by any disturbance. Class 2 represents the case where data transmission is disturbed by the interference signal from other wireless devices. Class 3 is an NLOS case: here the transmission path is blocked by a large object (machinery), and signal fading occurs. Class 4 again represents the case where both disturbances occur; signal fading due to blocking object (NLOS) and interference from other wireless devices.

Classes 1-4 represent different channel states. Our goal is to identify the current channel state and provide this information to the network controller (gateway). This will reveal the sources of the transmission problems and also allow the sensor network to adapt to changing conditions by reconfiguring the network parameters, like power control or routing.

In Fig. 19, the reference PDFs from different classes are presented. The estimated PDFs were acquired during the measurements under different channel conditions in an orderly manner. The shape of PDF of the received signal varies depending on the channel state (=class). The a parameter is the most affected in case of transforming from LOS channel state (=Class 1) to NLOS (=Class 4), since it reflects the magnitude of the dominant (usually LOS) component of the received signal. If the *a* value drops to zero, the amplitude distribution becomes Rayleigh. During our measurements the NLOS case was never Rayleigh, since in a strongly reflective environment the dominant path comes from a specular reflection; hence the a value decreased, but did not reach zero. Then again, the more

the signal is distorted, the more the PDF shape is scattered and the larger the sigma parameter.

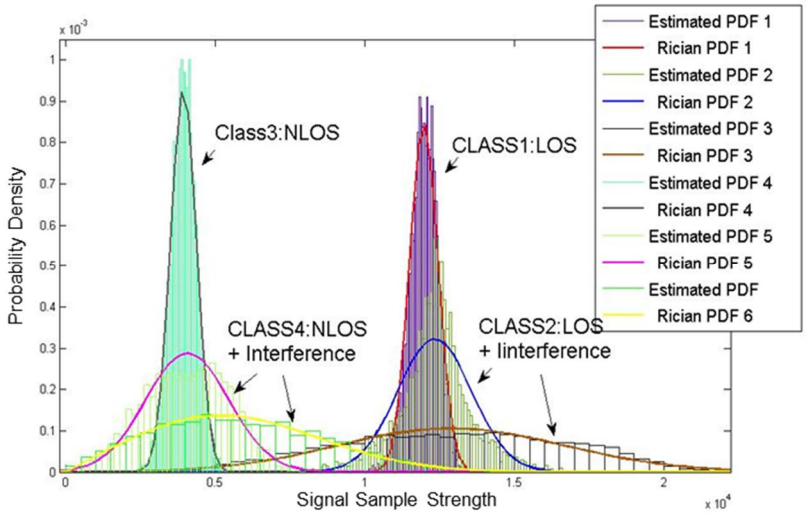

Figure 19. Reference histograms with matching Rician PDFs

In Fig. 20 the reference spectrograms of the received signal under different propagation conditions are presented. The horizontal axis represents time, the vertical axis is frequency; a third dimension indicating the amplitude of a particular frequency at a particular time is represented by the intensity or colour of each point in the image. The spectrogram provides us with additional information on whether there is an overlapping transmission on the same channel at the same time or not. In some cases, our signal is badly disturbed by the interference signal and cannot be recognised, but it can be discovered since we know the time windows of our signal transmissions. If needed, the interference signals can also be detected and their frequency parameters (*f, Δf* and *Δt*) obtained and analysed. This will increase our awareness of the frequency band occupancy.

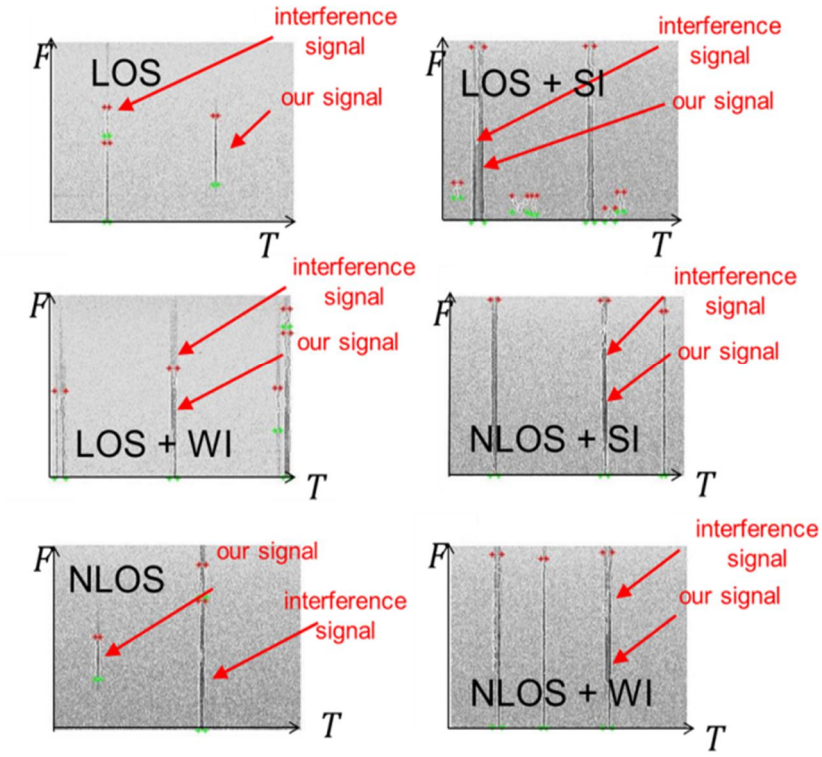

Figure 20. Reference spectrograms and RF objects

Here SI stands for strong interference and WI for weak interference. All interference objects that appeared in the plots in Fig. 20 are the WLAN signal transmissions. WLAN transmission strength observed by our radio receiver depends on the WLAN transmit power and the distance between the WLAN transmitter and our radio receiver. Two EIRP power limits exist for the 2.4 GHz band, one for 802.11b rates with CCK modulation (1, 2, 5.5 and 11 Mbps) and one for 802.11g/n rates with OFDM modulation. The limit is set to 20 dBm (100 mW) for OFDM and 18 dBm (63 mW) for CCK. The spectral power limitation of 10 dBm/MHz (10 mW/MHz) causes the lower power limit of 802.11b. As the spectral mask of the CCK modulation looks more like a sombrero, we see a high spectral power per MHz at the centre and a lower one at the edges. Therefore, if the Tx power is not lowered generally to 18 dBm, you exceed the spectral power limitation at the centre of a 802.11b 20 MHz channel. For OFDM, the spectral mask looks more like a rectangle, so the power is distributed almost equally, with an idealistic 7 dBm/MHz (5 mW/MHz) over a 20 MHz channel, for example, and the maximum power limit of 20 dBm can be used [91].

5. Measurements and test results

In this chapter the results of the measurements are presented. The goal of the measurements was to study how different radio channel disturbances affect signal propagation. Also, the classification test results are presented and discussed. In our work the algorithms were developed and extensively tested using desktop USPR N210, ETTUS SDR. Using the SDR only as a data collection device for research purposes is most beneficial, since the development overheads are relatively low, yet it can quickly verify new concepts. However, in the long run, developing the embedded version of the SDR tool is the only way of taking advantage of the SDR properties for the cognitive networks concept [85], [86], [87].

We performed comprehensive measurements to study the radio channel disturbances, their nature and effect on the received signal quality. During these measurements the data was recorded both by the SDR and the sensor node. The CRC functionality of the radio receiver (sensor node) was disabled to be able to receive all packets, including those that fail the CRC check. The BER was calculated over the data payload field of each received packet. The RSSI value was obtained from the radio receiver chip as well, and only for those packets which the radio was able to register. The data recorded with SDR was analysed in MATLAB.

The radio channel disturbances classifier was tested in easy and controllable environments such as the parking area and measurement hall, and the results showed that our analysis methods are applicable for the radio disturbance detection, identification and classification. However, in the real industrial environment the situation is much more complicated. Our final tests were performed in the factory hall during normal activity with workers and machinery moving around.

In this chapter we present the results of the measurements and tests, as well as the challenges we encountered in the industrial environment.

5.1 Measurements of BER, PER and PDF values

5.1.1 Design of the measurements

To collect data for the analysis of received signal behaviour within small-scale fading, the following test set-up was used, see Fig. 21. The test set-up is based on a radio transceiver pair and a source of radio interference.

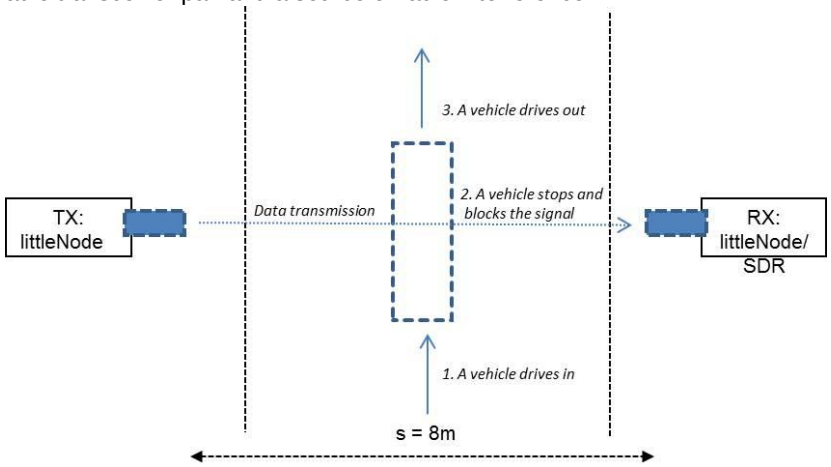

Figure 21. Experimental set-up

Transmitter and receiver antennas (TX and RX) were placed on the opposite sides of the road, which is about 8 metres wide. Three types of vehicles were used during the experiments; *Scenario 1*: a car, *Scenario 2*: a van, and *Scenario 3*: a truck. During the measurements a vehicle approached the line-of-sight between two radios, stopped for a moment to block the direct signal, and then drove away. We call the situation where no vehicle is blocking the signal the LOS channel state, meaning that the signal with shortest propagation path is not blocked or disturbed. We call the situation where a vehicle drives between the radios and blocks the signal the NLOS channels state, meaning that the signal with the shortest propagation path is blocked or disturbed. The data was recorded during the experiment both with the radio receiver (RX) and software-defined radio. From the RX radio we obtained the RSSI and BER values, and from the SDR the raw IQ data for further analysis. The first two scenarios (a car and a van) were performed in a parking area environment, and the last scenario (a truck) was performed in an industrial type environment.

The parking area environment is easy to control; it includes no obstacles close to transceivers and no active radio interference sources that may disturb the experiment results, see Figs. 22-23.

Figure 22. Parking area, a car.

Figure 23. Parking area, a van.

A typical industrial environment comprises concrete floors and walls, metal ceilings and metal machinery, and other industrial assets as well as strong radio interference. To perform the measurements with a truck, we chose the environment with strong radio interference and metal machinery nearby, see Fig. 24.

Figure 24. Industrial type area

The exemplary spectrograms for both the parking area and the industrial type area are presented in Fig. 25. In the industrial type area, the radio interference is much stronger than in the parking area. Our signal trace is indicated with an arrow, other traces on the figure are external radio interferences.

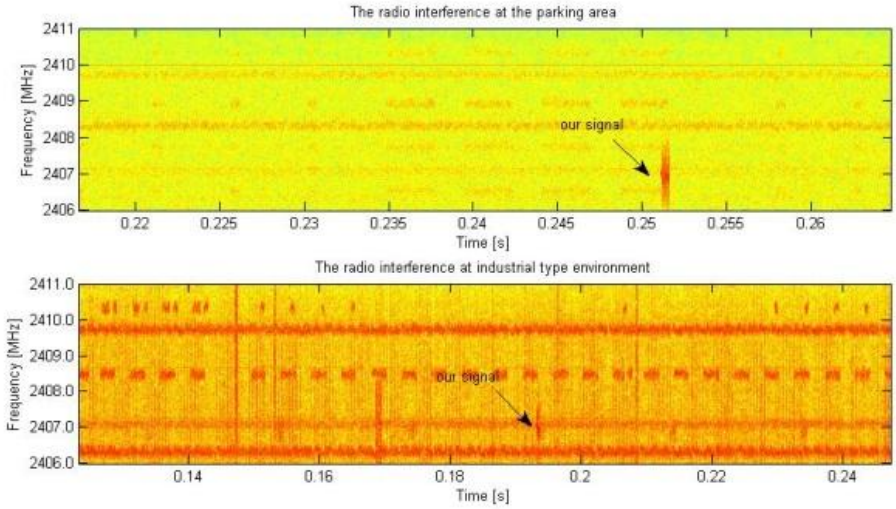

Figure 25. Exemplary spectrograms for the measurement environments: top: weak radio interference, below: strong radio interference, with test packet traces depicted with arrows.

Experimental Instrumentation

Transceivers:

- nRF51822, 2.4GHz radio (VTT littleNode)
- +4dBm output, 1Mbp/s mode
- Software-defined radio (USRP N210, RFX2400)

Antennas and cables:

- Receiver and transmitter: directive circular waveguide antenna (gain optimised for 2.4 GHz)
- 5m RG58 low loss antenna cables for transmitter and receiver antennas (attenuation ~0.7dB/m)
- Two camera stands for attaching the antennas.

Data collection:

- PC and a serial port interface for data collection.

5.1.2 Measurement results

In these measurements the BER and RSSI values were obtained by the radio receiver under different scenarios. The data was also recorded by the SDR, analysed with MATLAB tools, and the PDF shape parameters 'a' and 'σ' (=sigma) were obtained for each received packet.

Scenario 1: A car

When the line-of-sight was disturbed by the appearance of the passenger car, the consequences were clear and expected: the 10-20 dB drops in the signal RSSI values were registered during the measurements, indicating the temporal NLOS channel states. The blue coloured line in Fig. 26 shows the RSSI value drops, helping to track the channel state transitions. In the graph, the drops in the RSSI value appear to improve the readability of both RSSI and BER results. The y-axis indicates the RSSI value in -[dBm], and the number of erroneous bits per packet, and the x-axis indicates the index of the received packet. Erroneous bits are represented in red; during the LOS state the BER is zero, no bits (nor packets) were lost, but during the NLOS state the bit error bursts occur. The number of red points represents the number of packets that were received by the radio, but discarded because of bit errors.

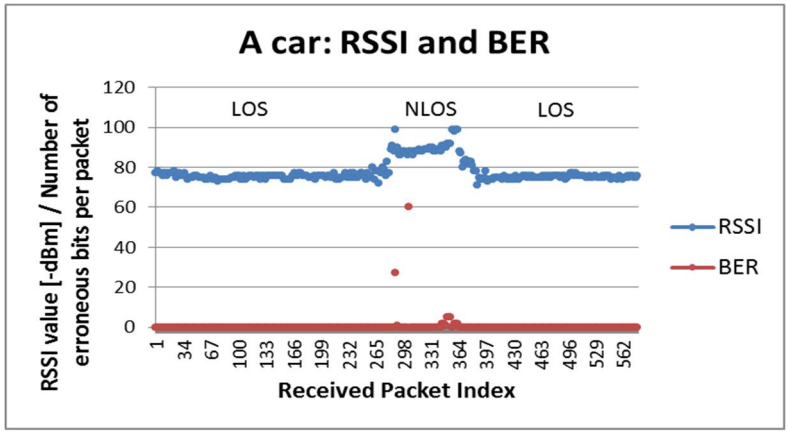

Figure 26. Received signal behaviour in a stationary LOS-NLOS-LOS scenario for a passenger car: RSSI and BER, Rician 'a' value (b) and Rician 'sigma' value (c).

PDF parameters change comparably, with substantial change both in "a" and "sigma" values, though the transience when the car is arriving in and leaving from the area between the transmitter and the receiver is somewhat turbulent, see Figs. 27-28.

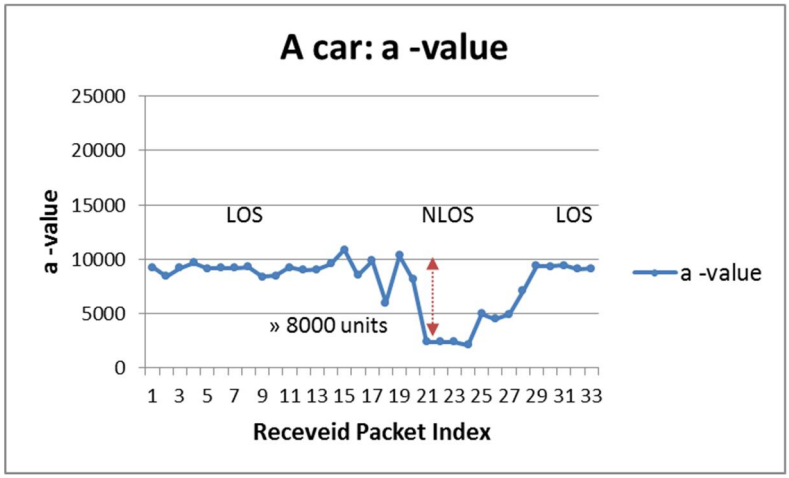

Figure 27. Received signal behaviour in stationary LOS-NLOS-LOS scenario for a passenger car: Rician 'a' value

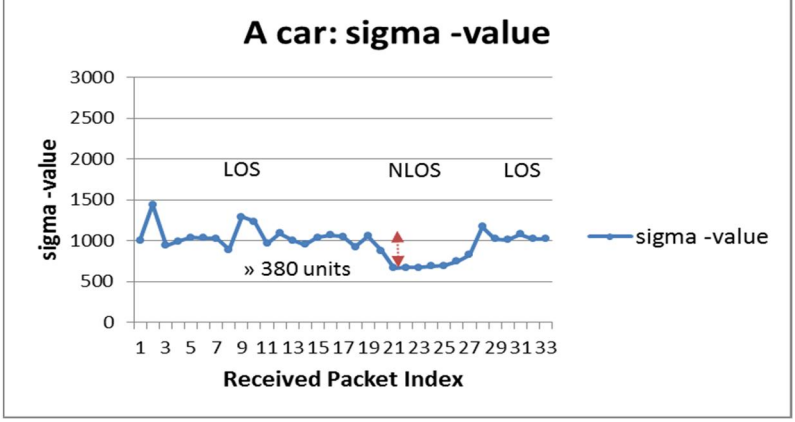

Figure 28. Received signal behaviour in stationary LOS-NLOS-LOS scenario for a passenger car: Rician 'sigma' value

Scenario 2: A van

In the case of the appearance of the van being the disturbance, see Fig. 29, the changes were stronger than for the passenger car: the RSSI value follows similar behaviour as for the passenger car; a reduction of 10-20 dB takes place within the change from LOS to NLOS. BER changes are more turbulent than in the case of the passenger car, the bit error bursts occur more frequently, and the test packets get more distorted: the number of erroneous bits per packet increases.

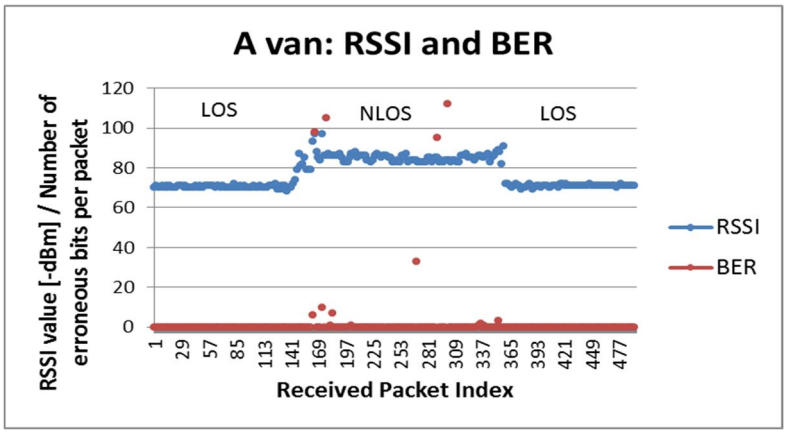

Figure 29. Received signal behaviour in stationary LOS-NLOS-LOS scenario for a van: RSSI and BER

PDF parameters change more strongly, with substantial change both in "a" and "sigma" values, though the transience when a van is arriving in and leaving from the area between the transmitter and the receiver is less turbulent than for the passenger car, see Figs. 30-31. This may be related to the shape of the vehicle: the passenger car has a gradual increase in height at the front; and when a car is approaching the line-of-sight, a metal object appears which at first does not block

the direct signal, but it does allow the signal components to reflect from the car's front part. A van does not have this kind of gradual increase; its front part is sharp.

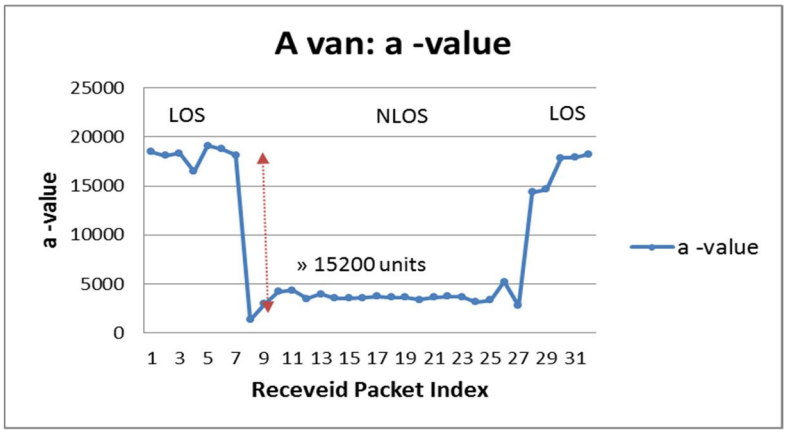

Figure 30. Received signal behaviour in stationary LOS-NLOS-LOS scenario for a van: "a" value

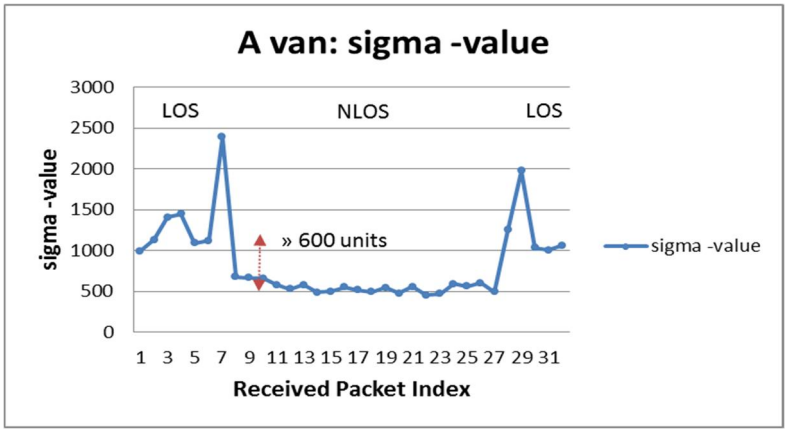

Figure 31. Received signal behaviour in stationary LOS-NLOS-LOS scenario for a van: "sigma" value

Scenario 3: A truck

In the case of the appearance of the truck being the disturbance, see Fig. 32, the changes were even stronger than for the van: the RSSI value has more scattering behaviour; a reduction of 20-25 dB takes place within the change from LOS to NLOS. BER changes are more turbulent even than in the case of the van, the

reason is that the truck blocks the LOS more effectively than the van and the passenger car. Here, the passive (obstacles, surfaces) and active (radio interference) environment is completely different to the first two scenarios, so we cannot compare the results directly. The BER bursts occur even when there is no vehicle blocking the signal, due to the disturbing radio traffic on the same frequency band.

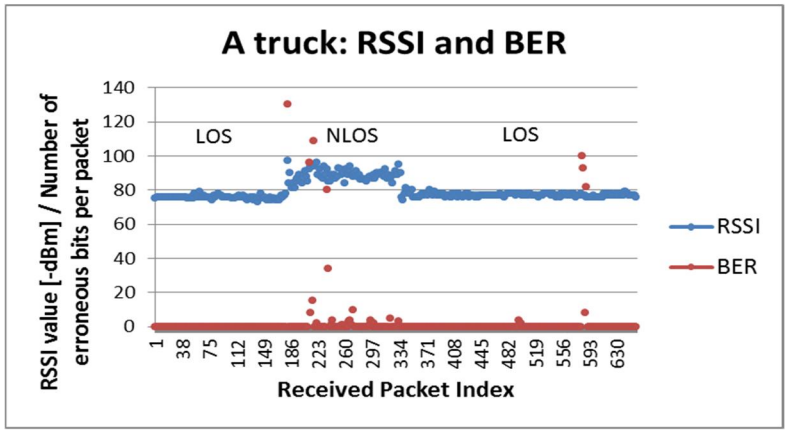

Figure 32. Received signal behaviour in stationary LOS-NLOS-LOS scenario for a truck: RSSI and BER

PDF parameters change even more strongly, with substantial change both in “a” and “sigma” values, and the transience when the truck is arriving in and leaving from the area between the transmitter and the receiver is less turbulent than for the passenger car, see Figs. 33-34. The intensified changes of the “a” and “sigma” values are explained by the increased signal scattering effect, due to the large and complex object that the signal must travel through (also the metal objects inside the truck affects the signal) and by the strong RF interference, which is seen as ‘a’ value turbulence during the whole experiment.

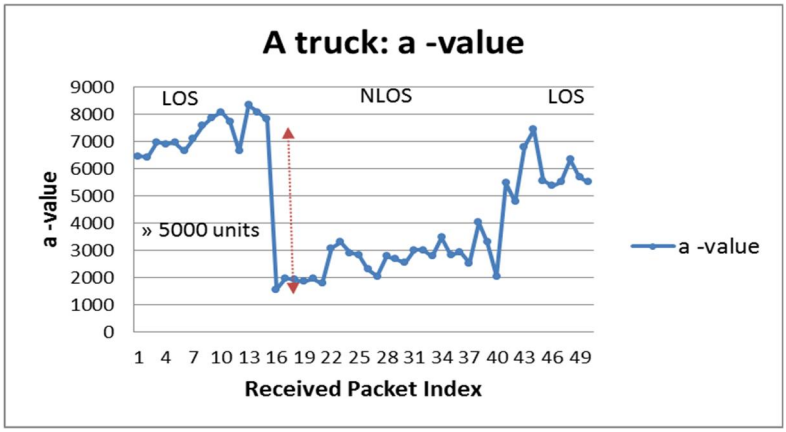

Figure 33. Received signal behaviour in stationary LOS-NLOS-LOS scenario for a truck: “a” value

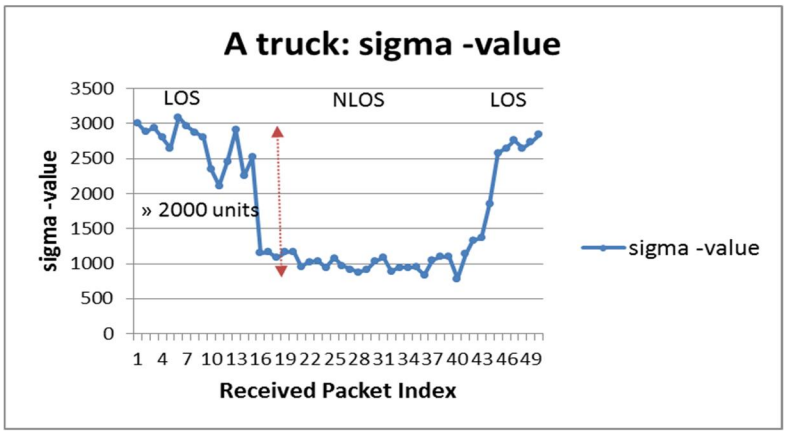

Figure 34. Received signal behaviour in stationary LOS-NLOS-LOS scenario for a truck: ”sigma” value

We also investigated the behaviour of “*a*” and “*sigma*” parameters in situations of strong radio interference. Here, the “*a*” value is not altered, but the “*sigma*” value changes dramatically due to the effect of two signals summing up, see Figs. 35-36.

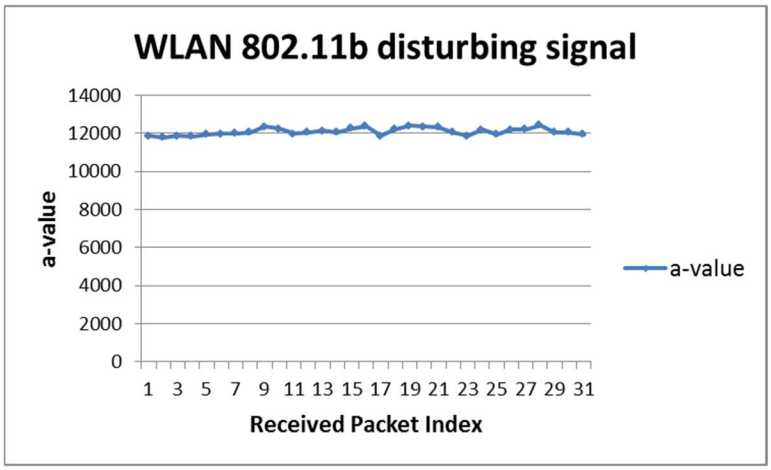

Figure 35. Received signal behaviour in LOS - LOS + Interference - LOS scenario: Rician 'a' value

The *sigma* value increases (=peaks) while the channel state changes from LOS to LOS + H, and drops while changing from LOS+H back to LOS. Here, "H" stands for radio interference (=WLAN 802.11b). The peaks of sigma values during LOS + H channel state means that these received packets were disturbed by the WLAN 802.11b signal.

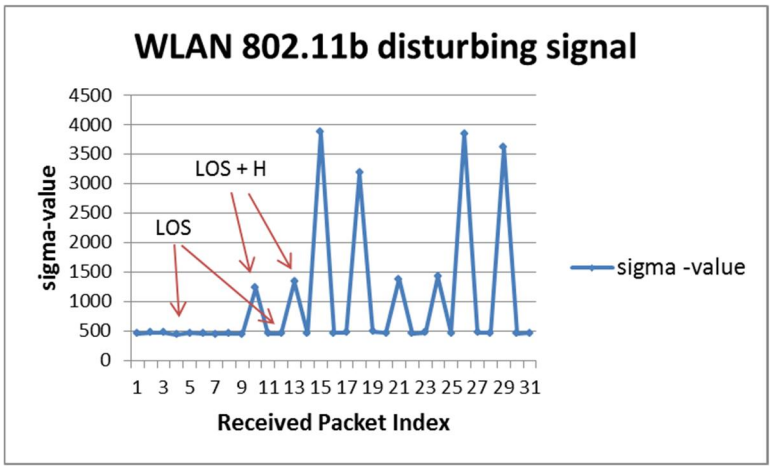

Figure 36. Received signal behaviour in LOS - LOS + Interference - LOS scenario: Rician 'sigma' value

5.2 Classifier tests

5.2.1 Design of real-life tests

The classifier performance analysis tests were performed before the final tests in a factory-like environment; see Figure 37. Here, we performed tests in a controllable manner to analyse the classifier performance for each class independently. A truck was used to block the signal during the tests.

Figure 37. Factory-like environment

Our final tests were performed in a real industrial environment with concrete floors and walls, metal ceilings, metal machinery and strong radio interference. During our final tests, the forklift was driven between the transmitter and receiver several times and workers performed their normal activity. Figure 38 shows the environment of the experiment, though the workers and the forklift are missing from the picture for confidential reasons.

Figure 38. Factory environment

The radio environment is characterised by the exemplary spectrogram; see Figure 39. The spectrogram shows the data recorded during one second from the 2410- 2415 MHz frequency channel in the industrial environment. The radio interference in such an environment is much stronger than in the offices.

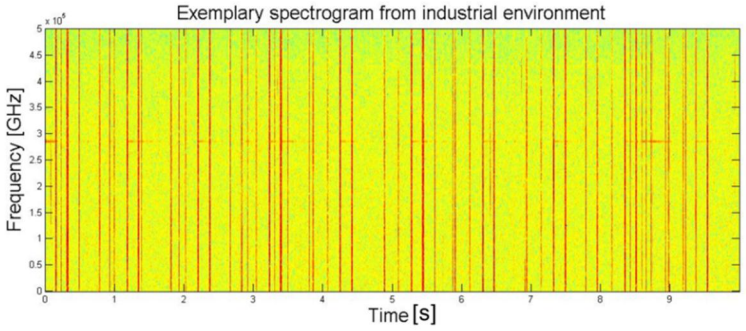

Figure 39. Spectrogram recorded in an industrial environment

Experimental instrumentation

During the measurements, two communicating radios were used: a 2.4 GHz Nordic nRF51422 radio transceiver as a transmitter (VTT littleNode) and a software

defined radio (USRP N210, RFX2400) as a receiver. The measurements data was recorded by the SDR, and analysed in MATLAB. The classification result for each received packet was obtained in real time with a 30-60s delay.

The basic philosophy of experimental design is to do all of the waveform-specific processing, such as PDF analysis and spectrogram analysis, classification and cognitive decisions on the host CPU (in MATLAB), and all of the high-speed operations like digital up and down conversion, decimation and the interpolation inside the FPGA of USRP. In USRP, the main ADC is a dual 14-bit, 100 MS/s, 2 auxiliary channel, 12-bit ADC for each daughter-board connector. The main DAC is a dual 16-bit, 400 MS/s, 2 auxiliary channel, 12-bit DAC. It supports a gigabit Ethernet connection; and it allows applications to simultaneously send 50 MHz of RF bandwidth with 8-bit samples and 25 MHz of RF bandwidth with 16-bit samples in and out of the USRP. The USRP is plugged directly into a dedicated Ethernet interface; USRP communicates at the IP/UDP layer over the gigabit Ethernet. In the USRP we can control centre frequency, transmission power and interpolation/decimation factor. The range for the centre frequency and the power are dependent on the attached daughter-board (RFX2400). The interpolation factors in the transmit path and decimation factor in the receive path [61].

5.2.2 Classifier performance analysis

The classifier performance was tested in a controllable, factory-like environment before the actual dynamic tests in a real industrial environment. The tests were run for each disturbance class independently, statically, and one class at a time. Classifier performance results for all classes indicate over 90% probability of correct results.

Fig. 40 shows the results for Class 1, which is a LOS case without any disturbances. The x-axis indicates the received packet index, and the y-axis the class the packet was classified to. There was some turbulence in the classification results at the beginning of the tests caused by a person walking between the radios; as he walks, the signal gets blocked, and the classifier detects channel state variations which are classified as Class 3 (NLOS). A couple of packets were classified as Class 2 and 4, meaning that there was some other radio transmission which interfered with our signal; this may be due to the person's phone traffic. After the turbulence, all the packets were classified correctly.

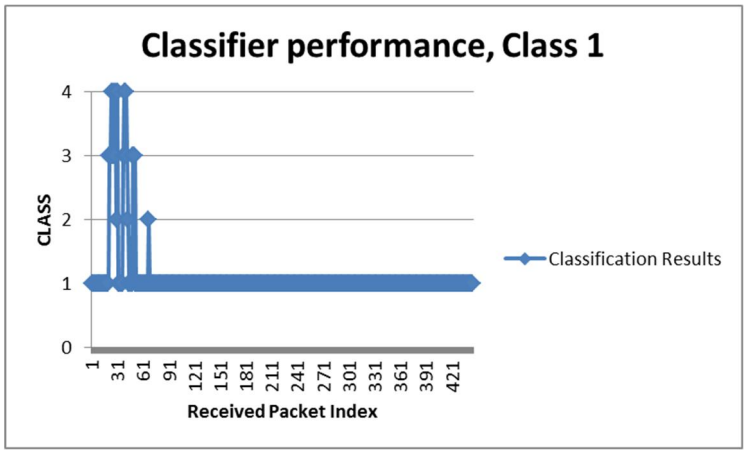

Figure 40. Classifier performance for Class 1, LOS

Fig. 41 presents the classifier results for Class 2. Here, our radio transmission was disturbed by the external radio interference. Some of the packets were incorrectly classified as Class 4 (NLOS + Interference) due to the radio interference signal being stronger than our signal. Then again, a couple of packets during the tests were classified as Class 1 (LOS) due to the radio interference being very weak and not causing much variation to the features obtained from the PDF analysis.

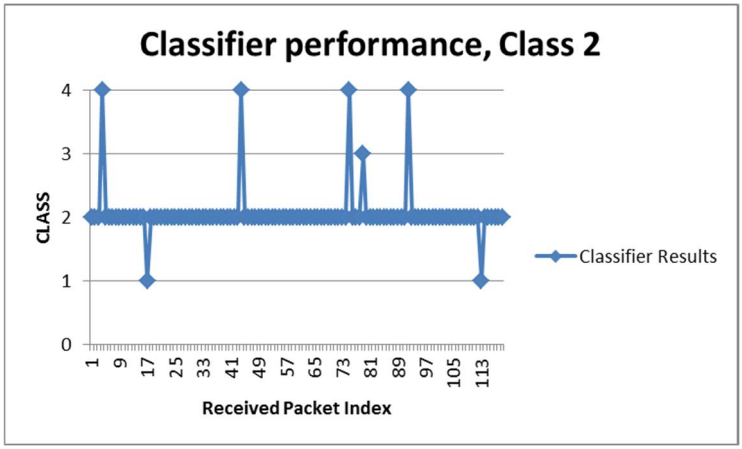

Figure 41. Classifier performance for Class 2, LOS + Interference

Fig. 42 demonstrates the classifier results for Class 3. Here, a truck was blocking the radio signal. Some of the packets were correctly classified as Class 4, since occasionally the signal was also disturbed by radio interference. If the interference

signal was too strong, some of the packets were erroneously classified as Class 2. This is caused by the fact that in the case of a strong radio interference signal, the features used to classify the packets are obtained from the interference signal, not our signal.

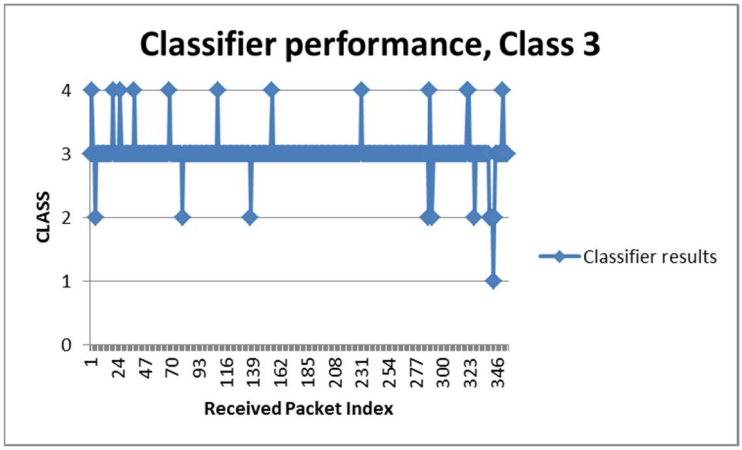

Figure 42. Classifier performance for Class 3, NLOS

Finally, Fig. 43 shows the classification results for the Class 4. Here, the truck was blocking the signal and external radio interference disturbed the signal transmission. To perform the analysis we picked only those packets which were proven to be disturbed by other radio transmissions. In addition, if the radio interference was stronger than our signal, the packets were erroneously classified as Class 2, and if the interference signal was very weak, the packets were classified correctly as Class 3.

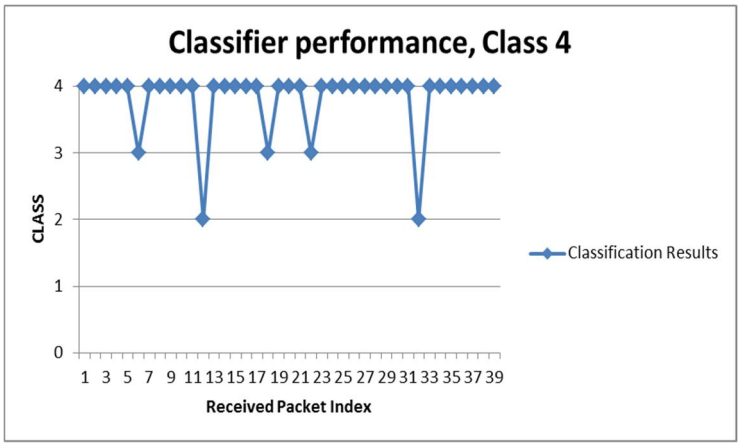

Figure 43. Classifier performance for Class 4, NLOS + Interference

5.2.3 Classification test results

The classification results for the set of data recorded during normal factory activity in a real industrial environment are presented. Normal activity in our case includes workers walking between the nodes, large and small forklifts driving between the nodes, and intense radio interferences, mostly IEEE 802.11.

The PDF is calculated for each received packet. In Figure 44 the PDFs of the received packets recorded during dynamic scenario are presented. The x-axis indicates the strength of the signal samples, the y-axis indicates the timeline, and the z-axis is the probability density for each signal sample's strength value.

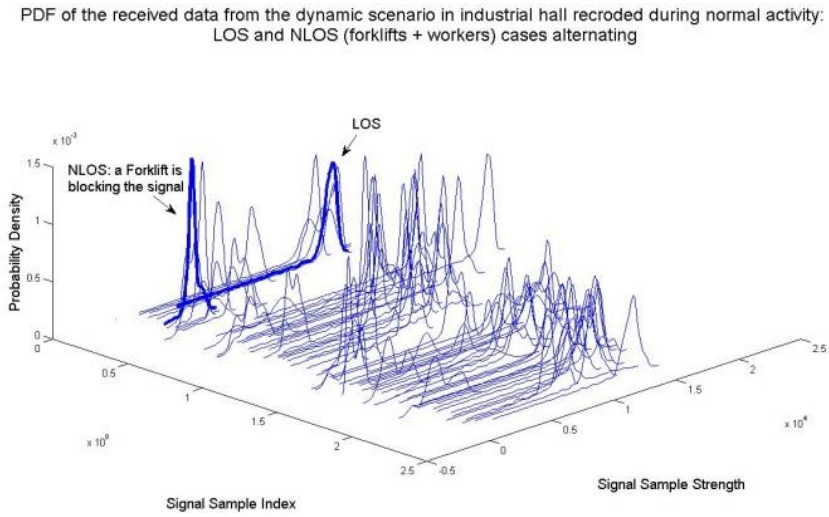

Figure 44. PDFs of the received data during the dynamic scenario

In the LOS case, the line-of-sight was temporarily disturbed by the workers walking between the nodes; the closer the worker was to the receiver, the more disturbed the received signal appeared to be. In [88] the effect of human body movement on wireless signals at 2.4GHz was studied. The authors found that there is significant impact on the signal fluctuations when the number of individuals and movement pace are taken into consideration. Slow-paced movement definitely reduces signal strength, while a fast pace will slightly decrease the signal strength from the baseline. The same observations were also made in an industrial environment with workers moving around; the signal level attenuated, but not as much as if there was a forklift blocking it, due to the dielectric properties of human biological tissue.

During the factory measurements, frequency-selective fading has occasionally occurred. In Fig. 45 two different channel states are shown, the upper plots present the state where the signal has not experienced frequency-selective fading, both a histogram and a spectrum of signal is given, and the plots below show how frequency-selective fading affects the signal.

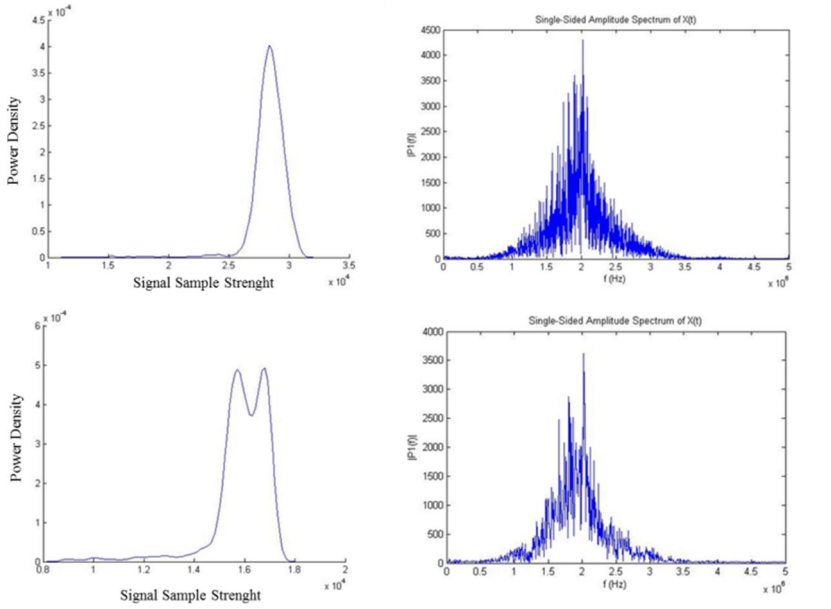

Figure 45. No frequency-selective fading vs frequency-selective fading

In any radio transmission, the channel spectral response is not flat. It has dips or fades in the response due to reflections, causing cancellation of certain frequencies at the receiver. Each of the multipath components have generally different relative propagation delays and attenuations which, when summing up in the receiver, result in a filtering effect on the received signal where different frequencies of the modulated waveform experience different attenuations and/or phase changes. In the measurements performed in the parking area, we did not observe such a clear case of frequency-selective fading. In the factory environment experiments, the classifier performance was not affected by this phenomenon, but the frequency-selective fading should be classified in its own class in future.

Figure 46 shows how environmental changes affect the shape parameters of the PDF. The blue PDFs represent the LOS case, where the transmitter and the receiver have line-of-sight for data transmission or near line-of-sight with workers walking between the nodes. The green PDFs represent the NLOS case, where data transmission is clearly blocked by the large object. In our case it is a forklift driving between the radios. The red PDFs represent the case where radio transmissions from other radios (mainly WLAN) are disturbing our data transmission.

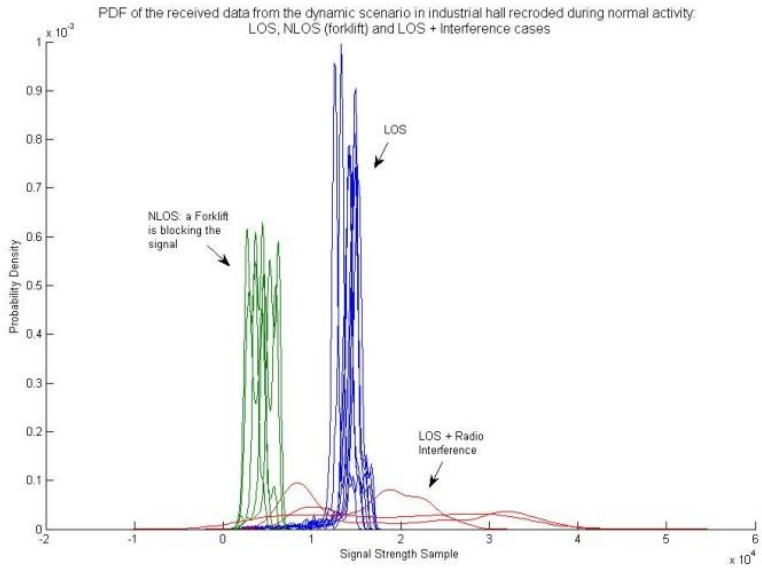

Figure 46. PDFs from different disturbance cases

The classification is based on the analysis of six feature values; how these values vary according to the environmental changes and their mutual influences. The curves in Figures 47-52 demonstrate the variations of these feature values during the dynamic case recorded in the factory environment. The dots on the curves indicate the data packets; the x-axis shows the index of the packet, and the y-axis shows the value of the feature. The variations of each feature value is not directly correlated with the channel state, but combing all six features into the feature vector and comparing it to the reference vector of each channel state class, we can classify the feature vector into one of four channel state classes presented before.

The centre frequency *f,* the width of the frequency band *Δf*, and the signal duration *Δt* feature values are obtained from the spectrum analysis by parametrising the RF object of our signal. In Fig. 47 the variations of the *f* feature value are shown. This value is decreased in the case of interference; the stronger the interference, the more the RF object of our signal in the spectrogram is affected by the RF object of the interference signal. In the case of NLOS, the *f* value is increased; the signal is attenuated, and the RF object of our signal in the spectrogram appears to be narrowed.

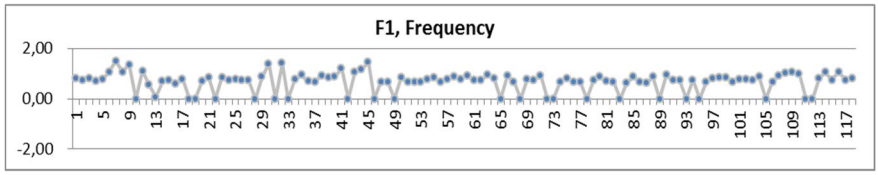

Figure 47. Variations of *f* value

The *Δf* value is affected in the same way as the *f* value, but it decreases in the NLOS case due to the decreased power of the received signal, and increases in the case of external radio interference, see Fig. 48.

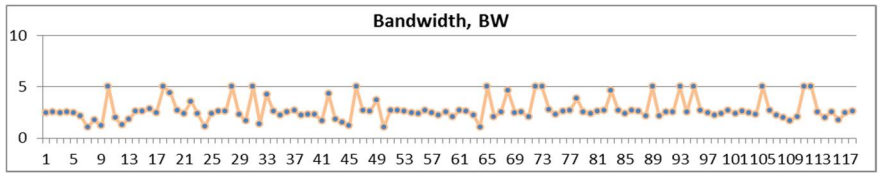

Figure 48. Variations of Δf value

In Fig. 49 the variations of *Δt* are shown. The *Δt* value is the same in the LOS and NLOS cases, because the decreased power of the signal does not affect the duration of the received signal, but in cases of interference the *Δt* value grows due to the interference signal overlapping with our signal, which can be seen in the spectrogram as two overlying RF objects.

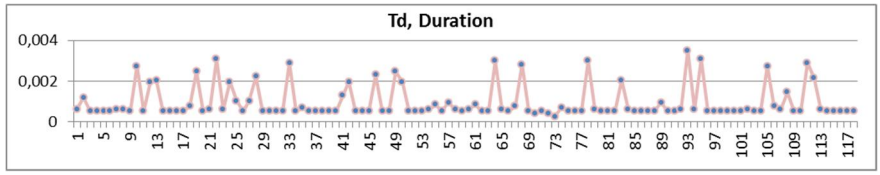

Figure 49. Variations of Δt value

The most significant differences occur in *a* and *sigma* values obtained from the PDF analysis. The *a* value in the NLOS case is only one-third of the *a* value in the LOS case. In the case of radio interference disturbing the signal, the a value is not altered, see Fig. 50.

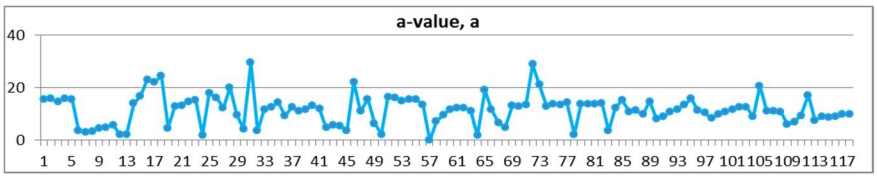

Figure 50. Variations of a value

In the presence of the interference, in both LOS and NLOS cases, the *sigma* value increases considerably; the stronger the interference, the more the *sigma* value escalates. In Fig. 51 the packets disturbed by the radio interference appear as peaks.

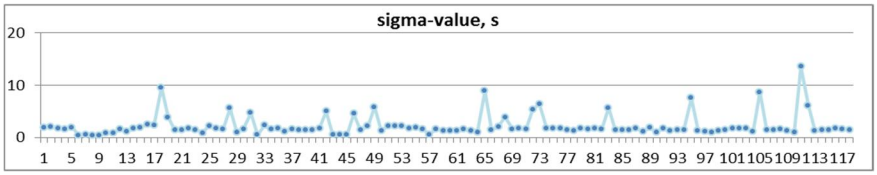

Figure 51. Variations of sigma value

In Fig. 52 the variations of the distribution fit error values are shown. The fit error value is sensitive to all disturbances, but the most for other radio disturbances; the less the histogram of the received signal resembles the Rician PDF, the larger the error.

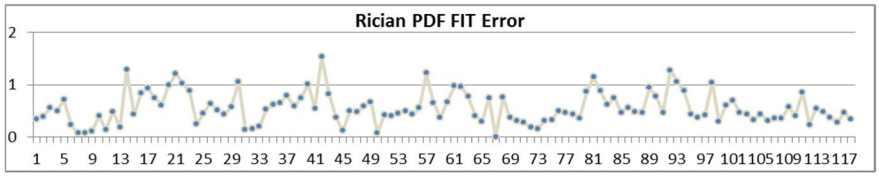

Figure 52. Variations of fit error value

The classification results for each received data packet are shown in Figure 53. Here, the snapshot of a dynamic situation is presented; a total of 118 packets are classified. Class 1 is the LOS case, Class 2 is the LOS + radio interference case, Class 3 is the NLOS case, and Class 4 is the NLOS + radio interference case.

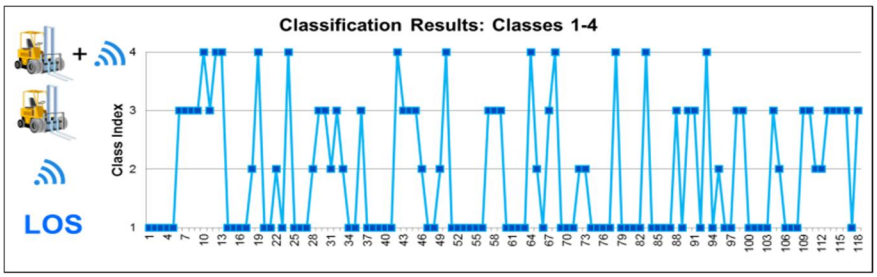

Figure 53. Classification results

In Fig. 53 the classification results illustrate that during the experiments, a forklift was driven several times between the transmitter and the receiver. In the case of workers crossing the line-of-sight of the radios, the classification result depends on how fast and how close the workers move towards the receiver and how much the signal is degraded because of it. The results also show that our signal is occasionally disturbed by the other wireless transmissions.

The feature vectors calculated from the received packets are compared with the reference feature vectors, and the minimum Euclidean distance is calculated. The reference feature vectors represent class-labelled decision regions where we want the measured feature vector calculated from each received data packet to be assigned. The reference feature vectors were obtained before starting the tests by calibrating the reference values. The calibration was performed in the following manner: the reference vectors for Class 1 (LOS case) and Class 3 (NLOS case) were calibrated by running measurements for a specific period of time. The mean values of measurement data were then used to compose the reference classes. The reference vectors for Class 2 and Class 4 were obtained computationally from calibrated reference values of classes 1 and 3.

Figures 54-57 shows the classification results The x-axis indicates the class index (1=LOS, 2=LOS + Interference, 3=NLOS and 4=NLOS + Interference), and the y-axis the Euclidean distance between the reference feature vector of a class and feature vector obtained from the received data. In Figure 54 the minimum distance is achieved between the feature vectors and Class 1, and thus packets are classified to Class 1.

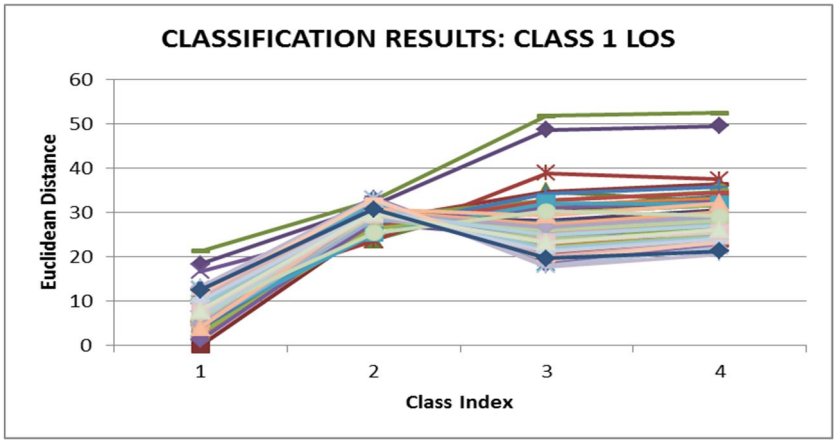

Figure 54. Classification results: Class 1

The results of classification of data packets recorded under the NLOS channel conditions are shown in Fig. 55. The Euclidean distance was calculated for the feature vectors obtained from the received data packets and reference feature vectors. Fig. 55 shows that each line has a clear minimum for the correct class, i.e. in each case the classification results in the correct class.

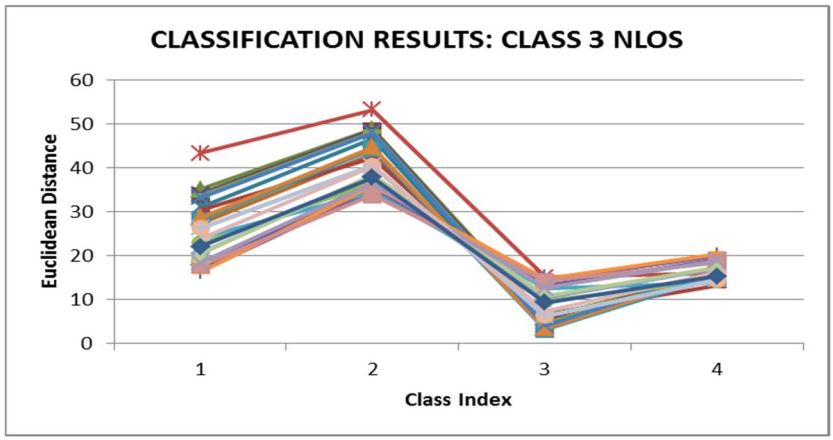

Figure 55. Classification results: Class 3

In Fig. 56 the results of classification of data packets recorded under the LOS channel state affected by a radio interference are presented. The strength of the disturbing signal varied from 50-80%, compared to our signal strength. Data packets are classified as Class 2, but where the radio interference summing up with our signal is weak, the minimum for the correct class is not so clear.

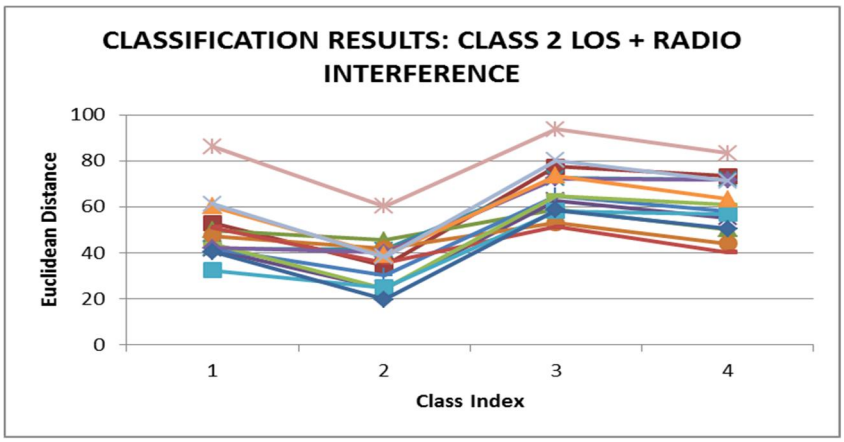

Figure 56. Classification results: Class 2

In Fig. 57 the results of classification of data packets recorded under the NLOS channel state disturbed by the radio interference are shown. In addition, overlapping with Class 3 may occur here if the radio interference is weak and the signal is only partially disturbed. This class is the most challenging to classify, since the data packets are strongly disturbed, and some are barely recognisable.

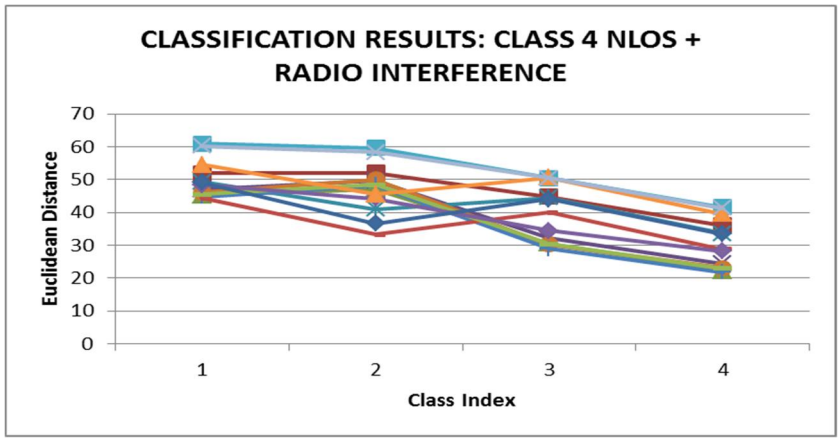

Figure 57. Classification results: Class 4

The stronger the disturbance, the clearer the classification results. The industrial environment is very complex. Usually there are several disturbances affecting the signal propagation at the same time, and in the case of a lack of dominant disturbance, classification uncertainty may occur. By testing the performance of the classifier in the parking area, we used six classes instead of four. We were

able to distinguish cases whether the radio interference affecting our signal is strong or weak, but due to the complexity of the industrial environment, we decided to classify the disturbances into four classes.

The classifier performance analysis was performed by monitoring the classifier results online while workers and forklifts occasionally blocked our signal transmission. The disturbances from the external radio interference were indicated afterwards using spectrograms recorded during the tests. The classifier performance was a bit weaker than in a static case due to the complexity of the environment, but still a correctness rate of over 90% was achieved.

6. Proposal for conceptual design of auto fault self-diagnostic system for industrial wireless sensor networks

In this chapter we present a conceptual design for an auto fault self-diagnostic system developed to address reliability issues in industrial wireless sensor networks.

The wireless sensor networks are always associated with functional uncertainty due to various disturbances in the radio channel. The most important features of the measurement network are easy installation and (re-)configuration, real-time monitoring, optimisation and alarming, also with regard to the radio network performance. The intelligent monitoring and optimisation of the radio network activity is seen by the users as operational reliability. The intelligent sensor network is also able to guide users in problem situations, for example in case the system requires a reconfiguration due to changes in the environment.

6.1 System architecture

An auto fault self-diagnostic system is being developed to improve the reliability of radio transmission in harsh environments. The system functionality is shown in Fig. 58.

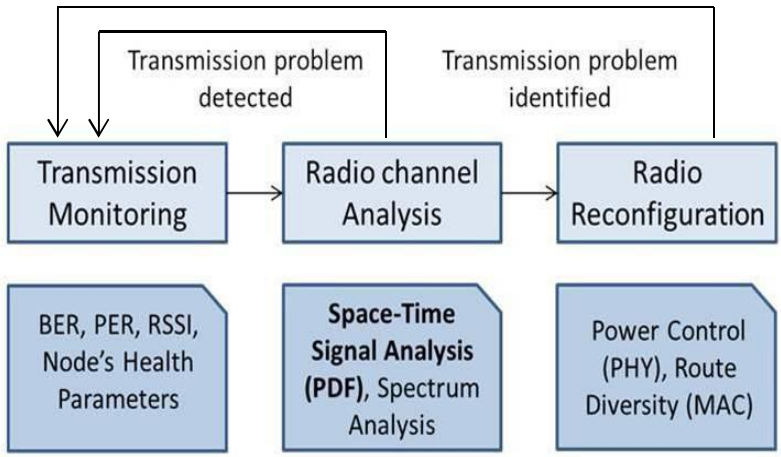

Figure 58. Auto fault self-diagnostic system

The auto fault self-diagnostic system comprises three self-contained tools; a transmission monitoring tool, a radio channel analysis tool, and a radio reconfiguration tool. The monitoring tool is developed to monitor the link quality between the nodes, the health parameters of each node (battery power, etc.), and the RSSI value if needed. The radio channel analysis tool aims to detect and identify radio transmission problems and provide channel condition information to the upper layers. The radio channel disturbance classification algorithm presented in this work forms the basis of the radio channel analysis tool. The radio reconfiguration tool is used to manage the wireless network parameters based on the information received from the radio channel analysis tool, which is in turn activated by the monitoring tool in case of transmission problems. The auto fault self-diagnostic system is planned to be integrated with the normal functionality of a WSN network and to provide additional intelligence to manage the WSN network and improve performance.

6.2 System design and implementation

The architecture of the WSN, including the SDR tool, is shown in Fig. 59. Here, the SDR is connected to the WSN gateway (GW) through 1 Gbit Ethernet. This gives the SDR the opportunity to analyse the same data which is captured by the GW, and on the other hand to reconfigure the network based on the SDR analysis through GW.

The measurement data collected by the WSN nodes is transferred to the gateway (GW), and then to the back-end system. Simple data pre-processing is performed in the WSN nodes, and more computational power required for processing

is performed in the gateway. The measurement data collected from WSN nodes may be fused either in the node or in the gateway if needed.

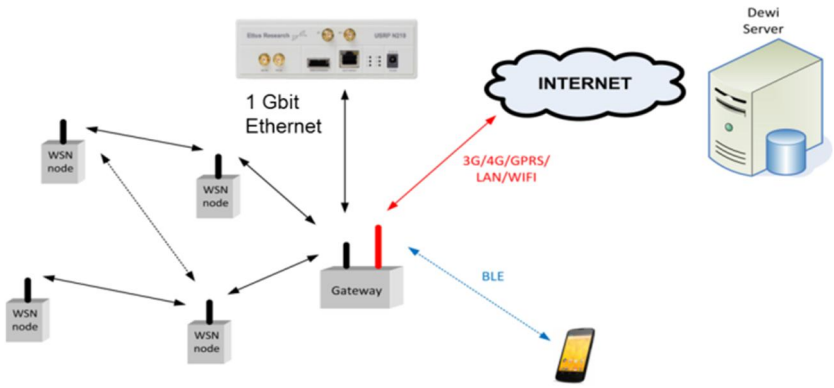

Figure 59. Wireless sensor network architecture with SDR tool

The GW monitors the quality of data transmission between the WSN nodes (RSSI, throughput), and in the case of transmission problems, the GW will activate the radio channel analysis tool (RCAT). The diagnostic tool aims to provide additional intelligence to manage the WSN network and improve performance. This tool will help the network to adapt to different transmission conditions and to optimise and ease the WSN installation process.

The communication between the GW and the back-end system is two-way and implemented using LAN, Wi-Fi or 3G/4G/GPRS. The configuration parameters – measurement-related and network performance-related – are obtained from the back-end system and transferred to the GW and WSN nodes. The WSN diagnostic information and the measurements data is transferred to the GW and the back-end system. The diagnostic information will help to optimise the network communication parameters and choose the right reconfiguration options to improve the data transmission reliability or to ease the network installation process.

6.2.1 Radio transmission monitoring tool

The radio transmission monitoring tool is used to monitor the link quality between the nodes (RSSI, packets throughput), the health parameters of each node, and to identify which node is faulty or/and which link does not work. This tool is ported to all WSN nodes, and in case of transmission problems, it sends an alarm to the GW, which decides whether there is a need to activate the radio channel analysis tool.

The main tasks of this tool are monitoring data packet transmission, the nodes' health parameters (HPs), links quality and RSSI values, identifying which node is faulty and/or which link does not work, and reporting it to the network controller, setting the network to testing mode if needed (stops data transmission), and reconfiguring the node's transmission parameters if needed (transmit power, frequency channel). This tool has been ported to VTT LittleNodes and tested in a real-life environment. The snapshot of a simple user interface is shown in Figure 60.

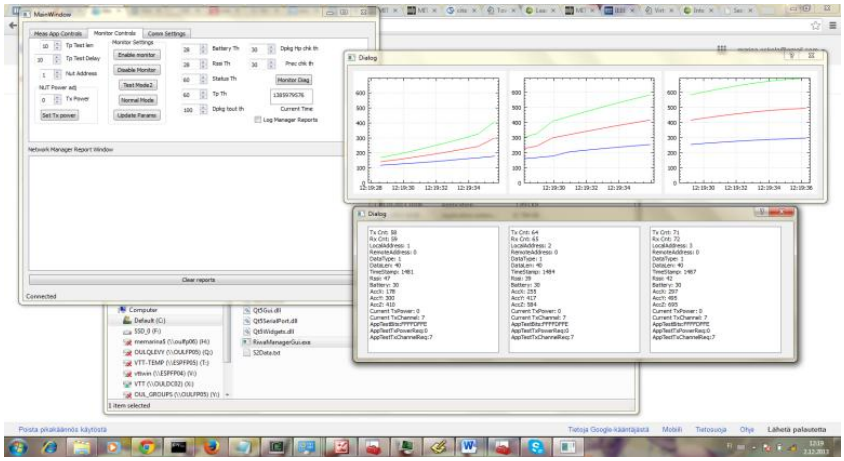

Figure 60. WSN monitoring and management tool

The user interface includes several dialogue windows; one with visualised sensor data, one with every node's HPs and every link's transmission quality information (here three nodes are used), and one where transmission parameters can be manually changed if needed. This tool will be further developed into an independent software packet that can be ported on any node. The related algorithms are described below in more details.

Nodes' health monitoring

A slave node (SN) sends its health information to a master node (MN) with every data packet (battery level, etc). The master node keeps track (table) of every node's health parameters. If some parameter exceeds the specified threshold value, the MN sends an alarm notification to the network controller (NC), here the gateway. Depending on the sensor network application (a data gathering app or an event-driven app), the MN periodically broadcasts (after specified timeout t) testing packets in order to ensure that all nodes are alive and achievable (event-driven app) or checks if a specific node is alive in case it has not sent a report after a specified timeout (t) (data gathering app); see Figures 61-62. In both cases

the MN keeps track of every node's state. Timeout t depends on how critical the data information is, and what the allowed latency is.

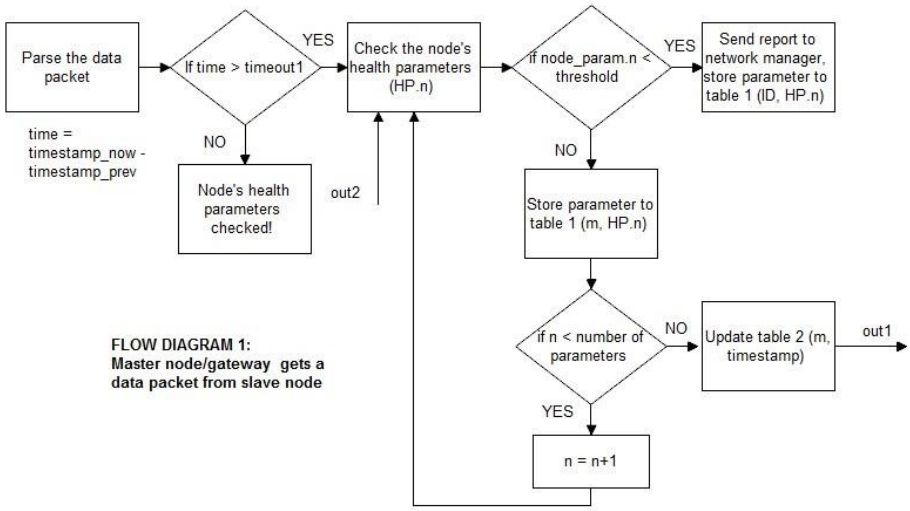

Figure 61. Data gathering app: parsing the data and checking the HPs

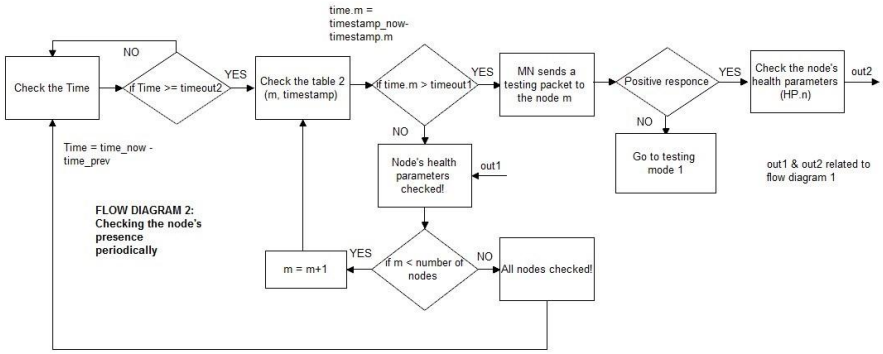

Figure 62. Event-driven app: checking the HPs periodically

If the MN does not get a response from a node, it first checks the previous values of its health parameters. If some of its values are near to its limit value (battery level is low), the MN sends a notification to the NC (here, the GW) containing the node's health condition information. If previous health values of this node are fine, the MN tries to reach the node again, and if there is still no answer, it triggers the neighbour nodes (NN) to send testing packets to this node (testing mode 1, Fig. 63).

If the NNs get a response from the node, the MN sends a notification to the NC about link quality problems between the node and the MN, and triggers Testing Mode 2. If neither of NNs get a response, the node is dead or unreachable, MN

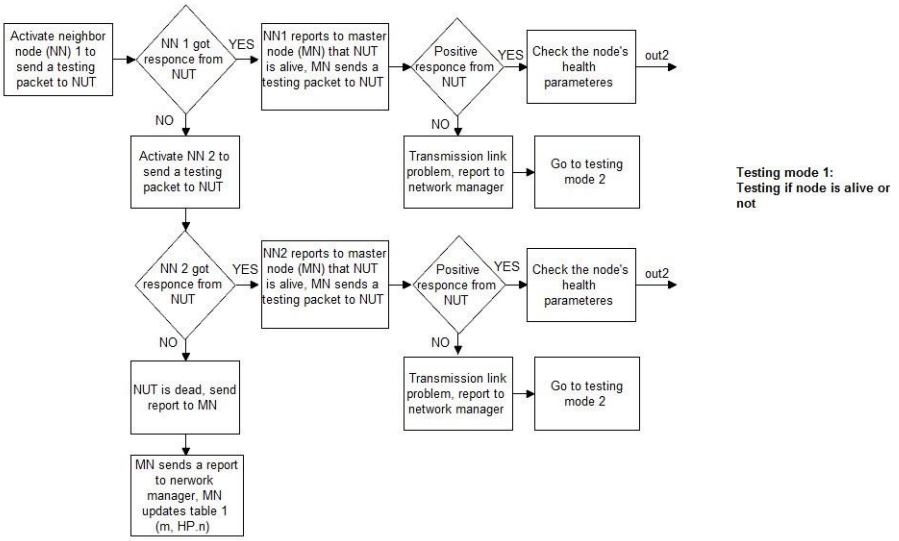

reports the situation to the NC.

Figure 63. Activating NNs, Testing Mode 1

Link state monitoring

The MN monitors the throughput (tp) and keeps a track (tables) of every SN-MN link state, see Fig. 64. If tp drops below the threshold value, the MN checks the HPs of the node. If the health parameters are OK, or if the node does not reply, the MN triggers NNs to test their radio links' state to this node (Testing Mode 2), sets the network to testing mode, and notifies the NC about the state of each link. If NNs are able to reach the node, but the MN cannot still reach the node, the radio channel analysis tool is activated in order to identify the transmission problem and reconfigure network parameters.

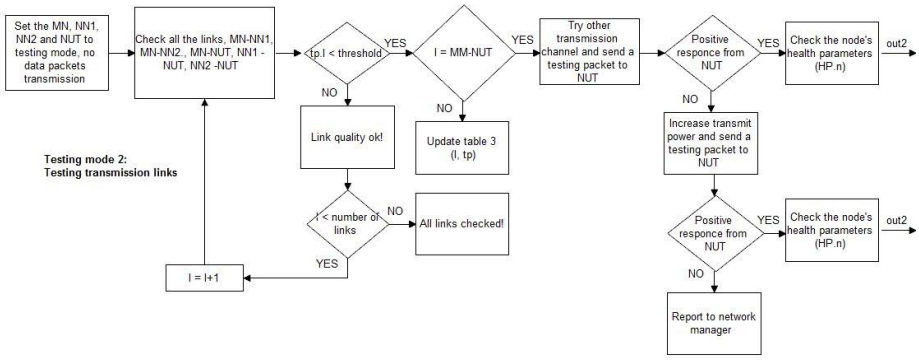

Figure 64. Testing Mode 2

6.2.2 Radio channel analysis tool

The radio channel analysis tool aims to identify the radio transmission problems and provide channel condition information to the upper layers or network management unit (here network management unit = GW). It utilises the software defined radio to enable the accurate radio channel state analysis and radio channel disturbances classifier. The classification algorithm is presented in details in previous chapters.

Considering the use of SDR in typical IWSN scenarios, the deployability in the context of portability and battery-based operation capability ensure the easy deployment of the SDR tool in a factory environment. Portability is determined by the physical size of the SDR and power consumption. Two types of platforms can be employed; desktop and embedded SDR. The desktop SDR is a high-end platform which relies on large FPGAs and powerful desktop computers. However, the price for high computing performance is limited portability. The embedded SDR systems are stand-alone devices optimised for compact size and low-power operation. The USPR-embedded platforms use both FPGA and an embedded CPU to provide a significant amount of computational resources in a power-efficient manner.

The actual steps to implement the algorithms onto embedded systems have not yet been taken, but they are included in our future plans. There are several design approaches for mapping the algorithms to the embedded SDR. The model-based design is a high-level approach that allows developers to program the board and generate code by building models using visual design software such as MATLAB/Simulink. MATLAB/Simulink has a variety of signal processing blocks and it can generate various types of code: C/C++ for MCU, DSP; VHDL/Verilog for FPGA/ASIC; and SPICE for Analogue Devices. The Simulink HDL Coder generates HDL code (VHDL/Verilog) for FPGAs from Simulink models. Developers also have the option of taking the board-based design approach and writing code in C

or HDL. The individual blocks of the MATLAB processing chain can also be progressively ported to the GNU Radio framework. GNU Radio is an open source software toolkit and it has support for Ettus USPR hardware. Signal processing blocks are written in C++ programming language. Python is used to connect these signal processing elements together to form a flow graph. Python uses a simplified wrapper and interface grabber (SWIG) for the purpose of interfacing C++ routines with python front end applications. There are more than 100 signal processing blocks in GNU Radio, such as mathematical calculation, frequency modulation, different filters, convolutional code, etc. Moreover, it is not difficult to add new signal processing block to GNU Radio. An important objective is to reuse signal processing blocks that are already available in GNU Radio whenever possible. GNU Radio has been working with OpenEmbedded on developing a way to build and deploy GNU Radio Linux systems on embedded devices. The purpose of using OpenEmbedded, or OE, is to provide a stable base and consistent behaviour between devices. Regardless of which design approach is taken, the exact same executable files are generated, and they must be downloaded onto the SDR for the board to be functional.

Our final goal is to implement the algorithms developed in MATLAB onto an embedded platform. A proposal for a flow graph of the classifier code blocks is depicted in Figure 65.

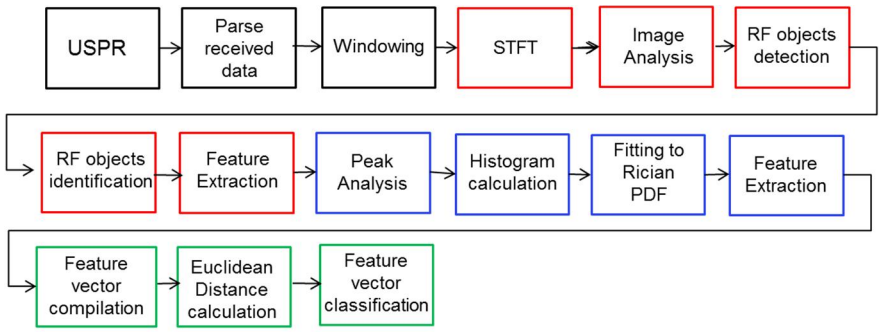

Figure 65. Flow graph of coding elements

The received data is collected using the rx_samples_to_file function provided by UHD/USPR, which stores data in complex float, which is in binary format. In the complex float format, the data is encoded with 64 bits, 32 bits for I and 32 bits for Q. The data is sampled with a 10Msps sample rate, and thus after parsing the binary data to the I + jQ format, we get a 1x10000000 complex double vectors of data samples, each from a 1-second period of time. The data is oversampled for research purposes, and the implementation phase can be reduced to the Nyquist sample rate. The vector of data is windowed, and STFT is calculated for each window of data.

The red blocks in the flow graph (Fig. 65) represent the signal analysis flow in the frequency domain. The spectrogram of a window of data is saved in image

format, and image analysis tools are applied to detect the RF objects from the spectrogram. From all detected RF objects, the RF object for our signal is identified and parametrised, and features (centre frequency *f,* width of the frequency band *Δf*, and signal duration *Δt*) are extracted.

The implementation issues in spectrum sensing for cognitive radios are broadly described in [83]. The critical design problem is the need to process the multi-gigahertz wide bandwidth and reliably detect the presence of primary users. This poses several challenges on the requirements related to the sensitivity, linearity, and dynamic range of the circuitry in the RF front end. In our case there is no need to process the whole gigahertz wide bandwidth, but only the bandwidth of our signal transmission. During the radio channel analysis, we aim to detect the interference signals that are disturbing our signal transmission in time and frequency domains. Thus, for spectrogram analysis we only need to know if there are any transmissions on the bandwidth used by our sensor nodes. In our tests we processed 5 MHz frequency bands (our signal BW = 2MHz), and obtained the required information on other radio transmissions using the same band and on the overlapping issues with our radio transmissions. Observing the recorded data (BW = 5MHz) in frequency and time domains, we can make a good guess as to which signal is disturbing our radio transmissions, WLAN or Bluetooth or signal from other sensor nodes in our network. If our signal BW is wider than the dynamic range of the RF front end, processing a frequency band narrower than the bandwidth of our signal will cause some limitations on the PDF analysis of our signal; see Figure 66.

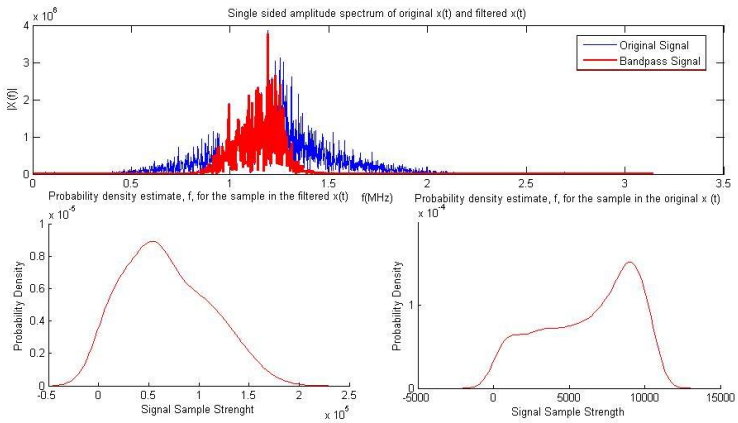

Figure 66. Bandpass filtered signal

We will lose useful information since it is important to analyse all the frequency components of the signal, and the interference signal may overlap with those frequency components of the signal which were filtered by the front end. In addition, the frequency-selective fading cannot be reliably detected. However, evi-

dence of signal attenuation and passive radio disturbances can still be detected (trucks, workers, etc.).

During the radio reconfiguration phase, we may need to obtain the information on the whole ISM band in order to choose the less crowded channel. The spectrum sensing in this case can be performed by scanning one frequency channel at a time, and merging the channels' spectrum data in a processing unit.

The coding blocks in blue in the flow diagram (Fig. 65) represent the signal analysis flow in the time domain. The peak analysis detects the exact time window of our signal. The histogram is calculated for the detected time window, matched to the Rician PDF, and features (*a* value, *sigma* value, and goodness of fit *fit_err*) are extracted. In this work we used MATLAB function (fitdist) to match the received signal samples with theoretical Rician distribution, but in the case of an embedded solution, the maximum likelihood estimation used by fitdist function is computationally too demanding. We propose to use a library of pre-simulated Rician distributions with different a and sigma parameters instead and match the histograms of the received signal magnitudes to these pre-simulated histograms of Rician PDFs, find the best match, and obtain the corresponding parameters (*a* value, *sigma* value, and goodness of fit *fit_err*). The indicative picture of the received signal's histogram matching to the predefined Rician PDFs is shown in Fig. 67.

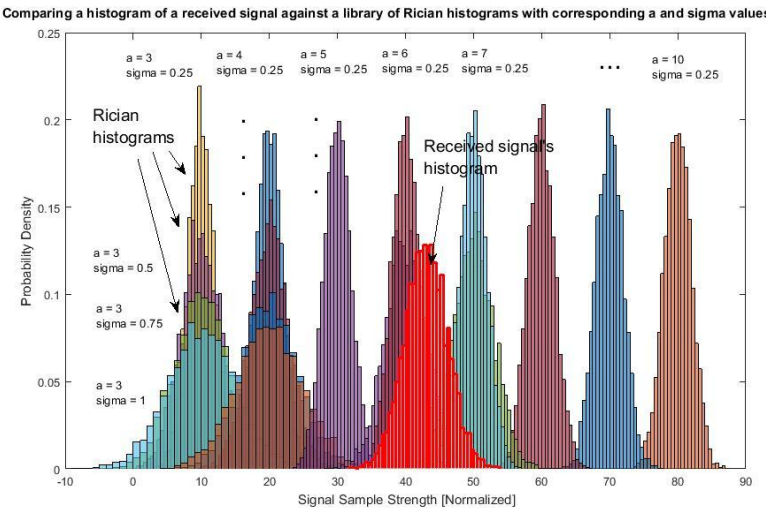

Figure 67. Histograms matching to predefined Rician PDFs

The histogram provides a graphical record of the shape of the data distribution. The x-axis shows all the possible values, and the y-axis shows the percentage of input samples that had each corresponding value. The continuously-valued counterpart of the histogram is the probability density function (PDF). The histogram is

simply an approximation of a PDF: the count of how many samples has each possible value in the range. The x-axis (=signal level strength) of both the pre-simulated Rician histograms and received data histograms must be scaled to avoid the dependence on the distances between the nodes, since in PDF analysis the variation of the histograms shape is essential, rather than an absolute level of the received signal strength. To compare the histograms of the received signal and predefined Rician histograms, and to find the histogram that matches the best, we use the chi-squared measure χ^2, which is typical for expressing similarities/differences in histograms [95]. The chi-squared histogram matching distance is calculated from Equation [14].

$$\chi^2(h_i, h_j) = \frac{1}{2}\sum_{m=1}^{K}\frac{[h_i(m)-h_j(m)]^2}{h_i(m)+h_j(m)} \quad [14]$$

Where
h_i = histogram i
h_j = histogram j
k = number of bins.

Thus, the histogram of the received signal is compared with the theoretical Rician histogram using the chi-squared method, and the features from the best match are obtained. The chi-squared measure has been successfully used for texture and object categories classification [100], near duplicate image identification [101], shape classification [102] and boundary detection [103]. Like other bin-to-bin distances such as the L1 and the L2 norms, it is sensitive to quantisation effects and depends on the number of bins. If the number of bins is low, the distance is robust, but not discriminative; if it is high, the distance is discriminative, but not robust [104]. The histogram comparison is presented in [100].

The green boxes in the flow diagram (Fig. 65) indicate the classification process; the obtained feature vector is compared with the reference vectors and the minimum Euclidean distance is calculated. The implementation process from MATLAB code to embedded platforms is also described in general in [63] - [67].

6.2.3 Radio reconfiguration tool

The radio reconfiguration tool is used to manage the network parameters based on the information received from the radio channel analysis tool. The decision is made either in GW or in the back-end system. The reconfiguration parameters are then transferred to the WSN nodes. In our network we can reconfigure the following transmission parameters of the sensor nodes: transmit power, data rate, frequency channel (PHY level). We can also provide the channel condition information to the upper layers (MAC and higher), i.e. to optimise the routing algorithms.

We performed BER tests at different data rates (250 kbits, 2 Mbits) and transmission power levels (+4 dBm, -8 dBm) in order to study which radio parameters should be reconfigured in a case of temporal fading to minimise the BER value. The results show that BER tends to sensitively increase at higher transmission rates in industrial environments. Note that higher transmission rates are achieved by using more aggressive modulation schemes (denser constellations with more closely located points), making the data transmission more vulnerable to disturbances. The impact of transmit power configurations on the BER value was smaller than expected, but naturally it affects the number of the packets that the receiver did not receive at all in cases where the RSSI value dropped below the receiver's sensitivity value. The number of erroneous bits observed in the NLOS states is randomly distributed and strongly affected by radio configurations (transmit power, data rate). The results of these tests are reported in [97].

In the network design phase, the transmission parameters should be set very carefully. In [89] the authors have investigated the optimal common transmission power for wireless sensor networks. As opposed to following the conventional graph-theoretic approach, they consider connectivity from a more realistic viewpoint by taking into account the characteristics of a wireless communication channel. The study shows that, for a given data rate and a given maximum tolerable BER at the end of a multihop route, there exists an optimal transmit power. Moreover, for a given value of the maximum tolerable route BER, there exists a global optimal data rate for which the optimal common transmit power is the minimum possible. This suggests that the data rate, if chosen carefully, can guarantee significant savings in terms of transmit power, prolonging the battery life of devices and network lifetime.

However, even careful design cannot predict all the factors that can lead to connectivity degradation in WSN. Therefore, effective and efficient mechanisms should be provided to achieve reliability with low energy expenditure. Different WSN applications have different reliability requirements. For instance, industrial control or military applications might require nearly 100% reliability. On the other hand, environmental monitoring applications might tolerate message loss, leading to a trade-off between energy conservation and reliability. For energy efficiency, the WSN protocol stack needs to be tuned according to actual needs. The traffic and network conditions in a WSN are often very dynamic, due to the noisy wireless channel and the failure probability of sensor nodes (e.g. when they run out of battery power). Thus, energy-aware and reliable data collection mechanisms should be able to adapt to the actual operating conditions. In [107] the authors propose an adaptive and cross-layer approach for reliable and energy-efficient data collection in WSNs based on IEEE 802.15.4/ZigBee standards. Their approach involves an energy-aware adaptation module that captures the application's reliability requirements and autonomously configures the MAC layer, based on the network topology and current traffic conditions. The ADaptive Access Parameters Tuning (ADAPT) algorithm has been developed based on an analytical study of the IEEE 802.15.4 standard. ADAPT is simple and lightweight, and uses only information local to the sensor nodes. As a result, it is fully distributed, and

has a very low complexity, thus being well suited for resource-constrained sensor nodes.

The radio reconfiguration tool is an algorithm that aims to choose the optimal transmission parameters based on the information provided by the radio channel analysis tool. In the same manner as the ADAPT tool, it applies the cross-layer approach and adapts to varying transmission conditions by autonomously configuring the transmission parameters. Unlike the ADAPT tool, it uses the measurement information obtained from the physical level to adapt to varying channel states.

The principles of employing the auto fault self diagnostic system in real environments are shown in Fig. 68.

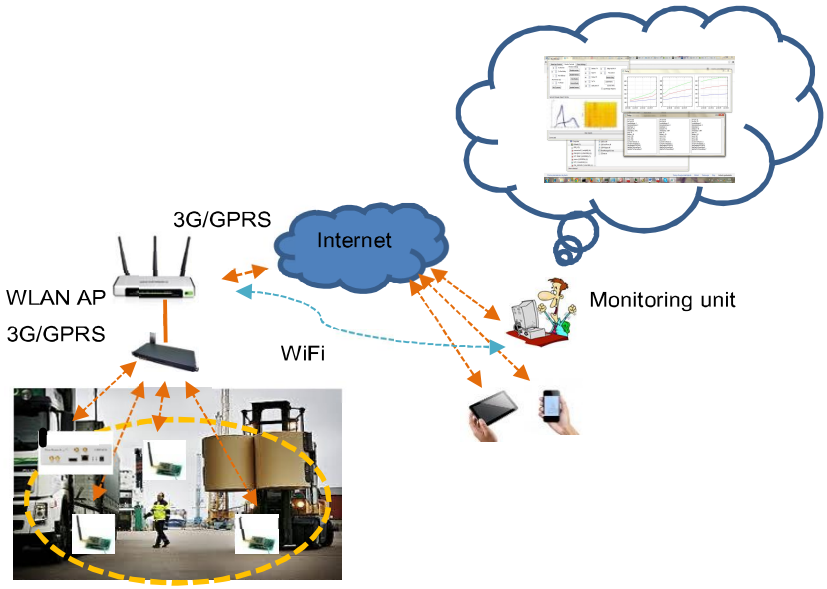

Figure 68. Auto fault self-diagnostic system

The sensor nodes autonomously monitor their health parameters and link quality, and in the case of transmission problems, the information is sent through the GW to the cloud, from where it can be obtained by the monitor unit (PC, tablet, smartphone). The channel analysis tool can be turned on automatically or manually and remotely. After the transmission problem is identified, the optimal decision for the network reconfiguration can be done, also either automatically or manually and remotely.

7. Discussion and future directions

The transmission links between the nodes in wireless sensor networks should be reliable and secure, even in extreme conditions. Changes in external environmental factors and radio conditions along with the multipath propagation phenomena lead to unpredictable signal fading and may cause poor performance in a communication system. Detection and identification of a physical phenomenon that is behind the transmission problem will help us to choose the right actions to overcome the degradation of link quality by providing channel condition information to the upper layers (MAC, network and higher layers). Depending on the interference type (fading or radio interference), we must apply specific adaptation algorithms, like power control (PHY layer) or route diversity (network layer) to overcome the transmission problems caused by radio channel disturbances.

In this work we have described a signal analysis and classification procedure to detect and identify radio disturbances, and introduced the results from the tests performed in a real industrial environment. The PDF-based radio channel analysis method can be used to detect passive radio disturbances, also when RSSI and BER data is not available. Spectrum analysis offers additional valuable information on the radio frequency channel congestion state for disturbance classification. The performed tests showed that our analysis methods are applicable to radio disturbance detection, identification and classification. The classifier proved capable of distinguishing between passive (obstacle, truck) and active disturbances (radio interference) affecting the radio signal propagation.

Leaning on our results, we propose a cognitive radio paradigm for wireless sensor networks to cope with radio channel disturbances. The definition of cognitive radio (CR) is given in the IEEE 1900.1 WG draft: “CR is radio in which communication systems are aware of their environment, internal state, and location and can make decisions about their radio operating behaviour based on that information. Cognitive radio utilises software-defined radio, adaptive radio, and other technologies to autonomously adjust its behaviour or operations to achieve the desired objectives.” Cognitive radio can be exploited to address the unique challenges of IWSN applications, which are time and space-varying spectrum characteristics, reliability and latency, harsh propagation conditions, and energy constraints for low-power sensor nodes.

Recent studies have reported on radio interference cognition, spectrum sensing, monitoring and management. In our work, we aimed to expand the environmental awareness to also include physical environment cognition (obstacles, trucks). Besides industrial wireless sensor networks, this can also be beneficial in many future applications, such as for self-driving delivery robots on city pavements having issues with reflections from surrounding buildings, leading to self-localisation errors.

The auto fault self-diagnostic tool is planned to be integrated with the normal functionality of a WSN network and to provide additional intelligence to manage the WSN network and improve performance. Our final goal is to implement WISE-NEMO sub-tools, the radio transmission monitoring tool (RTMT), the radio channel analysis tool (RCAT) and the radio reconfiguration tool (RRT) as independent software packages which can be ported to the embedded platforms. This will require the optimisation of the code and lightening of the algorithm. The RTMT is already ported to the sensor nodes, and has been in use in different WSN applications. The RCAT is the biggest software package, requiring the high computational and energy resources of a platform. The RRT is to be ported on all sensor nodes, including sink nodes and gateway. The sub-tools can be applied all together to improve radio transmission reliability, or as independent packages for different applications.

8. Conclusion

We have presented the performance results of the radio channel disturbance classifier, and its applicability to industrial environments. The harsh signal propagation conditions in environments like factories may cause substantial degradation of wireless link performance, and lead to loss of time and money. We discussed the most disruptive disturbances of signal transmission in factory environments; disturbances caused by other wireless devices (co-channel and adjacent interference), environmental characteristics such as metal constructions and the presence of heavy equipment (signal fading), and by electrical and mechanical equipment (noise).

In this work, we described the methods and principles to identify and classify radio channel disturbances. The probability density function (PDF) channel state analysis method is based on the idea that changes in statistical properties of the received signal are strongly correlated with the transitions of the channel states. Spectral analysis is based on the spectrograms calculation of the received signal and obtaining the statistical information of the radio interferences with image analysis tools. By combining the results of signal analysis in time and frequency domains, we constructed a classifier to classify the radio channel disturbances. We tested the classifier functionality in a real industrial environment, and discussed the development process of the classifier towards an embedded SDR platform. The classifier proved to be a feasible solution for improving the reliability of wireless transmission and will be further developed into a portable, small-sized SDR-based tool.

Especially for cases where errors are too severe for the successful demodulation of the signal, and where RSSI or BER values cannot be accessed due to lost packets, the PDF parameters can provide the necessary information on the current channel state and possible disturbance objects. Identification of a physical phenomenon that is behind transmission problems will help to predict and successfully solve these problems by providing channel condition information to the upper layers. Depending on the interference type (fading or radio interference), specific adaptation algorithms must be applied, like power control (PHY layer) or route diversity (network layer) to overcome transmission problems.

9. References

1. A. Willig, K. Matheus & A. Wolisz (2005) Wireless Technology in Industrial Networks, Proc. IEEE, vol. 93, no. 6, pp. 1130–1151
2. A. Willig (2008) Recent and Emerging Topics in Wireless Industrial Communication, IEEE Trans. Industrial Informatics, vol. 4, no. 2, pp. 102–124
3. V.C. Gungor & G.P. Hancke (2009) Industrial Wireless Sensor Networks: Challenges, Design Principles, and Technical Approaches, IEEE Trans. Industrial Electronics, vol. 56, no. 10, pp. 4258–4265
4. M. Paavola & K. Leivisk (2010) Wireless Sensor Networks in Industrial Automation, Factory Automation, book edited by Javier Silvestre-Blanes, ISBN 978-953-307-024-7
5. Ian F. Akyildiz & Mehmet Can Vuran (2010) Wireless Sensor Networks, book, ISBN 978-047-051-519-8
6. L. Xu (2011) Enterprise systems: State-of-the-art and future trends, IEEE Trans. Ind. Inf., vol. 7, no. 4, pp. 630–640
7. J. Zheng, D. Simplot-Ryl, C. Bisdikian & H.T. Mouftah (2011) The internet of things, IEEE Commun. Mag., vol. 49, no. 11, pp. 30–31
8. J. Åkerberg, M. Gidlund & M. Bjorkman (2011) Future Research Challenges in Wireless Sensor and Actuator Networks Targeting Industrial Automation, 9th IEEE International Conference on Industrial Informatics (INDIN), pp. 410–415
9. M. Nobre, I. Silva & L.A. Guedes (2014) Reliability Evaluation of WirelessHART Under Faulty Link Scenarios, 12th IEEE International Conference on Industrial Informatics, pp. 676–682
10. S. Petersen & S. Carlsen (2009) Performance Evaluation of WirelessHART for Factory Automation, 14th IEEE International Conference on Emerging Technologies & Factory Automation, pp. 1–9
11. "ISA100", http://www.isa100wci.org/
12. T. Lennvall, S. Svensson, & F. Hekland (2008) A Comparison of WirelessHART and Zigbee for Industrial Applications, IEEE International Workshop on Factory Communication System, pp. 85–88
13. S. Petersen & S. Carlsen (2011) WirelessHART vs ISA100.11a: The Format War Hits the Factory Floor, IEEE Industrial Electronics Magazine, Volume: 5, Issue: 4, pp. 23–34

14. K. Gravogl, J. Haase & C. Grimm (2011) Choosing the best wireless protocol for typical applications, 24rd International Conference on Architecture of Computing Systems (ARCS), pp. 279–184
15. D. Cavalcanti, S. Das, J. Wang & K. Challapali (2008) Cognitive Radio-based Wireless Sensor Network, Proceedings of 17th International Conference on Computer Communications and Networks, pp. 1–6
16. M. Conti & S. Giordano (2007) Multihop Ad Hoc Networking: The Reality, IEEE Communications Magazine, Volume: 45, Issue: 4, pp. 88–95
17. A. Willing (2008) Recent and Emerging Topics in Wireless Industrial Communications: A Selection, IEEE Transactions On Industrial Informatics, Vol. 4, No. 2, pp. 102–124
18. L. Zheng (2010) Industrial Wireless Sensor Networks and Standardizations, The Trend of Wireless Sensor Networks for Process Automation, Proceedings of SICE Annual Conference, pp. 1187–1190
19. L. Hou & N. Bergmann (2010) System Requirements for Industrial Wireless Sensor Networks, Proceedings of 15th IEEE International Conference on Emerging Technologies and Factory Automation, pp. 1–8
20. J. Åkerberg, M. Gidlund & M. Björkman (2011) Future Research Challenges in Wireless Sensor and Actuator Networks Targeting Industrial Automation, 9th IEEE International Conference on Industrial Informatics (INDIN), pp. 410–415
21. K.S. Low, W.N.N. Win & M.J. Er (2005) Wireless Sensor Networks for Industrial Environments, International Conference on Computational Intelligence for Modelling, Control and Automation and International Conference on Intelligent Agents, Web Technologies and Internet Commerce, (Volume: 2), pp. 271–276
22. J. Song, A.K Mok, D. Chen & M. Nixon (2006) Using real-time logic synthesis tool to achieve process control over wireless sensor networks, Proceedings of the 12th IEEE International Conference on Embedded and Real-Time Computing Systems and Applications (RTCSA'06), pp. 420–426, ISBN 0-7695-2676-4
23. J. Heo, J. Hong & Y. Cho (2009) EARQ: Energy aware routing for real-time and reliable communication in wireless industrial sensor networks, IEEE Transactions on Industrial Informatics, Vol. 5, No. 1, pp. 3–11, ISSN 1551-3203
24. J. Al-Karaki & A. Kamal (2004) Routing techniques in wireless sensor networks: A survey. IEEE Wireless Communications, Vol. 11, No. 6, pp. 1536–1284, ISSN 1536-1284
25. I.F. Akyildiz, W. Su, Y. Sankarasubramaniam & C. Cayirci (2002) Wireless sensor networks: a survey. Computer Networks, Vol. 38, No. 4, pp. 293–442, ISSN 1389-1286
26. A. Rowe, R. Mangharam & R. Rajkumar (2008) RT-link: a global time-synchronized link protocol for sensor networks. Ad Hoc Networks, Vol. 6, No. 8, November 2008, pp. 1201–1220, ISSN 1570-8705.
27. A. Flammini, D. Marioli, E. Sisinni & A. Taroni (2007) A real-time wireless sensor network for temperature monitoring, Proceedings of the IEEE International Symposium on Industrial Electronics, ISIE 2007, pp. 1916–1920, ISBN 978-1-4244-0755-2

28. P. Neumann (2007) Communication in industrial automation – What is going on? Control Engineering Practice, Vol. 15, No.11, November 2007, pp. 1332–1347, ISSN 0967-0661
29. T. Watteyne, S. Lanzisera, A. Mehta & K. Pister (2010) Mitigating multipath fading through channel hopping in Wireless Sensor Networks, IEEE International Conference on Communications (ICC), pp. 1–5, ISSN 1550-3607
30. K. Srinivasan & P. Levis (2006) RSSI is Under Appreciated, Proceedings of the Third Workshop on Embedded Networked Sensors (EmNets)
31. "WINA", http://www.wina.org
32. I. Howit, W.W. Manges, P.T. Kuruganti, G. Allgood & J.A. Gutierrez (2006) Wireless industrial sensor networks: Framework for QoS assessment and QoS management, ISA transactions, Vol. 45, No 3, pp. 347–359
33. R. Zurawski (2014) Industrial Communication Technology Handbook, book CRC Press, 1756 p.
34. S. Peterson & S. Carlsen (2009) Performance Evaluation of WirelessHART for Factory Automation, IEEE Conference on Emerging Technologies & Factory Automation, pp. 1–9, ISSN 1946-0759
35. A. Araujo, J. Blesa, E. Romero & D. Villanueva (2012) Security in cognitive wireless sensor networks. Challenges and open problems, EURASIP Journal on Wireless Communications and Networking, ISSN 1687-1499
36. A. Willig, M. Kubisch, C. Hoene & A. Wolisz (2002) Measurements of a Wireless Link in an Industrial Environment Using an IEEE 802.11 – Compliant Physical Layer. IEEE Transactions of Industrial Electronics, vol. 49, no. 6, pp. 1265–1282
37. V.C. Gungor & G.P. Hancke (2009) Industrial wireless sensor networks: Challenges, design principles, and technical approaches, IEEE Trans. Ind. Electron., vol. 56, no. 10, pp. 4258–4265
38. Y. Yang, Y. Xu, X. Li & C. Chen (2011) A Loss Inference Algorithm for Wireless Sensor Networks to Improve Data Reliability of Digital Ecosystems, IEEE Transactions of Industrial Electronics, vol. 58, no. 6, pp. 2126–2137.
39. A. Ulusoy, O. Gurbuz, & A. Onat (2011) Wireless Model-Based Predictive Networked Control System Over Cooperative Wireless Network. IEEE Transactions on Industrial Informatics, vol. 7, no. 1, pp. 4 –51.
40. A. Kato & K. Ohnishi (2005) RTLinux based bilateral control system with time delay over network, in Proc. IEEE Int. Symp. Ind. Electron., pp. 1763–1768
41. K. Srinivasan & P. Levis (2006) RSSI is Under Appreciated, Proceedings of the Third Workshop on Embedded Networked Sensors (EmNets)
42. A. Vlavianos, L.K. Law, I. Broustis, S. V. Krishnamurthy & M. Faloutsos (2008) Assessing Link Quality in the IEEE 802.11 Wireless Networks: Which is the Right Metric, IEEE 19th International Symposium on Personal, Indoor and Mobile Radio Communications, pp. 1–6, ISSN 978-1-4244-2643-0
43. P. Ängskog, C. Karlsson, J.F. Coll, J. Chilo & P. Stenumgaard (2010) Sources of Disturbances on Wireless Communication in Industrial and Factory Environments, Asia-Pacific International Symposium on Electromagnetic Compatibility, pp. 281–284, ISSN 978-1-4244-5621-5

44. P. Stenumgaard, J. Chilo, J.F. Coll & P. Ängskog (2013) Challenges and Conditions for Wireless Machine-to-Machine Communications in Industrial Environments, IEEE Communications Magazine (Volume: 51, Issue: 6), pp. 187–192, ISSN 0163-6804
45. E. Sisinni, P. Archetti, M. Manenti & E. Piana (2012) High availability wireless temperature sensors for harsh environments, IEEE Sensors Applications Symposium (SAS), pp. 1–6, ISSN 978-1-4577-1724-6
46. T.S. Rappaport (1989) Indoor Radio Communications for Factories of the Future, IEEE Communications Magazine
47. W. Jakes (1974) Microwave Mobile Communications, Wiley
48. R.S. Kennedy (1969) Fading Dispersive Communication Channels, Wiley
49. P. Yegani & C.D. McGillem (1991) Statistical Model for the Factory Radio Channel, IEEE Transactions On Communications, Vol 39, No 10, pp. 1445–1454, ISSN 0090-6778
50. E. Toscano & L.L. Bello (2008) Cross-Channel Interference in IEEE 802.15.4 Networks IEEE International Workshop on Factory Communication Systems, pp. 139–148, ISSN 978-1-4244-2349-1
51. S.Y. Shin, H.S. Park, S. Choi & W.H. Kwon (2005) Packet Error Rate Analysis of IEEE 802.15.4 under IEEE 802.11b Interference, Proc. Wired/Wireless Internet Commun., pp. 279–288
52. S.Y. Shin, H.S. Park, S. Choi & W.H. Kwon (2007) Packet Error Rate Analysis of ZigBee Under WLAN and Bluetooth Interferences, IEEE Trans. on Wireless Comm, vol. 6, no. 8, pp. 2825–2830
53. J. Heo, J. Hong, & Y. Cho (2009) EARQ: Energy Aware Routing for Real-Time and Reliable Communication in Wireless Industrial Sensor Networks, IEEE Transactions on Industrial Informatics, vol. 5, no. 1, pp. 3–11, ISSN 1551-3203
54. J. Niu, L. Cheng, Y. Gu, L. Shu & S.K. Das (2014) R3E: Reliable Reactive Routing Enhancement for Wireless Sensor Networks, IEEE Transactions On Industrial Informatics, Vol. 10, No. 1, pp. 784–794, ISSN 1551-3203
55. P. Suriyachai, U. Roedig & A. Scott (2012) A Survey of MAC Protocols for Mission-Critical Applications in Wireless Sensor Networks, IEEE Communications Surveys & Tutorials, Vol. 14, No. 2, pp. 240–264, ISSN 1553-877X
56. D. Yang, Y. Xu, H. Wang, T. Zheng, I. Zhang, H. Zhang & M. Gidlund (2015) Assignment of Segmented Slots Enabling Reliable Real-Time Transmission in Industrial Wireless Sensor Networks, IEEE Transactions on Industrial Electronics, vol. 62, no. 6, pp. 3966–3977, ISSN 0278-0046
57. K. Mikhaylov, J. Tervonen, J. Heikkilä & J. Känsäkoski (2012) Wireless Sensor Networks in Industrial Environment, 2nd Baltic Congress Future Internet Communications (BCFIC). pp. 271–276, ISSN 0-7695-2504-0
58. E. Tanghe, W. Joseph, L. Verloock, L. Martens, H. Capoen, K. Herwegen & W. Vantomme (2008) The Industrial Indoor Channel: Large-Scale and Temporal Fading at 900, 2400, and 5200 MHz, IEEE Transactions on Wireless Communications, (Volume: 7, Issue: 7), pp. 2740–2751, ISSN 1536-1276

59. T.S. Rappaport & C.D. McGillem (1989) UHF Fading in Factories, IEEE Journal on Selected Areas in Communications, (Volume: 7, Issue: 1), pp. 40–48, ISSN 0733-8716
60. G.D. Durgin (2003) Space-Time Wireless Channels, Prentice Hall Communication Engineering and Emerging Technologies Series, 335 p.
61. Ettus, http://www.ettus.com/
62. J.S.C. Turner, M.F. Ramli, L.M. Kamarudin, A. Zakaria, A.Y.M. Shakaff, D.L. Ndzi, C.M. Nor, N. Hassan & S.M Mamduh (2013) The Study of Human Movement Effect on Signal Strength for Indoor WSN Deployment, IEEE Conference on Wireless Sensors (ICWiSe2013), pp. 30–35
63. D. Xu, R. Tongret, Y.F. Zheng & R.L. Ewing (2010) Wavelet-Modulated Pulse for Compressive Sensing in SAR, Proceedings of the IEEE National Aerospace and Electronics Conference (NAECON), pp. 197–202, ISSN 0547-3578
64. Y. Ren, D. Yao & X. Zhang (2011) The Implementation of TETRA using GNU Radio and USRP, IEEE 4th International Symposium on Microwave, Antenna, Propagation, and EMC Technologies for Wireless Communications (MAPE), pp. 363–366, ISSN 978-1-4244-8265-8
65. A. Mate, K. Lee & I. Lu (2011) Spectrum Sensing Based on Time Covariance Matrix Using GNU Radio and USRP for Cognitive Radio, IEEE Long Island Systems, Applications and Technology Conference (LISAT), pp. 1–6, ISSN 978-1-4244-9878-9
66. P. Fuxjäger, A. Costantini, D. Valerio, P. Castiglione, G. Zacheo, T. Zemen & F. Ricciato (2013) IEEE 802.11p Transmission Using GNURadio, 6th Karlsruhe Workshop on Software Radios, pp. 1–4
67. T.J. O'Shea, T.C. Clancy & H.J. Ebeid (2007) Practical Signal Detection And Classification in Gnu Radio, SDR Forum Technical Conference
68. C.A. Levis, J.T. Johnson & F.L. Teixera (2010) Radiowave Propagation, Physics and Applications, Wiley, 295 p.
69. J. Han, S. Lee, H. Kim & Y. Lee (2011) Performance improvement of IEEE 802.15.4 in the presence of co-channel interference, IEEE Wireless Communications and Networking Conference (WCNC), pp. 49–54, ISSN 1525-3511
70. B. Saleh, M.J.N. Sibley & P. Mather (2014) Energy efficient cluster scheduling and interference mitigation for IEEE 802.15.4 network, International Computer Science and Engineering Conference (ICSEC), pp. 244–250, ISSN 978-1-4799-4965-6
71. N.J. LaSorte, S.A. Rajab & H.H. Refai (2012) Developing a Reproducible Non-Line-of-Sight Experimental Setup for Testing Wireless Medical Device Coexistence Utilizing ZigBee, IEEE Transactions on Biomedical Engineering, (Volume: 59, Issue: 11), pp. 3221–3229, ISSN 0018-9294
72. G. Breed (2003) Bit Error Rate: Fundamental Concepts and Measurement Issues, High Freq. Electron., vol. 2, no. 1, pp. 46–47
73. J. Zhao & R. Govindan (2003) Understanding packet delivery performance in dense wireless sensor networks, in Proc. ACM SENSYS, pp. 1–13.
74. G. Zhou, T. He, J.A. Stankovic, & T. Abdelzaher (2005) RID: Radio interference detection in wireless sensor networks, in Proc. IEEE INFOCOM, pp. 891–901

75. M. Zuniga & B. Krishnamachari (2007) An analysis of unreliability and asymmetry in low-power wireless links, ACM Trans. Sensor Netw., vol. 3, no. 2, pp. 1–30
76. K. Srinivasan & P. Levis (2006) RSSI is under appreciated, in Proc. EMNETs
77. D. Son, B. Krishnamachari & J. Heidemann (2006) Experimental analysis of concurrent packet transmissions in low-power wireless networks, in Proc. ACM SENSYS, pp. 237–250
78. W. Xu, W. Trappe & Y. Zhang (2007) Channel Surfing: Defending Wireless Sensor Networks from Interference, in Proceedings of the IEEE/ACM International Conference on Information Processing in Sensor Networks (IPSN), pp. 499–508, ISSN 978-1-59593-638-7
79. L. Stabellini & J. Zander (2008) Interference Aware Self-Organization for Wireless Sensor Networks: a Reinforcement Learning Approach, in Proceedings of the 4th annual IEEE Conference on Automation Science and Engineering (CASE 2008), pp. 560–565
80. S. Geirhofer, L. Tong & B.M. Sadler (2007) Dynamic Spectrum Access in the Time Domain: Modeling and Exploiting White Space, in IEEE Communication Magazine, Vol. 45, No. 5, pp. 66–72, ISSN 0163-6804
81. L. Stabellini & J. Zander (2010) Energy-Aware Spectrum Sensing in Cognitive Wireless Sensor Networks: a Cross Layer Approach, IEEE Wireless Communications and Networking Conference (WCNC), pp. 1–6, ISSN 1525-3511
82. Z. Qui, Y. Xui & S. Yin (2014) A novel clustering-based spectrum sensing in cognitive radio wireless sensor networks, IEEE 3rd International Conference on Cloud Computing and Intelligence Systems (CCIS), pp. 695–699
83. D. Cabric, S.M. Mishra & R.W. Brodersen (2004) Implementation Issues in Spectrum Sensing for Cognitive Radios, Proc. 38th Asilomar Conf. Sig., Sys. and Comp. 2004, pp. 772–76
84. I.F. Akyildiz, W. Lee, M.C. Vuran & S. Mohanty (2008) A Survey on Spectrum Management in Cognitive Radio Networks, IEEE Communication Magazine on Cognitive Radio Communications and Networks, pp. 40–48, ISSN 0163-6804
85. R.V. Prasad, P. Pawelczak, J.A. Hoffmeyer & H.S. Berger (2008) Cognitive Functionality in next generation wireless networks standardization efforts, IEEE Communications Magazine, vol. 46, no. 4, pp. 72–78, ISSN 0163-6804
86. M. Mueck et al. (2010) ETSI reconfigurable radio systems: status and future directions on software defined radio and cognitive radio, IEEE Communications Magazine, (Volume: 48, Issue: 9), pp. 78–86, ISSN 0163-6804
87. A.A. Tabassam, F.A. Ali, S. Kalsait & M.U. Suleman (2011) Building Software-Defined Radios in MATLAB Simulink – A Step Towards Cognitive Radios, 13th International Conference on Computer Modelling and Simulation (UKSim), pp. 492–497
88. J.S.C. Turner, M.F. Ramli, L.M. Kamarudin, A.Zakaria, A.Y.M. Shakaff, D.L. Ndzi, C.M.Nor, N. Hassan & S.M Mamduh (2013) The Study of Human Movement Effect on Signal Strength for Indoor WSN Deployment, IEEE Conference on Wireless Sensors (ICWiSe2013), pp. 30–35

89. S. Panichpapiboon, G. Ferrari & O.K. Tonguz (2006) Optimal Transmit Power in Wireless Sensor Networks, IEEE Transactions On Mobile Computing, Vol. 5, No. 10, pp. 1432–1447, ISSN 1536-1233
90. P.J. Crepeau (1992) Uncoded and Coded Performance of MFSK and DPSK in Nakagami Fading Channels, IEEE Transactions On Communications, Vol. 40, No. 3, pp. 487–493, ISSN 0090-6778
91. ETSI EN 300 328 v1.8.1, http://www.etsi.org
92. Commission F.C. 1998 Title 47, Code for Federal Regulations, Part 15
93. N. Golmie (2001) Interference in the 2.4 GHz ISM Band: Challenges and Solutions, Workshop on Services and App. in the Wireless Public Infrastructure, [Online]. Available: http://w3.antd.nist.gov/pubs/golmie.pdf
94. M. Eskola & T. Heikkilä (2012) Deriving test procedures of Low-Rate Wireless Personal Area Networks, International Symposium on Performance Evaluation of Computer and Telecommunication Systems (SPECTS), pp. 1–8
95. M. Eskola, T. Heikkilä & T. Peippola (2013) Identification of radio disturbances of wireless sensor networks, SCSC '13 Proceedings of the 2013 Summer Computer Simulation Conference, ISBN: 978-1-62748-276-9
96. M. Eskola & T. Heikkila (2014) Detection of short-term radio signal disturbances in industrial wireless sensor networks, International Symposium on Performance Evaluation of Computer and Telecommunication Systems (SPECTS), pp. 612–617
97. M. Eskola & T. Heikkila (2014) Metrics for short-term radio signal disturbances detection in wireless sensor networks, 6th International Congress on Ultra-Modern Telecommunications and Control Systems and Workshops (ICUMT), pp. 318–325
98. M. Eskola & T. Heikkila (2015) Detection of short-term radio signal disturbances in Industrial Wireless Sensor Networks, Journal of Networks, Vol. 10, No. 4, pp. 201–208
99. M. Eskola & T. Heikkilä (2016) Classification of Radio Frequency Disturbances in Industrial Wireless Sensor Networks, Elsevier Ad Hoc Networks, Vol. 42, 15 May 2016, pp. 19–33
100. O. Cula & K. Dana (2004) 3D texture recognition using bidirectional feature histograms, International Journal of Computer Vision, August 2004, Vol. 59, Issue 1, pp. 33–60
101. D. Xu, T. Cham, S. Yan, L. Duan & S. Chang (2010) Near duplicate identification with spatially aligned pyramid matching, IEEE Transactions on Circuits and Systems for Video Technology, Volume: 20, Issue: 8, pp. 1068–1079, ISSN 1051-8215
102. H. Ling & D. Jacobs (2007) Shape classification using the inner-distance, IEEE Transactions on Pattern Analysis and Machine Intelligence, Volume: 29, Issue: 2, pp. 286–299, ISSN 0162-8828
103. D. Martin, C. Fowlkes & J. Malik (2004) Learning to detect natural image boundaries using local brightness, colour, and texture cues, IEEE Transactions on Pattern Analysis and Machine Intelligence, Volume: 26, Issue: 5, pp. 530–549, ISSN 0162-8828

104. O. Pele & M. Werman (2010) The Quadratic-Chi Histogram Distance Family, Chapter, Computer Vision – ECCV 2010, Volume 6312 of the series Lecture Notes in Computer Science, pp. 749–762
105. N. Hanik, A. Gladisch, C. Caspar & B. Strebel (1999) Application of amplitude histograms to monitor performance of optical channels, Electronics Letters, Volume: 35, Issue: 5, pp. 403–404, ISSN 0013-5194
106. E. Azzouz & A.K. Nandi (1998) Algorithms for Automatic Modulation Recognition of Communication Signals, IEEE Transactions On Communications, Vol. 46, No. 4, pp. 431–436, ISSN 0090-6778
107. M. Di Francesco, G. Anastasi, M. Conti, S.K. Das & V. Neri (2011) Reliability and Energy-Efficiency in IEEE 802.15.4/ZigBee Sensor Networks: An Adaptive and Cross-Layer Approach, IEEE Journal On Selected Areas in Communications, Vol. 29, No. 8, pp. 1508–1524, ISSN 0733-8716
108. D.M. Dobkin (2005) RF Engineering for Wireless Networks: Hardware, Antennas, ans Propagation, Elsevier, 448 p.
109. N. Kushalnagar, G. Montenegro & C. Schumacher (2007) IPv6 over Low-Power Wireless Personal Area Networks (6LoWPANs): Overview, Assumptions, Problem Statement, and Goals, RFC 4919, Internet Engineering Task Force
110. T. Winter, P. Thubert, A. Brandt, J. Hui, R. Kelsey, P. Levis, K. Pister, R. Struik, J.P. Vasseur & R. Alexander (2012) RPL: IPv6 Routing Protocol for Low-Power and Lossy Networks, RFC 6550, Internet Engineering Task Force
111. Z. Shelby, K. Hartke, C. Bormann & B. Frank (2011) Constrained Application Protocol (CoAP), IETF CoRE Working Group
112. K. Pister & L. Doherty (2008) TSMP: Time Synchronized Mesh Prootocol, Proc. of Int. Symp. Distributed Sensor Networks (DSN), Florida, USA
113. M.R. Palattella, P. Thubert, X. Vilajosana, T. Watteyne, Q. Wang & T. Engel (2014) 6TiSCH Wireless Industrial Networks: Determinism Meets IPv6, in S. C. Mukhopadhyay (Ed.) Internet of Things: Challenges and Opportunities, Springer-Verlag, Lecture series of Smart Sensors, Instrumentation and Measurements

Series title and number

VTT Science 138

Title	**Strategy for wireless transmission disturbances detection and identification in industrial wireless sensor networks**
Author(s)	Marina Eskola
Abstract	This doctoral thesis presents a novel method for detecting and identifying radio channel disturbances. Wireless transmission in factory environments occasionally becomes degraded due to harsh radio signal propagation conditions. The most disruptive disturbances are caused by other wireless devices (co-channel and adjacent interference), environmental characteristics such as metal constructions and heavy equipment (signal fading), and electrical and mechanical equipment (noise). We have performed extensive measurements in different industrial environments to study the effects of different radio channel disturbances on signal propagation. The obtained measurement results led us to develop signal analysis methods and a disturbance detector based on a classifier. The classifier was tested in a real industrial environment; these tests showed an encouraging detection performance. Signal analysis is performed both in time and frequency domains. In the time domain, the probability density function (PDF) method is used. It is based on detecting the PDF shape variations calculated from the received signal and their correlation to the environmental changes in the radio channel. In the frequency domain, spectrogram analysis is performed. Here, we calculate the spectrogram of each received data packet, and by applying image analysis tools on the spectrograms, we obtain the required information on the received signal and on other radio transmissions which may have disturbed our radio signal transmission. The recognition and identification of the radio channel disturbances is based on the fusion of the signal magnitude analysis (PDF) and spectrogram analysis with a classifier. We also discuss the development process of a classifier-based tool towards an embedded solution. The classifier was developed and extensively tested using USPR N210, ETTUS SDR (Software Defined Radio). The classifier proved to be a feasible solution for detecting and identifying reliability flaws of wireless transmission in the industrial environment, and will be further developed into a portable, small-sized SDR-based tool.
ISBN, ISSN, URN	ISBN 978-951-38-8468-0 (Soft back ed.) ISBN 978-951-38-8467-3 (URL: http://www.vttresearch.com/impact/publications) ISSN-L 2242-119X ISSN 2242-119X (Print) ISSN 2242-1203 (Online) http://urn.fi/URN:ISBN:978-951-38-8467-3
Date	October 2016
Language	English, Finnish abstract
Pages	101 p.
Name of the project	
Commissioned by	
Keywords	Radio channel disturbances, software defined radio, classifier, Rician distribution, reliability, industrial wireless sensor networks
Publisher	VTT Technical Research Centre of Finland Ltd P.O. Box 1000, FI-02044 VTT, Finland, Tel. 020 722 111

Julkaisun sarja ja numero

VTT Science 138

Nimeke	**Strategia langattoman tiedonsiirron häiriöiden havaitsemiseen ja tunnistamiseen teollisissa langattomissa anturiverkoissa**
Tekijä(t)	Marina Eskola
Tiivistelmä	Tässä väitöskirjassa esitellään uusi menetelmä radiokanavan häiriöiden havaitsemiseksi ja tunnistamiseksi. Langaton tiedonsiirto tehdasympäristöissä häiriintyy ajoittain, mikä johtuu haastavista radiosignaalin etenemisolosuhteista. Eniten häiriöitä aiheuttavat muut langattomat laitteet (saman lähetyskanavan sekä viereislähetyskaavan häiriöt), ympäristöolosuhteet, kuten metallirakenteet ja raskaat ajoneuvot (signaalin häipyminen), sekä sähkö- ja mekaaniset laitteet (kohina). Tutkimuksessa suoritettiin laajoja mittauksia erilaisissa teollisuusympäristöissä tutkiakseen radiokanavan häiriöiden vaikutusta signaalin etenemisen. Työssä kehitettiin signaalinanalyysimenetelmiin ja häiriön ilmaisimeen perustuva luokittelija ja testattiin sen suorituskykyä oikeassa teollisuusympäristössä. Testit osoittivat, että luokittelijalla on hyvä radiohäiriöiden havaintokyky. Signaalin analyysi suoritetaan sekä aika- että taajuustasossa. Aikatasossa käytetään todennäköisyystiheysfunktion (PDF) laskemiseen pohjautuvaa menetelmää. Tämä menetelmä perustuu vastaanotetun signaalin PDF-muodon vaihteluiden havaitsemiseen ja näiden vaihteluiden vastaavuussuhteeseen radiokanavan muutosten kanssa. Taajuusalueessa suoritetaan spektrogrammien analyysi. Spektrogrammi lasketaan jokaiselle vastaanotetulle paketille ja soveltamalla kuvananalysointitekniikoita spektrogrammeihin saadaan tarvittavat tiedot sekä vastaanotetusta signaalista että muista radiolähetyksistä, jotka saattavat häiritä radiosignaalin lähetystä ja vastaanottamista. Radiohäiriön tunnistaminen perustuu signaalin voimakkuuden analyysiin (PDF) ja spektrogrammianalyysin fuusioon luokittelijaksi. Työssä esitetään myös luokittelijaan pohjautuvan työkalun kehitysprosessin vaiheet ja haasteet kohti sulautettua ratkaisua. Luokittelija on kehitetty ja testattu laajasti käyttäen USPR N210, ETTUS SDR (Software Defined Radio) -työkalua. Luokittelija on osoittautunut toteuttamiskelpoiseksi ratkaisuksi langattoman tiedonsiirron ongelmien havaitsemiseksi ja tunnistamiseksi teollisessa ympäristössä, ja sitä tullaan kehittämään edelleen osaksi kannettavaa, pienikokoista SDR-pohjaista työkalua.
ISBN, ISSN, URN	ISBN 978-951-38-8468-0 (nid.) ISBN 978-951-38-8467-3 (URL: http://www.vtt.fi/julkaisut) ISSN-L 2242-119X ISSN 2242-119X (Painettu) ISSN 2242-1203 (Verkkojulkaisu) http://urn.fi/URN:ISBN:978-951-38-8467-3
Julkaisuaika	Lokakuu 2016
Kieli	Englanti, suomenkielinen tiivistelmä
Sivumäärä	101 s.
Projektin nimi	
Rahoittajat	
Avainsanat	Radiokanavan häiriöt, ohjelmistoradio, luokittelija, Rician jakauma, luotettavuus, teollinen langaton sensoriverkko
Julkaisija	Teknologian tutkimuskeskus VTT Oy PL 1000, 02044 VTT, puh. 020 722 111

Strategy for wireless transmission disturbances detection and identification in industrial wireless sensor networks

This doctoral thesis studies novel methods for detecting and identifying radio channel disturbances in industrial environments. Wireless transmission in factory environments occasionally becomes degraded due to harsh radio signal propagation conditions. The most disruptive disturbances are caused by other wireless devices (co-channel and adjacent interference), environmental characteristics such as metal constructions and heavy equipment (signal fading), and electrical and mechanical equipment (noise).

The extensive measurements have been performed in different industrial environments to study the effects of different radio channel disturbances on signal propagation. The obtained measurement results led us to develop signal analysis methods and a disturbance detector based on a classifier.

In this work the development process of a classifier-based tool towards an embedded solution is also discussed. The classifier was developed and extensively tested using USPR N210, ETTUS SDR (Software Defined Radio). The classifier proved to be a feasible solution for detecting and identifying reliability flaws of wireless transmission in the industrial environment, and will be further developed into a portable, small-sized SDR-based tool.

ISBN 978-951-38-8468-0 (Soft back ed.)
ISBN 978-951-38-8467-3 (URL: http://www.vttresearch.com/impact/publications)
ISSN-L 2242-119X
ISSN 2242-119X (Print)
ISSN 2242-1203 (Online)
http://urn.fi/URN:ISBN:978-951-38-8467-3